TRANSMEMBRANE DOMAINS IV, V, VI, AND VII CONTRIBUTE TO HUMAN ANGIOTENSIN II TYPE 1 RECEPTOR HOMOMER FORMATION

by

Brent M. Young

Submitted in partial fulfilment of the requirements
for the degree of Master of Science

at

Dalhousie University
Halifax, Nova Scotia
June 2015

To my parents and grandparents,

who have taught me to never stop chasing my dreams.

...and to Danny,

who has helped me keep two feet on the ground during the process.

TABLE OF CONTENTS

LIST OF TABLES

LIST OF FIGURES

ABSTRACT

From schizophrenia to asthma, GPCRs have an important role in drug therapy. This work focuses on the AT1R; a GPCR with widespread use in the treatment of cardiovascular disease. Specifically, this work examines the structural aspects of AT1R dimerization, which has been shown to have profound effects on receptor pharmacology. We hypothesized that AT1R homomer formation is driven by hydrophobic amino acids that are exposed to the phospholipid bilayer. A three-dimensional homology model of the AT1R was developed and subsequently validated by a recently published crystal structure. This model was used to guide site-directed mutagenesis, and BRET was used to characterize receptor mutants. The data presented herein demonstrates that hydrophobic amino acids within TMs III, IV, V, VI, and VII contribute to AT1R-AT1R affinity. These findings provide the first glimpse at AT1R homomer structure using GOMoDo and may provide a foundation for the development of drugs that target AT1R dimers.

LIST OF ABBREVIATIONS AND SYMBOLS USED

7TM	seven transmembrane-spanning
ADORA1	adenosine receptor A1
ADORA2A	adenosine receptor A2a
Ang II	angiotensin II
ASA	accessible surface area
AT1R	angiotensin II type 1 receptor
AT2R	angiotensin II type 2 receptor
β1AR	β_1-adrenergic receptor
β2AR	β_2-adrenergic receptor
B2R	bradykinin B2 receptor
BRET	bioluminescence resonance energy transfer
CB1R	cannabinoid receptor type 1
coIP	coimmunoprecipitation
CXCR4	C-X-C chemokine receptor type 4
δOR	δ-opioid receptor
D1R	dopamine D1 receptor
D2R	dopamine D2 receptor
DOPE	discrete optimized protein energy
ECL	extracellular loop
FBS	fetal bovine serum
FRET	fluorescence resonance energy transfer
$GABA_BR$	γ-aminobutyric acid B receptor
GFP	green fluorescent protein
GOMoDo	GPCR Online Modeling and Docking Server
GPCR	G protein-coupled receptor
GPCRDB	GPCR Database
HEK	human embryonic kidney
hERG	human ether-a-go-go-related gene potassium channel
ICL	intracellular loop
IP	inositol phosphate
IUPHAR	International Union of Basic and Clinical Pharmacology
μOR	μ-opioid receptor
M3R	muscarinic acetylcholine receptor M3
PAGE	polyacrylamide gel electrophoresis
PCR	polymerase chain reaction
PEI	polyethylenimine
PS	penicillin-streptomycin
RAAS	renin-angiotensin-aldosterone system
RET	resonance energy transfer
*R*luc	*Renilla* luciferase
RMSD	root-mean-square deviation
S.E.	standard error
T_m	melting temperature

TM	transmembrane
VADAR	Volume Area Dihedral Angle Reporter
WT	wild-type
YFP	yellow fluorescent protein

ACKNOWLEDGEMENTS

First and foremost, I would like to thank my supervisor Dr. Denis J. Dupré who, through patience and guidance, has nurtured my success as a graduate student. I would also like to extend a sincere thank you to past and present members of the Dupré Lab as well as the Denovan-Wright Lab. Your ongoing support has been integral to the success of this project. I would like to express my appreciation for Dr. Christopher Sinal, Dr. Jana Sawynok, and Dr. Jan Rainey, who have always been available as members of my scientific advisory committee. Additionally, I would like to thank Dr. Patrice Côté, Dr. Kishore Pasumarthi, and Dr. Jana Sawynok, who have generously volunteered their time as members of my examining committee. My progress as a graduate student has been facilitated by the administrative support of Luisa Vaughan, Sandi Leaf, and Cheryl Bailey. To you, I owe many thanks. The Indspire Health Careers Award Program and The Dalhousie Medical Research Foundation Adopt-a-Researcher Program have supported this work through generous scholarship funding. This project was made possible by grant funding from the Natural Sciences and Engineering Research Council of Canada (NSERC Grant RGPIN-355310-2013).

CHAPTER 1 INTRODUCTION

1.1 G Protein-Coupled Receptors

More than 800 receptors belong to the G protein-coupled receptor (GPCR) superfamily, and it is one of the largest protein families encoded by the human genome[1-3]. The GPCR signature can also be found in the genome of every known eukaryotic species, highlighting the evolutionary significance of these integral membrane proteins[4]. Over half of human GPCRs are thought to be involved in the olfactory system[1]; however, receptor function can range from phototransduction[5] to bronchodilation[6]. This vast diversity has given the GPCR superfamily a central role in drug therapy. Indeed, nearly half of all pharmaceuticals on the market target only a small fraction of these receptors[7,8]. Thus, it can be speculated that, with further characterization, the GPCR superfamily will be an important tool for disease treatment for years to come.

Current use of GPCRs in drug therapy includes almost every organ system. Diseases affecting the respiratory, cardiovascular, and central nervous systems are perhaps the most notable. Among the most common GPCR targets are the angiotensin II type 1 receptor (AT1R), the dopamine receptor, the 5-hydroxytryptamine receptor, and the adrenergic receptors. Blockade of the AT1R, for example, is widely used for the treatment of hypertension, congestive heart failure, and diabetes mellitus-induced renal damage[9]. While antagonists of the β_1- and/or β_2-adrenergic receptors (β_1/β_2AR) are used to treat coronary heart

disease, hypertension, and congestive heart failure[10], β_2AR agonists are central in the treatment of asthma and chronic obstructive pulmonary disease[11]. Looking at the central nervous system, dopamine receptor antagonists are used for the treatment of schizophrenia, while agonists of the same receptor are used for the treatment of Parkinson's disease[12].

The widespread use of GPCRs as drug targets is derived in large part from the flexibility of GPCR signaling. In the canonical model of GPCR signaling, activated GPCRs act as guanine nucleotide exchange factors that promote the switch of GDP to GTP within the α subunit of specific heterotrimeric G proteins (Gαβγ; Figure 1A). These GTP-bound G proteins go on to activate numerous intracellular effector proteins, which ultimately yield a physiological response[13]. In recent years, however, the canonical model of GPCR signaling has been modified as it has become apparent that GPCRs are also capable of signaling without the use of G protein transducers[13]. The discovery of GPCR signaling via a class of adaptor proteins known as arrestins (Figure 1B) has broadened our understanding of GPCR signaling, and it has highlighted the functional diversity among this superfamily of receptors.

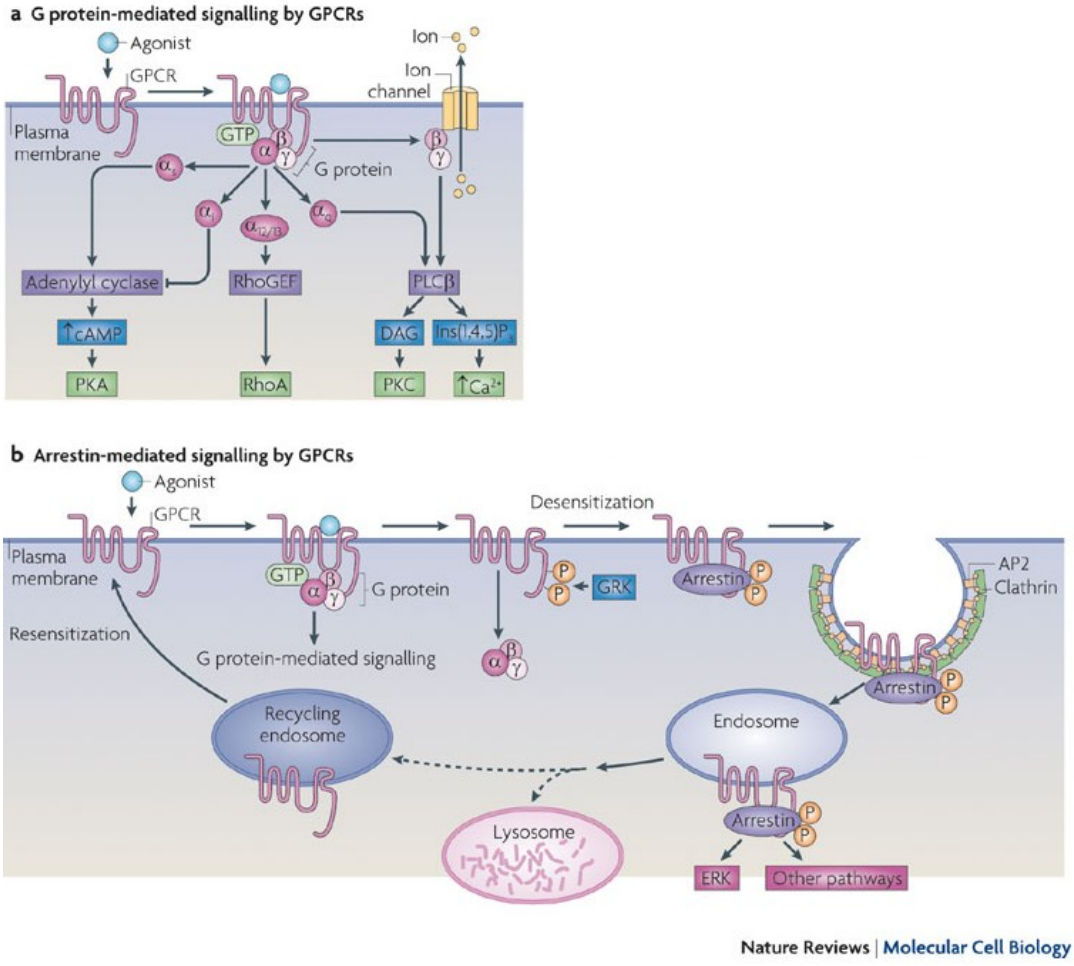

Figure 1 **Canonical GPCR signaling pathways.** (A) General overview of G protein-mediated signaling by GPCRs. (B) Overview of arrestin-mediated signaling by GPCRs. Adapted by permission from Macmillan Publishers Ltd: Nature Reviews Molecular Cell Biology (Ritter *et al.*, 2009)[13], Copyright © 2015.

1.2 GPCR CLASSIFICATION

Function, however, is not the sole source of variability among GPCRs. Structural diversity within the GPCR superfamily creates a significant challenge for receptor classification and, indeed, several classification systems have emerged over the years. Some of these systems are based on structural features, such as the

location of the binding pocket, while others are based on phylogenetic data[14]. Kolakowski (1994) developed one of the first GPCR classification systems for the GCRDb database, and it consisted of seven distinct classes (A-F and O) organized according to sequence identity[15]. While this database has since become obsolete, the Kolakowski classification system has been modified to include six classes (A-F), and it has been incorporated into the current database known as the GPCR Database (GPCRDB)[16].

The A-F system divides the GPCR superfamily into six classes based on sequence identity within the transmembrane region. These families are better known as the Class A rhodopsin-like receptors, Class B secretin-like receptors, Class C metabotropic glutamate receptors, Class D pheromone receptors, Class E cAMP receptors, and the Class F frizzled/smoothened receptors. These six classes are further divided into subclasses, which are denoted by roman numerals. Class A is the largest family of receptors as it encompasses over 80% of all GPCRs. Members of this family are functionally diverse and tend to bind peptides, biogenic amines, or lipid-like ligands[17]. Class B receptors bind larger peptides such as secretin, parathyroid hormone, glucagon, and calcitonin[18], while Class C receptors bind glutamate, an excitatory neurotransmitter[19]. The Class F frizzled/smoothened receptors are a minor family; however, they have a key role in animal development through Wnt binding and hedgehog signaling[20]. Despite the A-F system being designed to incorporate both vertebrate and invertebrate GPCRs, some classes do not include human GPCRs at all. Classes D and E, for example, consist of fungal pheromone receptors and cAMP receptors, which are

involved in chemotaxis. Neither of these classes are expressed in humans. Overall, this diversity complicates GPCR classification, and it has led to the development of systems that classify only human GPCRs.

Human GPCRs are most often organized using a five family system known as the GRAFS classification system.[1] This system was established by Fredriksson *et al.* (2003), and it has since been used extensively in other studies[1,14,21]. The five families that make up the GRAFS system are known as the glutamate, rhodopsin, adhesion, frizzled/taste2, and secretin families. Similar to the A-F system, this five family system of classification is based primarily on sequence data within the transmembrane (TM) region; however, the GRAFS system goes one step further in organising GPCRs into distinct phyla[1]. Despite this, each GPCR within a given GRAFS family may possess a unique signalling capability by coupling with specific G protein subtypes, signaling via distinct G protein-independent pathways, and binding only specific ligands[22]. The sheer number and diversity of members among the rhodopsin family alone highlights the challenges associated with classifying GPCRs based solely on sequence data. A better understanding of tertiary receptor structure may facilitate classification given the subtle differences in structure that lead to such a multifaceted functionality[22].

1.3 GPCR Structure

Despite having limited sequence homology, every GPCR has a similar topology that consists of seven TM-spanning (7TM) α-helices that form a barrel-like structure connected by three extracellular loops and three intracellular loops[23].

Typically, the 7TM region is enriched with hydrophobic amino acids, and it provides an ideal environment for small molecule binding (photons, biogenic amines, nucleosides, and sphingosine 1-phosphate)[24]. Upon ligand binding, the 7TM region relays conformational changes to the intracellular face of the receptor, activating the signaling cascade. In addition to the 7TM region, GPCRs possess an extracellular N-terminus, and an intracellular C-terminus. The 7TM region tends to be more conserved when compared to the loops and termini; however, this sequence identity only exists within any given receptor class[22,25]. While the length of each terminus can vary significantly, a total length of 200-300 amino acids is characteristic of GPCRs[26].

Several regions and motifs have been identified as key in determining GPCR function. The extracellular surface, for example, has been shown to be highly variable among GPCRs, and it has an important role in binding larger molecules such as peptides and glycoproteins (oxytocin, vasopressin, opioids, thyrotropin-stimulating hormone, and follitropin-stimulating hormone)[24]. The N-terminus and second extracellular loop (ECL2) are often shown to influence solvent accessibility of the binding pocket[22]. Looking at the N-terminus, it tends to be more structured in rhodopsin as a result of glycosylation, and it serves to limit accessibility of the binding pocket. Within the same receptor, ECL2 forms a β-sheet that renders the covalently bound ligand, 11-*cis* retinal, inaccessible to solvents[27,28]. However, looking at the β-adrenergic receptors and the adenosine receptor A2a (ADORA2A), the N-terminus lacks a predominant secondary structure, and it does not impede solvent accessibility. Likewise, ECL2 of the β_1-

and β_2-adrenergic receptors (β1/β2AR) forms an α-helix that does not influence accessibility of the binding pocket. Looking at the ADORA2A, ECL2 has no predominant secondary structure and, similarly, it does not prevent solvent accessibility.

At the intracellular surface, there are some key structural features that influence GPCR activity[22]. The E/DRY motif on TMIII, for instance, holds members of the rhodopsin family in the inactive state by forming an "ionic lock" with a glutamate residue on TMVI[29]. Looking at the β2AR, mutation of the E/DRY motif leads to constitutive activity[30,31]. Further analysis has indicated that full and partial agonists act to disrupt this interaction in the β-adrenergic receptors as well as ADORA2A. This leads to destabilization of the inactive-state conformation and results in receptor activation. A conserved tyrosine that resides in an α-helix found in intracellular loop 2 (ICL2) of the β1AR and the ADORA2A is also known to form a hydrogen bond with the E/DRY motif on TMIII. Much like the glutamate residue found on TMVI, this residue serves to hold the receptor in the inactive state. The fact that this tyrosine is not found in the β2AR , but it is found in the β1AR , may explain why the β2AR has a higher basal activity compared to the β1AR[22].

Another common structural feature at the intracellular surface of some GPCRs is known as the NPxxY motif[32]. Found at the cytoplasmic end of TMVII and similar to the E/DRY motif, the NPxxY motif contributes to conformational changes that result in receptor activation. This motif has been identified in rhodopsin, the

β_2AR, the thyrotropin receptor, and the muscarinic acetylcholine receptor M3 (M3R), to name a few[32-35]. The proline residue found in this motif promotes distortion of the TMVII α-helix, and it forms a water pocket lined by TMII, TMIII, TMVI, and TMVII. Ordered water molecules found in this pocket are thought to stabilize the inactive state conformation of the receptor; however, the weak nature of these interactions is thought to allow for rapid toggling from the inactive state to the active state upon ligand binding[36,37].

1.4 Emergence of the GPCR Oligomerization Paradigm

Evidence for receptor tyrosine kinase oligomerization preceded that of GPCR oligomerization by more than a decade[38-40]. Early studies involving radioligand binding[41-43], radiation inactivation[44-47], and receptor crosslinking[48] provided data that pointed to the existence of high order GPCR structures[49]; however, the notion of GPCR oligomerization only began to garner support in 1993 when Maggio *et al.* developed two chimeric receptors[39]. These mutants, dubbed the α_2/M3 and M3/α_2 receptors, were comprised of the α_{2c}-adrenergic receptor and the M3R with TMs VI and VII swapped between each GPCR. Characterization of these mutants demonstrated that both receptors were binding-deficient and non-functional when expressed alone. However, it was noted that receptor coexpression reinstated ligand binding and receptor function that was comparable to the wild-type (WT) receptors[39]. This was the first *trans*-complementation experiment that involved GPCRs, and it served as a catalyst for further studies in the field of GPCR oligomerization[50].

A few years later, the concept of GPCR dimerization gained momentum when Hébert *et al.* (1996) demonstrated that a peptide derived from TM VI of the β_2AR was sufficient to disrupt β_2AR dimerization as visualized using a western blot[51]. Remaining doubts were minimized in 1998 when it was shown that heterodimerization is a requisite for proper gamma-aminobutyric acid B receptor ($GABA_BR$) trafficking and signalling[52-54]. Specifically, these studies showed that two $GABA_BR$ subtypes, $GABA_BR1$ and $GABA_BR2$, are non-functional when expressed individually; however, the receptors were shown to regain function and bind GABA with high affinity when coexpressed. A C-terminal interaction was reported between the two receptors in human embryonic kidney (HEK) cells[53], and both genes were shown to be expressed in individual neurons[54]. This was the first time GPCR dimerization was shown to have functional consequences *in vivo* and, since this time, an entire field of research has been devoted to GPCR oligomerization[50,55-57].

1.5 Pharmacological Aspects of GPCR Oligomerization

One of the first studies to highlight the pharmacological consequences of GPCR dimerization came from Barki-Harrington *et al.* (2003)[58]. This study demonstrated that a single antagonist was sufficient to inhibit both AT1R and β_2AR signalling. When examining mouse cardiomyocytes, it was shown that angiotensin II (Ang II)-induced contractility is attenuated by selective inhibition of the β_2AR with propranolol. Interestingly, propranolol-mediated inhibition was virtually identical when either Ang II or isoproterenol, a potent β2AR agonist,

were used to stimulate contractility[58]. These experiments indicated that a *trans*-inhibitory mechanism must exist between the AT1R and the β_2AR. Confocal microscopy suggested that an interaction between the AT1R and the β_2AR is the underlying mechanism of *trans*-inhibition as the two receptors were shown to co-localize. To determine whether or not this finding was physiologically relevant, the researchers demonstrated that an isoproterenol-induced increase in heart rate can be reduced in mice that are pretreated with valsartan, an angiotensin receptor blocker[58]. It was hypothesized that this *trans*-inhibition occurs via functional uncoupling of the G protein from the adjacent receptor. Indeed, pre-treatment of cardiomyocytes with either valsartan or propranolol respectively disrupts either isoproterenol- or angiotensin-mediated [^{35}S]GTPγS binding to G_α at the adjacent receptor. This inhibition was also observed in downstream signalling, with isoproterenol-stimulated cAMP formation and angiotensin-stimulated inositol-phosphate (IP) accumulation being disrupted by antagonist binding at the adjacent receptor[58]. This study was one of the first in-depth examinations of the pharmacological consequences of GPCR oligomerization, and several others have emerged in recent years.

Agonist-induced signaling changes are not the only pharmacological consequences of GPCR oligomerization. It has been shown that GPCRs themselves can act as allosteric modulators of other receptors upon complex formation. For example, the bradykinin B2 receptor (B2R) increases AT1R signaling via heteromer formation, even in the absence of Ang II[47]. On the contrary, an interaction between the AT1R and the angiotensin II type 2 receptor

(AT2R) has been shown to reduce AT1R signaling independent of downstream crosstalk[59]. Similarly, the somatostatin receptor 2A has been shown to act as a negative allosteric modulator of the somatostatin receptor 3[60]. This evidence suggests that there is therapeutic potential in the modulation of GPCR oligomerization as it may be an alternative approach for modulating GPCR signaling.

While GPCR oligomerization can lead to changes in both basal and ligand-stimulated signaling, it has also become apparent that agonists can influence the receptor-receptor interaction itself. For example, treatment with a dopamine D1 receptor (D1R) agonist has been shown to decrease heteromer formation between the adenosine receptor A1 (ADORA1) and the D1R. On the contrary, treatment with an ADORA1 agonist increases this complex formation[61]. Another example of this phenomenon can be observed with the thyrotropin-releasing hormone receptor 1. Here, ligand binding potentiates receptor dimerization[62]. However, the opposite holds true for the δ-opioid receptor[63], the κ-opioid receptor[64], and the neuropeptide Y Y4 receptor[65], which transition from dimers to monomers in the presence of agonist. While the phenomena mentioned above represent some of the most profound oligomerization-induced changes in GPCR pharmacology, a comprehensive list of GPCR-GPCR interactions and their corresponding pharmacological effects can be found in Table 1.

Table 1 Summary of the known pharmacological effects of GPCR complex formation.

GPCR Complex	Pharmacological Effect of Complex Formation
5-Hydroxytryptamine 2A receptor – dopamine D2 receptor[66,67]	Increased binding affinity and decreased signaling by dopamine D2 receptor agonist
Adenosine A1 receptor – adenosine $A2_A$ receptor[68]	Decreased binding affinity and agonist signaling
Adenosine A1 receptor – β_2-adrenergic receptor[69,70]	Decreased β_2-adrenergic receptor signaling upon coactivation
Adenosine A1 receptor – dopamine D1 receptor[61]	Decreased dopamine D1 receptor signaling upon coactivation
Adenosine $A2_A$ receptor – cannabinoid receptor type 1[71]	Coactivation of adenosine $A2_A$ receptor required for cannabinoid receptor type 1 signaling
Adenosine $A2_A$ receptor – dopamine $D2_L$ receptor[72-77]	Decreased agonist binding affinity and cointernalization
α_{1A}-adrenergic receptor – α_{1B}-adrenergic receptor[78,79]	Increased binding affinity and decreased signaling by dopamine D2 receptor agonist
α_{1A}-adrenergic receptor – histamine H1 receptor[80]	Increased signaling
α_{1B}/β_2-adrenergic receptor – α_{1D}-adrenergic receptor[81,82]	Increased cell surface expression and increased signaling of α_{1D}-adrenergic receptor
α_{2A}-adrenergic receptor – β_1-adrenergic receptor[83]	Cointernalization
α_{2A}-andrenergic receptor – μ-opioid receptor[84]	Decreased α_{2A}-adrenergic receptor signaling with morphine stimulation

GPCR Complex	Pharmacological Effect of Complex Formation
Angiotensin II type 1 receptor – bradykinin B2 receptor[47,85,86]	Increased binding affinity and signaling of angiotensin II
Angiotensin II type 1 receptor – β_1/β_2-adrenergic receptor[58]	Decreased signaling in the presence of antagonist
Angiotensin II type 1 receptor – dopamine D– receptor[87]	Decreased dopamine D_2 receptor signaling in the presence of angiotensin II type 1 receptor antagonist
Angiotensin II type 1 receptor – cannabinoid receptor type 1[88]	Increased angiotensin II signaling and G protein switch (cannabinoid receptor type 1 controls G protein signaling)
Angiotensin II type 1 receptor – angiotensin II type 2 receptor[59]	Decreased signaling of the angiotensin II type 1 receptor
β_1-adrenergic receptor – β_2-adrenergic receptor [89]	Increased signaling in the presence of agonist, but decreased binding affinity
β_2-adrenergic receptor – δ-opioid receptor[90]	Cointernalization
β_2-adrenergic receptor – oxytocin receptor[91]	Decreased agonist signaling
Cannabinoid receptor type 1 – dopamine D2 receptor[92-94]	Decreased agonist binding and G protein switch ($G\alpha_{i/o}$ to $G\alpha_s$)
Cannabinoid receptor type 1 – δ-opioid receptor[95,96]	Cannabinoid receptor type 1 expression increased at cell surface, agonist signaling via cannabinoid receptor type 1 decreased, and δ-opioid receptor binding affinity increased by cannabinoid receptor type 1 agonist
Cannabinoid receptor type 1 – μ-opioid receptor[96]	Decreased signaling in the presence of agonist

GPCR Complex	Pharmacological Effect of Complex Formation
C-C chemokine receptor type 2 – C-C chemokine receptor type 5[97,98]	Decreased agonist binding
C-C chemokine receptor type 2 – μ-opioid receptor[99]	Decreased signaling
C-X-C chemokine receptor type 2 – δ-opioid receptor[100]	Increased δ-opioid receptor signaling in the presence of C-X-C chemokine receptor type 2 antagonist
δ-opioid receptor – κ-opioid receptor[64]	Decreased binding of selective agonist and antagonist, but increased binding of partially selective ligand
δ-opioid receptor – μ-opioid receptor[101-105]	Increased binding affinity and signaling by combination of μ-agonist and δ-antagonist. G protein switch from $G\alpha_i$ to $G\alpha_z$, and $G\alpha_i$ to β-arrestin). Decreased internalization
δ-opioid receptor – dopamine D1 receptor[106]	G protein switch with a preference for $G\alpha_i$ over $G\alpha_s$
Dopamine D1 receptor – dopamine D2 receptor[107-109]	G protein switch from $G\alpha_{i/o}$ to $G\alpha_{q/11}$ with cointernalization
Dopamine D1 receptor – dopamine D3 receptor [110,111]	Increased agonist binding and increased dopamine D1 receptor signaling
Dopamine D1/D2 receptors – histamine H3 receptor[112]	Decreased signaling by histamine H3 receptor agonists
Dopamine D2 receptor – dopamine D2 receptor[113]	Ligand dependent changes in signaling
Dopamine D2 receptor – dopamine D3 receptor[114,115]	Increased binding of agonists selective for the dopamine D3 receptor

GPCR Complex	Pharmacological Effect of Complex Formation
Dopamine D2 receptor – somatostatin receptor type 5[116]	Increased agonist binding and signaling
Dopamine $D2_L$ receptor – neurotensin receptor 1[117]	Decreased agonist binding with neurotensin receptor 1 coactivation
μ-opioid receptor – somatostatin receptor type 2_A[118]	Cointernalization
Somatostatin receptor type 1 – somatostatin receptor type 5[119]	Cointernalization
Somatostatin receptor type 2 – somatostatin receptor type 3[60]	Increased somatostatin receptor type 2_A signaling and decreased somatostatin receptor type 3 signaling. Decreased internalization in the presence of agonist
Vasopressin $V1_A$ receptor – vasopressin V2 receptor[120]	Cointernalization and increased binding to β-arrestin

1.6 TECHNIQUES USED TO CHARACTERIZE GPCR OLIGOMERS

1.6.1 Immunoblotting and Coimmunoprecipitation

Common biochemical approaches such as non-denaturing polyacrylamide gel electrophoresis (PAGE), immunoblotting, and coimmunoprecipitation (coIP) have played a key role in the identification and investigation of GPCR oligomers. PAGE coupled with immunoblotting is perhaps the most minimalist among these approaches. This technique is based on the asssumption that GPCRs will migrate as complexes during PAGE, and that these complexes will appear as immunoreactive bands with a molecular weight that is two or more times larger

than that of each monomeric receptor[49]. There are, however, some limitations to consider when using this approach. With untagged receptor homomers, for example, it is difficult to determine whether or not the additional molecular weight is derived from a receptor-receptor interaction or a receptor-protein interaction. It can also be difficult to obtain an antibody with specificity for untagged receptors[121]. As a result, many studies have exploited heterologous expression of tagged GPCRs. With differentially tagged receptors, each GPCR can be probed individually to determine whether or not both GPCRs of interest appear at the predicted molecular weight of the oligomer. This approach is commonly used in studies involving coIP[51,64,122].

With coIP, cell lysates are probed with a receptor- or epitope-specific antibody, and the immunoprecipitated protein is analyzed using PAGE and immunoblotting. The appearance of an immunoreactive band for the secondary receptor is indicative of either a direct or indirect interaction between each receptor. It is most common to use coIP for the examination of heterologous expression systems with epitope-tagged receptors; however, coIP has also been used for the examination of GPCR oligomer formation in native tissues. This has played a key role in strengthening the notion that GPCR oligomerization occurs *in vivo*, and it has demonstrated that oligomerization is not simply an artifact of heterologous expression[49,123-125]. Overall, biophysical methods have been used to characterize over 50 endogenous and exogenous GPCR-GPCR complexes. A comprehensive list of these complexes can be found below (Table 2).

Table 2 GPCRs shown to form homomeric and heteromeric complexes using biochemical methods.

GPCR	Receptor Expression
5-Hydroxytryptamine 2A receptor – dopamine D2 receptor[66,67]	Exogenous
5-Hydroxytryptamine 4 receptor – 5-hydroxytryptamine 4 receptor [126]	Exogenous
Adenosine A1 receptor – adenosine A1 receptor[127]	Endogenous
Adenosine A1 receptor – adenosine $A2_A$ receptor[68]	Exogenous
Adenosine A1 receptor – dopamine D1 receptor[61]	Endogenous, Exogenous
Adenosine $A2_A$ receptor – cannabinoid receptor type 1[71]	Endogenous
Adenosine $A2_A$ receptor – dopamine $D2_L$ receptor[72-77]	Endogenous, Exogenous
α_{1A}- adrenergic receptor – α_{1A}- adrenergic receptor [79]	Exogenous
α_{1A}-adrenegic receptor – α_{1B}-adrenergic receptor[78,79]	Exogenous
α_{1B}-adrenergic receptor – α_{1B}-adrenergic receptor[79]	Exogenous
α_{1B}/β_2-adrenergic receptor – α_{1D}-adrenergic receptor[82]	Exogenous
α_{2A}-adrenergic receptor – β_1-adrenergic receptor[83]	Exogenous

GPCR	Receptor Expression
Angiotensin II type 1 receptor – angiotensin II type 1 receptor [59]	Endogenous, Exogenous
Angiotensin II type 1 receptor – angiotensin II type 2 receptor[59,61]	Endogenous, Exogenous
Angiotensin II type 1 receptor – bradykinin receptor B2[47,85,86]	Endogenous, Exogenous
Angiotensin II type 1 receptor – β_1-/β_2-adrenergic receptors[58]	Exogenous
Angiotensin II type 1 receptor – cannabinoid receptor type 1[88]	Exogenous
Angiotensin II type 1 receptor – dopamine D– receptor[87]	Endogenous, Exogenous
β_2-adrenergic receptor – β_2-adrenergic receptor [51,128,129]	Exogenous
β_2-adrenergic receptor – δ-opioid receptor[90]	Exgenous
β_2-adrenergic receptor – oxytocin receptor[91]	Exogenous
Calcium-sensing receptor – calcium-sensing receptor [130,131]	Endogenous, Exogenous
Cannabinoid receptor type 1 – δ-opioid receptor[95]	Exogenous
C-C chemokine receptor 2 – C-C chemokine receptor 2[132]	Endogenous, Exogenous
C-C chemokine receptor 5 – C-C chemokine receptor 5[133]	Exogenous
C-X-C chemokine receptor 1 – C-X-C chemokine receptor 1[134]	Exogenous

GPCR	Receptor Expression
C-X-C chemokine receptor 2 – C-X-C chemokine receptor 2[134,135]	Exogenous
C-C chemokine receptor 2b – C-C chemokine receptor 5[97,98]	Exogenous
C-C chemokine receptor 5 – μ-opioid receptor[99]	Exogenous
C-X-C chemokine receptor 2 – δ-opioid receptor[100]	Exogenous
δ-opioid receptor – δ-opioid receptor [63,104,136]	Exogenous
δ-opioid receptor – κ-opioid receptor[64]	Exogenous
δ-opioid receptor – μ-opioid receptor[101-105]	Endogenous, Exogenous
Dopamine D1 receptor – dopamine D1 receptor [137]	Exogenous
Dopamine D1 receptor – dopamine D2 receptor[107-109,138]	Endogenous, Exogenous
Dopamine D1 receptor – dopamine D3 receptor[110,111]	Endogenous, Exogenous
Dopamine D2 receptor – dopamine D2 receptor[139,140]	Exogenous
Dopamine $D2_L$ receptor – neurotensin receptor 1[117]	Exogenous
Dopamine D3 receptor – dopamine D3 receptor [141]	Endogenous, Exogenous
κ-opioid receptor – κ-opioid receptor [64]	Exogenous

GPCR	Receptor Expression
κ-opioid receptor – μ-opioid receptor[142]	Exogenous
Melatonin M1 receptor – melatonin M1 receptor[143]	Exogenous
Melatonin M2 receptor – melatonin M2 receptor [143]	Exogenous
Metabotropic glutamate receptor 1 – metabotropic glutamate receptor 1[144]	Endogenous, Exogenous
Metabotropic glutamate receptor 5 – metabotropic glutamate receptor 5[145]	Endogenous, Exogenous
μ-opioid receptor – μ-opioid receptor [104]	Exogenous
μ-opioid receptor – somatostatin receptor 2A[118]	Exogenous
Muscarinic acetylcholine receptor M3 – muscarinic acetylcholine receptor M3[146]	Exogenous
Neuropeptide Y Y4 receptor – neuropeptide Y Y4 receptor [65]	Exogenous
Oxytocin receptor – vasopressin $V1_A$/V2 receptors[147]	Exogenous
Somatostatin receptor 2 – somatostatin receptor 3[60]	Exogenous
Somatostatin receptor 2A – somatostatin receptor 2A [60,62]	Exogenous
Somatostatin receptor 5 – somatostatin receptor 5[119]	Exogenous
Thyrotropin receptor – thyrotropin receptor [148]	Exogenous

GPCR	Receptor Expression
Thyrotropin-releasing hormone receptor 1 – thyrotropin-releasing hormone receptor 1[62]	Exogenous

While coIP has proven to be invaluable for the study of GPCR oligomers, there are some caveats to consider when using this technique[149]. For example, the use of a detergent during cell lysis may increase the likelihood of protein aggregate formation[49,150,151]. This is especially true given the hydrophobic nature of GPCRs. Where low detergent concentrations have been shown to exaggerate these interactions via protein aggregate formation, high detergent concentrations have been shown to disrupt the hydrophobic interactions between oligomers[149]. Theoretically, the former conditions would yield false positives, while the latter would yield false negatives. Some have circumvented this problem by developing a control that involves expressing each GPCR in individual cell populations and mixing these cells prior to lysis. Indeed, it has been shown that complexes can only be obtained when receptors are expressed in the same cell[64,121]. Moreover, it has been shown that receptor-receptor interactions observed via coIP can be disrupted by reducing agents. For example, the calcium-sensing receptor and the metabotropic glutamate receptor 1 appear as dimers in the absence of a reducing agent; however, in the presence of a reducing agent, these receptors appear as monomers[130,144]. This demonstrates that covalent linkages exist between GPCRs prior to solubilisation, and cell lysis does not necessarily result in non-specific receptor interactions. Ultimately, with proper controls, coIP can be used to identify GPCR oligomers. However, it is inherently limited in its ability to detect

small changes in receptor-receptor affinity, and biophysical methods have emerged as a quantitative alternative for examining these structures.

1.6.2 Resonance Energy Transfer

Biophysical techniques based on resonance energy transfer (RET) have emerged as important tools to complement and, sometimes, replace biochemical techniques in the examination of GPCR oligomerization[152]. These techniques involve the transfer of energy from a donor fluorophore to an acceptor fluorophore and, thus, require the heterologous expression of fluorophore-tagged proteins. Despite this, RET-based techniques are advantageous because they can be used to examine proteins that are expressed in intact, living cells[153]. This alleviates some of the solubilisation issues that arise with the biochemical methods mentioned above, and it provides a much more quantitative means for assessing protein-protein interactions. RET has played a prominent role in the examination of GPCR oligomerization in recent years[154]. A list of GPCR-GPCR complexes that have been observed using RET can be found in Table 3.

Table 3 A list of GPCRs shown to form dimers and oligomers using resonance energy transfer

Receptor
5-hydroxytryptamine 2A receptor – dopamine D2 receptor[66,67]
5-hydroxytryptamine 4 receptor – 5-hydroxytryptamine receptor 4[126]
Adenosine receptor A1 – adenosine receptor A2a[68]
Adenosine receptor A2a – cannabinoid receptor type 1[71]
Adenosine receptor A2a – Dopamine $D2_L$ receptor[72-77]
α_{1A}-adrenergic receptor – α_{1B}-adrenergic receptor[78,79]
α_{2A}-adrenergic receptor – μ-opioid receptor[84]
Angiotensin II type 1 receptor – bradykinin B2 receptor[47,85,86]
Angiotensin II type 1 receptor – cannabinoid receptor type 1[88]
β_1-adrenergic receptor – β_1-adrenergic receptor[128,129]
β_2-adrenergic receptor – β_2-adrenegic receptor[51,128,129]
β_2-adrenergic receptor – oxytocin receptor[91]
Cannabinoid receptor type 1 – dopamine D2 receptor[92-94]
Cannabinoid receptor type 1 – δ-opioid receptor[95,96]
Cannabinoid receptor type 1 – μ-opioid receptor[96]
Cholecystokinin 2 receptor – μ-opioid receptor[155]
C-C chemokine receptor type 2b – C-C chemokine receptor type 5[97,98]

Receptor
C-X-C chemokine receptor type 1 – C-X-C chemokine receptor type 1[134]
C-X-C chemokine e receptor type 2 – C-X-C chemokine receptor type 2[134]
C-X-C chemokine receptor type 2 – δ-opioid receptor[100]
δ-opioid receptor – μ-opioid receptor[101-105]
Dopamine D1 receptor – dopamine D2 receptor[107-109]
Dopamine D1 receptor – dopamine D3 receptor[110,111]
Dopamine D1/D2 receptors – histamine H3 receptor [112]
Dopamine D2 receptor – dopamine D3 receptor[114,115]
K-opioid receptor – μ-opioid receptor[142]
Melatonin M1 receptor – melatonin M1 receptor[143]
Melatonin M2 receptor – melatonin M2 receptor[143]
Neuropeptide Y Y4 receptor – neuropeptide Y Y4 receptor [65]
Vasopressin $V1_A$ receptor – vasopressin V2 receptor[120]
Vasopressin $V1_A$/V2 receptors – oxytocin receptor[147]

In order for RET to occur, an overlap of 30% or more is required between the emission spectrum of the donor fluorophore and the absorption spectrum of the acceptor fluorophore[156]. Additionally, specific spatial requirements must be met in order of achieve this energy transfer. First, RET can only occur when the two tags come within a distance of 100 Å of one another[157]. Second, RET is dependent

on the relative orientation of each tag. Specifically, the emission and absorption dipoles of the donor and acceptor fluorophores must be oriented at an angle other than 90°, otherwise self-cancelling oscillations occur, and RET is abolished[154,157]. Ultimately, a ratio of acceptor emission to donor emission can be calculated, and this ratio indicates whether or not there is a protein-protein interaction. With this in mind, it is important to note that a low RET ratio does not necessarily mean that there is no interaction. This could simply indicate that the spatial requirements for RET, which are mentioned above, have not been met. Likewise, a high RET ratio does not necessarily mean a direct interaction is occurring between the two proteins of interest. This could mean that the receptors are within close enough proximity for RET to occur, but the interaction is indirect. Despite this, RET is thought to be ideal for the study of GPCR dimers because, looking at the crystal structure of rhodopsin, the centre-to-centre distance between two monomers within a dimer is predicted to be 40-50 Å[158,159]. This leaves little room for indirect interactions to be observed between two GPCRs.

There are two common variations of RET. These techniques are known as fluorescence resonance energy transfer (FRET; Figure 2C) and bioluminescence resonance energy transfer (BRET; Figure 2A & B). As outlined above, both techniques require two tags that are compatible for energy transfer; however, they differ in the sense that FRET utilizes an external light source and a fluorescent protein as the energy donor, while BRET utilizes a bioluminescent molecule as the energy donor[160]. With BRET, an enzyme known as *Renilla*

luciferase (*R*luc) occupies the role of the energy donor as it hydrolyzes a substrate known as coelenterazine. This reaction results in the emission of energy, which is subsequently transferred to the acceptor molecule on the interacting protein. In the case of BRET[1], yellow fluorescent protein (YFP) acts as the acceptor molecule (Figure 2B) and, in the case of BRET[2], green fluorescent protein (GFP) acts as the acceptor molecule (Figure 2A).

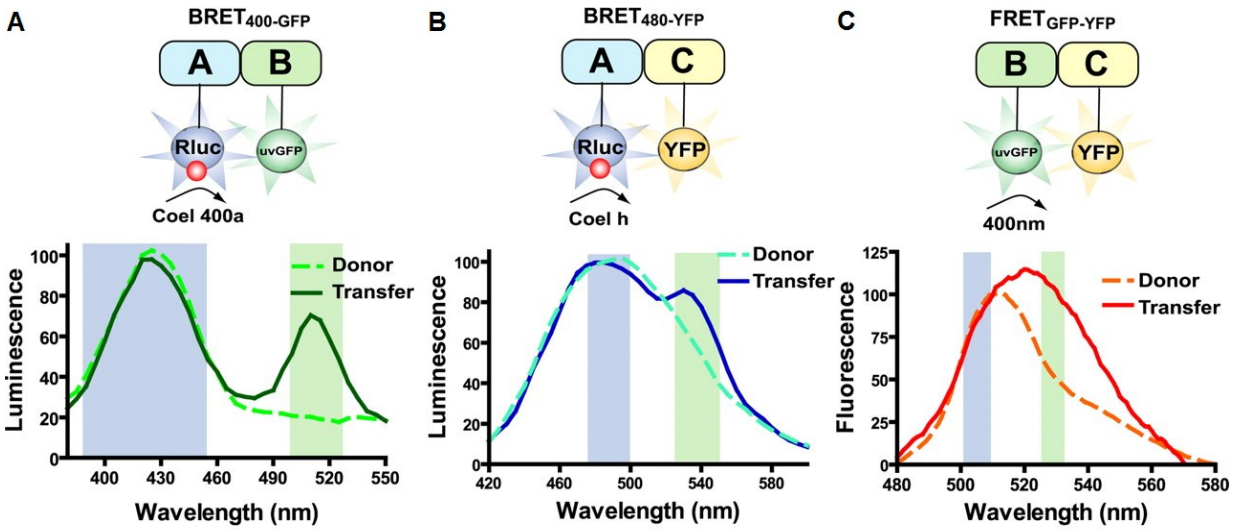

Figure 2 **Schematic and graphical representation of biophysical techniques based on resonance energy transfer.** (A) BRET[2] involves the transfer of energy for *R*luc to GFP. This technique has the highest peak-to-peak resolution between the donor and acceptor spectra. (B) BRET[1] involves the transfer of energy between *R*luc and YFP. The resolution between acceptor/donor emission spectra is lower in BRET[1] when compared to BRET[2]. This decreases signal-to-noise ratio. (C) FRET differs from BRET in the sense that it uses GFP as the energy donor and YFP as the energy acceptor. The spectral resolution between these two tags is the lowest among all of the techniques mentioned above. This, and the use of an external light source, gives FRET the lowest signal-to-noise ratio. Adapted by permission from FASEB Office of Publications: The FASEB Journal (Breton *et al.*, 2010)[152], Copyright © 2015.

Among the three techniques outlined in Figure 2, BRET^2 is the most sensitive because there is a higher peak-to-peak resolution between the emission spectrum of the energy donor and the emission spectrum of the energy acceptor. This results in a higher signal-to-noise ratio. Based solely on the signal-to-noise ratio, FRET is the least favourable technique. Additionally, BRET is often chosen over FRET because it does not rely on an external light source. As with any fluorescence technique, the use of an external light source in FRET can lead to fluorophore photobleaching as well as autofluorescence[160]. The autofluorescence of molecules that are external to the FRET system increases noise and, ultimately, decreases FRET sensitivity. While FRET has more use in the visualization of subcellular protein localization, BRET is often chosen for its quantitative advantages.

Mercier *et al.* (2002) were the first to use a BRET saturation assay to quantitatively assess the specificity of a GPCR-GPCR interaction[129]. With this approach, different cell populations are transfected with a constant amount of donor-labelled protein and increasing amounts of acceptor-labelled protein. In the event of a specific interaction, each donor-labelled protein eventually becomes saturated with acceptor-labelled proteins, and the BRET ratios plateau. On the contrary, with non-specific interactions, the BRET signal increases in a nonsaturable, quasi-linear fashion as the concentration of acceptor-labelled protein increases[129]. Overall, BRET saturation experiments are particularly useful because they provide a $BRET_{50}$ value. This value represents the acceptor/donor

ratio that provides 50% of the maximal BRET response, and it is inversely proportional to the affinity between each GPCR.

1.6.3 Functional Complementation

While biochemical and biophysical approaches have successfully demonstrated that GPCRs can be found within close proximity of one another, functional complementation studies have demonstrated that direct interactions do occur between GPCRs[55]. With functional complementation, two non-functional receptor-G protein complexes are coexpressed with the assumption that function will be restored should an interaction occur. Each of the fusion proteins used in functional complementation assays consist of either a non-functional receptor and a functional G protein, or a functional receptor and a non-functional G protein. By coexpressing these two complexes, one of two outcomes can be achieved. In the case of non-interacting receptors, signaling is not reconstituted. In the case of interacting receptors, however, signaling is reconstituted. While functional complementation was initially observed with endogenous $GABA_B$ receptors[52-54], it has since been shown with heterologous expression of α_{1A}-adrenergic –histamine H1 receptor heteromers[80], δ-opioid–D1R heteromers[106], and dopamine D2 receptor (D2R) homomers[113]. While functional complementation can distinguish between direct and indirect interactions, it is limited in its ability to detect small changes in receptor-receptor affinity. When quantifying the affinity between two receptors, biophysical methods are more advantageous.

1.6.4 Receptor Crystallization

The first glimpse of the 7TM architecture of GPCRs came in 1993 with the analysis of two-dimensional rhodopsin crystals[161,162]. Almost a decade later, in 2000, the first three-dimensional crystal structure of rhodopsin emerged[158]. This stands as the first three-dimensional GPCR crystal structure to be solved[22]. Since this time, 25 three-dimensional GPCR crystal structures have been elucidated (Table 4), and only a handful of these are receptor dimers.

Table 4 List of GPCRs with a known high resolution crystal structure.

GPCR	Elucidation Date
Rhodopsin[158]	2000
β_2-adrenergic receptor[163]	2007
Adenosine $A2_A$ receptor[164]	2008
β_1-adrenergic receptor[165]	2008
C-X-C chemokine receptor type 4[166]	2010
Dopamine D3 receptor[167]	2010
Histamine H1 receptor[168]	2011
δ-opioid receptor[169]	2012
κ-opioid receptor [170]	2012
μ-opioid receptor[171]	2012
Muscarinic acetylcholine receptor M2[172]	2012
Muscarinic acetylcholine receptor M3[173]	2012
Neurotensin receptor 1[174]	2012
Nociceptin/orphanin FQ receptor[175]	2012
Protease-activated receptor 1[176]	2012
Sphingosine-1-phosphate receptor 1[177]	2012

GPCR	Elucidation Date
5-hydroxytryptamine receptor 1B[178]	2013
5-hydroxytryptamine receptor 2B[179]	2013
C-C chemokine receptor type 5[180]	2013
Corticotropin-releasing factor 1 receptor[181]	2013
Glucagon receptor[182]	2013
Smoothened receptor[183]	2013
Metabotropic glutamate receptor 1[184]	2014
Purinergic $P2Y_{12}$[185]	2014
Angiotensin II type 1 receptor[186]	2015

Several obstacles complicate GPCRs crystallization. First, GPCRs have low endogenous expression levels, which makes heterologous expression essential for the production of large quantities of receptor. Furthermore, these flexible proteins must be isolated from the plasma membrane in a functional and biochemically stable form. Once stable crystallization is achieved, diffraction properties must be optimized in order to produce a high quality structure of the receptor. However, recent acceleration in the publication of GPCR crystal structures demonstrates that here has been some progress in the field[187].

1.6.5 Summary

Functional complementation was one of the earliest techniques used to characterize GPCR oligomers. While this approach is credited with stimulating interest in the field of GPCR oligomerization, it has only provided indirect evidence of this phenomenon. More recent studies have turned to biochemical and biophysical methods, which have provided direct evidence of receptor-receptor interactions. These techniques have led to the widespread acceptance of GPCR oligomerization; however, there are some caveats to consider when using these approaches. Adequate controls and, sometimes, a combination of different methods are required to ensure experimental reliability. This additional burden, coupled with the ongoing challenges associated with receptor crystallization, has led to a broad push for the development of computational techniques that can be used to model GPCRs.

1.7 Computational Techniques Used to Model GPCRs

Given the technical challenges associated with elucidation of tertiary and quaternary GPCR structure[187], there has been a growing push towards computational modelling of GPCRs[188]. The GPCR Online Modeling and Docking server (GOMoDo) was developed by Sandal *et al.* to address this issue[189]. This web-based program serves as a single, user-friendly interface for GPCR modelling and ligand docking. While there were no novel modelling programs developed specifically for GOMoDo, the server is unique because it is the first web-based platform to incorporate multiple pre-existing bioinformatics tools for GPCR

modelling[189]. Using the GOMoDo interface, non-expert researchers can produce a robust sequence alignment[190-193], compile and assess a series of homology models based on existing GPCR crystal structures[194-197], and perform ligand docking using either blind[198] or information-driven docking[199-201].

The server also incorporates a program known as Volume Area Dihedral Angle Reporter (VADAR), which can be used for quantitative structural analysis of selected GPCR models[202]. This program is particularly helpful as it can be used to predict exposed residues that may be involved in GPCR dimerization. By rolling a virtual hydrogen atom around the exterior of the receptor, an algorithm calculates the accessible surface area (ASA) of each amino acid side chain within the protein. Those with a high ASA are assumed to be highly exposed, and those with a low ASA are assumed to be buried deep within the receptor. Therefore, ASA can be used to predict which amino acids have the highest potential to participate in complex formation.

In order to develop a three-dimensional model of a GPCR using GOMoDo, the user may either select a GPCR sequence from a database that is provided or input an amino acid sequence that was obtained from an external source. Given this information, the server uses a program known as HHsearch to develop a profile-profile comparison[191]. This differs from traditional sequence-sequence alignments because it represents both the query and database sequences as *sequence profiles*. These profiles are derived from an alignment of multiple related sequences, which accounts for the degree of conservation at specific

positions within the protein. This allows for the identification of conserved motifs such as the transmembrane helices that are characteristic of GPCRs. As a result, HHsearch has been identified as one of the most effective protein comparison tools to date[203].

Following analysis with HHsearch[191], a program known as MODELLER is used to produce a comparative model of tertiary receptor structure[194]. GOMoDo provides MODELLER with the alignment that was processed via HHsearch and, given this, the program calculates a three-dimensional model of the GPCR. The model is calculated using a method referred to as the *satisfaction of spatial constraints*[196]. With this method, the location of each atom within the receptor is predicted using a set of geometric criteria. These criteria are derived from a template GPCR with a known tertiary structure. GOMoDo compiles a series of three-dimensional models for the target receptor, with each model being based on experimental data from another GPCR[189]. MODELLER assesses each model using two scoring functions. These functions are known as the discrete optimized protein energy (DOPE) and the GA341 scores.

The DOPE score is a statistical potential based on atomic distance[204]. Scoring parameters are derived from a sample of 1472 existing crystal structures. The DOPE score is particularly useful as it can be used to assess either the entire model or discrete regions of the model. This allows for the identification of problematic regions within the model. Just as native structures have the lowest free energy of all states under native conditions, models that are closest to the

native state, as determined statistically, have lower DOPE scores[204]. Similar to the DOPE score, the GA341 score is a statistical potential that is used to assess model quality[205]. However, unlike the DOPE score, the GA341 score is based on sequence identity between the target and template. A high degree of sequence identity between the model and template results in a higher GA341 score[206].

By plotting the normalized DOPE score for each model as a function of the GA341 score, GOMoDo allows users to select the best template and, therefore, model based on energetics and sequence identity. With successful modelling, there is a relatively loose negative correlation between the normalized DOPE score and the GA341 score. If there appears to be a positive correlation or no correlation at all between these scoring functions, modelling may be deemed unsuccessful. A low normalized DOPE score and high GA341 score is indicative of a high quality model; therefore, when looking at a plot of these scoring functions, the best models can be found at the lower right corner of the Cartesian plane[189].

1.8 The Renin-Angiotensin-Aldosterone System and the Human AT1R

The renin-angiotensin-aldosterone system (RAAS) is an important endocrine axis that has a key role in cardiovascular function. This system differs from most endocrine mediators because the synthesis of its main peptide hormone, Ang II, is extracellular. Through the synthesis of Ang II, the RAAS provides tight regulation of arterial pressure, and it has emerged as an important tool for the treatment of cardiovascular disease[207].

The RAAS begins with the synthesis of an enzyme known as renin in the renal glomerulus. This enzyme is synthesized as a proenzyme or precursor protein, and it is activated by the proteolytic cleavage of 43 N-terminal amino acids. The activated enzyme is stored by juxtaglomerular cells and secreted into circulation in a calculated manner[207]. There are four factors that influence renin secretion. These include renal perfusion pressure, NaCl concentration, stimulation via the sympathetic nervous system, and feedback from Ang II[208]. Regulation of renin secretion is the main regulatory checkpoint of the RAAS[207].

Upon activation and secretion, renin catalyzes the conversion of angiotensinogen to Ang I (Figure 3). Plasma levels of angiotensinogen, which is secreted by the liver, are relatively stable; however, synthesis can be increased in response to glucocorticoids, sex hormones, and Ang II[209]. While increased levels of angiotensinogen are associated with an increased risk of hypertension, there is some evidence to suggest that decreased renin secretion serves as a mechanism to compensate for this. Following the conversion of angiotensinogen to Ang I, an enzyme known as angiotensin converting enzyme (ACE) catalyzes the conversion of Ang I to Ang II. This enzyme is expressed on the surface of vascular endothelial cells, renal proximal tubule cells, and neuroepithelial cells. Aside from catalyzing the synthesis of Ang II, ACE also catalyzes the inactivation of vasodilator molecules such as bradykinin and kallidin. Ultimately, this shifts the balance of vascular tone from vasodilation to vasoconstriction.

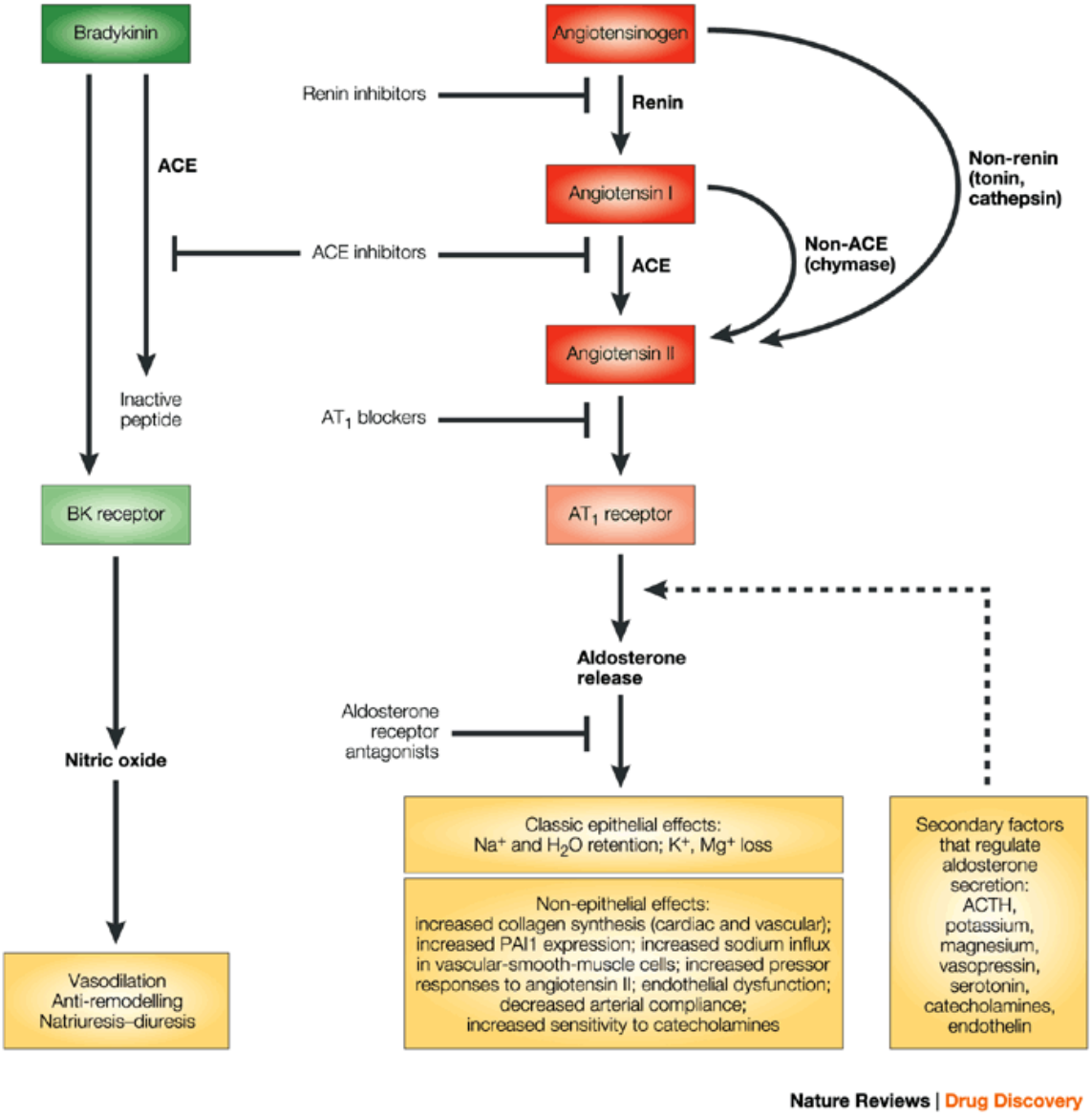

Figure 3 **Overview of the RAAS.** Angiotensinogen is secreted from the liver and converted to Ang II by a series of proteolytic cleavages within the plasma. Ang II serves as the ligand for the AT1R, which promotes vasoconstriction, Na^+/H_2O retention, and an increase in blood pressure. Reprinted by permission from Macmillan Publishers Ltd: Nature Reviews Drug Discovery (Zaman *et al.*, 2002)[210], Copyright © 2015.

Ang II-mediated signalling via the AT1R uses a variety of cellular mechanisms to produce an increase in blood pressure (Figure 4)[210]. The classical effect of Ang II is seen with vascular smooth muscle cells. Here, Ang II-induced AT1R signaling results in intracellular Ca^{2+} release and cellular contraction. Ultimately, this culminates in vasoconstriction. In the kidneys and adrenal glands, Ang II-mediated signaling via the AT1R results in Na^{+}/H_2O retention, which increases blood volume. More recent evidence suggests that Ang II-mediated signaling also has a neurogenic component. In the central nervous system, signalling of the AT1R has been shown to increase cardiac output and water ingestion. All of these phenomena produce an increase in blood pressure and can contribute to cardiovascular disease[210]. Furthermore, studies have shown that Ang II-stimulated AT1R signalling results in both cardiac hypertrophy and vascular stiffness. This provides an explanatory mechanism for cardioprotective effects of AT1R blockade[211].

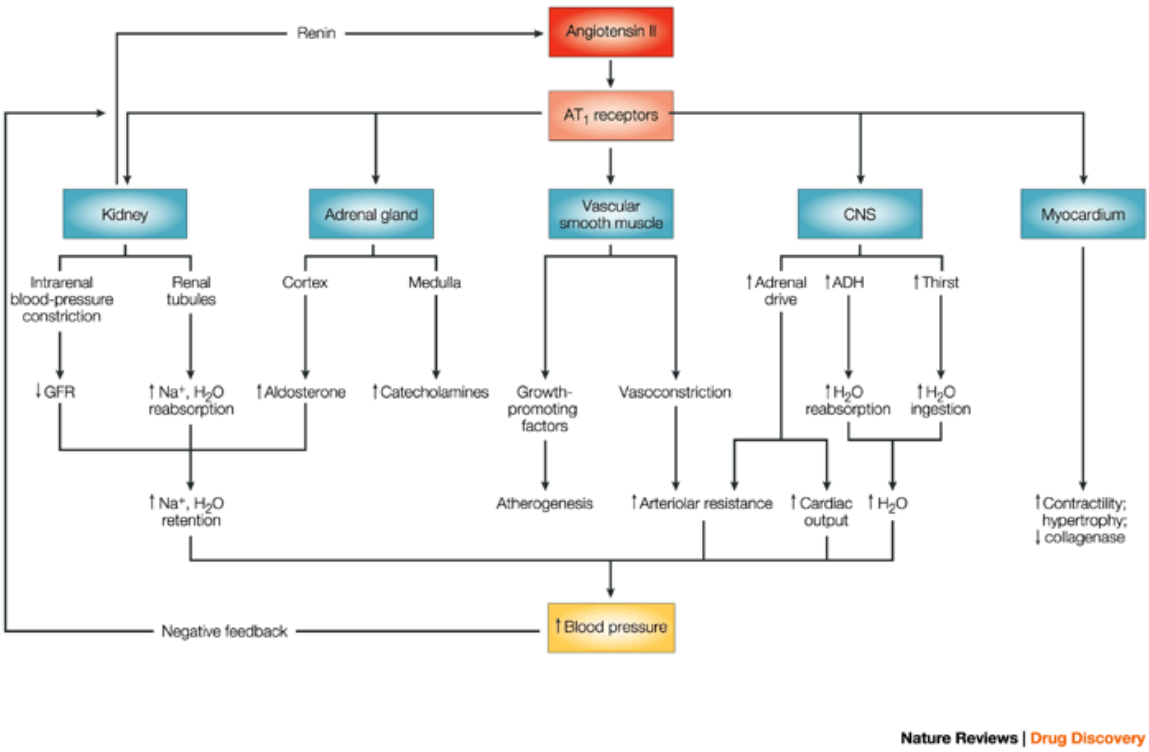

Figure 4 **Overview of the mechanisms by which the AT1R regulates blood pressure.** Upon binding Ang II, the AT1R has various effects that increase blood pressure. Within the vasculature, Ang II promotes vasoconstriction via AT1R. Secondary sites of AT1R expression include the kidney and central nervous system, which contribute to an increase in blood pressure by promoting Na^+/H_2O retention and an increase in cardiac output.. Reprinted by permission from Macmillan Publishers Ltd: Nature Reviews Drug Discovery (Zaman *et al.*, 2002)[210], Copyright © 2015.

1.9 AT1R Structure

Until recently, there has been very little success in elucidating AT1R structure. In fact, the majority of the work presented herein was performed in the absence of a published crystal structure. However, with the advent of a technique known as serial femtosecond crystallography, Zhang *et al.* (2015) have produced a crystal structure of the human AT1R in complex with a selective antagonist known as

ZD7155[186]. These results show that the AT1R has a prototypical GPCR structure consisting of an extracellular N-terminus, three extracellular loops, 7TM α-helices, three intracellular loops, and an intracellular C-terminus[186]. As a class A GPCR, it shares a high level of sequence identity with the chemokine receptors (36% shared with C-X-C chemokine receptor type 4 [CXCR4]) and the opioid receptors (33% shared with the κ-opioid receptor)[166,170]. Looking at the overall fold of the receptor, again, it is highly similar to the chemokine and opioid receptors. In particular, the root-mean-square deviation (RMSD) for 80% of α-carbon atoms within the AT1R crystal structure is 1.8 Å from those of the κ-opioid receptor[186,212]. This signifies that 80% of AT1R α-carbons fall within an average distance of 1.8 Å from those of the κ-opioid receptor.

In terms of structural features that modulate AT1R signaling, Asn111 (TMIII) and Asn295 (TMVII) have been shown to stabilize the inactive state conformation of the receptor via hydrogen bonding. Indeed, binding of Ang II to the WT receptor has been shown to disrupt the interaction between Asn111 and Asn295 to allow Asn295 to interact with Asp74 within TMII. Accordingly, mutation of Asn111 and Asn295 has been shown to result in constitutive activation of the receptor[213,214].

Interestingly, Asp74, Asn111, and Asn295, coupled with Trp253 from the WxP motif and Asn298 from the NPxxY motif, have been identified as a putative sodium binding pocket in the AT1R[215]. This sodium pocket is highly conserved when compared to the crystal structure of the δOR[216]; however, in the AT1R, Asn295 is expressed in lieu of a serine residue[186]. This suggests that the hydrogen

bond between Asn111 and Asn295 may be influenced by sodium binding, resulting in a destabilization of the inactive state. This may provide a structural mechanism for the increase in blood pressure that is associated with high dietary sodium intake [217].

1.10 Pharmacological Relevance of AT1R Dimerization

The specific expression of GPCR oligomers in certain tissues or disease states provides an excellent opportunity for drug development. Theoretically, these drugs would be highly selective and have fewer adverse effects when compared to their non-selective counterparts[55]. Looking at the AT1R, this opportunity presents itself with the existence of AT1R - B2R heterodimers. Expression of these complexes is elevated in pre-eclampsia and experimental hypertension, where they increase Ang II sensitivity and promote an increase in blood pressure[85,218]. Selective blockade or disruption of these heterodimers could provide a novel means for treating these diseases. However, there is a lack of structural data that could be used to design drugs selective for these complexes. First, the AT1R homomer interface must be elucidated in order to identify receptor-specific mechanisms of complex formation.

1.11 OBJECTIVES

The objectives of this study were two-fold and can be summarized as follows:

1. Develop a three-dimensional model of the AT1R to identify amino acids that are potential contributors to receptor homomerization.

2. Use site-directed mutagenesis to characterize specific combinations of these amino acids in terms of their effect on receptor-receptor affinity.

CHAPTER 2 MATERIALS AND METHODS

2.1 REAGENTS

Reagents were obtained as follows: Human AT1R cDNA was obtained from OriGene Technologies (Rockville, MD, USA). The pcDNA 3.1(+) mammalian expression vector, heat inactivated fetal bovine serum (FBS) and penicillin-streptomycin (PS) were purchased from Life Technologies, Inc. (Burlington, ON, Canada). Polyethylenimine (PEI) was purchased from Polysciences, Inc. (Warrington, PA, USA), and coelenterazine-400a was purchased from Cedarlane Labs (Burlington, ON, Canada). Phusion® High-Fidelity PCR Kit, T4 DNA Ligase Kit, and all restriction endonucleases were obtained from New England BioLabs® Inc. (Ipswich, MA, USA). Dulbecco's Modified Eagle's Medium (DMEM), Angiotensin II human, and all other chemicals were purchased from Sigma-Aldrich Canada (Oakville, ON, Canada) unless otherwise noted.

2.2 IDENTIFICATION OF CANDIDATES FOR MUTAGENESIS

GOMoDo was the primary interface used to perform all modelling and analysis of the AT1R[189]. A FASTA formatted amino acid sequence was obtained from the UniProt database for the human AT1R[219]. This sequence was used as an input for GOMoDo. After performing two rounds of sequence alignment using BLAST[192], PSI-PRED was used to add secondary structure information to the alignment via GOMoDo[193]. GOMoDo developed a hidden Markov model (HMM) using HHmake, and suitable templates for modelling were selected from a database of

GPCR HMMs using HHsearch[190,191]. MODELLER was used to develop three-dimensional homology models of the AT1R without loop refinement. The GOMoDo output included a list of all models and respective scoring data obtained from MODELLER[194]. The best model was chosen based on the lowest normalized DOPE score and highest GA341 score[189].

VADAR was used to assess this model by producing a Ramachandran plot and calculating fractional ASA[202]. The Ramachandran plot was used to validate the selected model, and fractional ASA data was used to determine which amino acids were exposed to the phospholipid bilayer. Fractional ASA is similar to absolute ASA; however, this value represents the absolute ASA of an amino acid divided by the ASA of the same amino acid surrounded by two glycine residues[202]. This accounts for size variations that exist between amino acids. Visual inspection of the model was used to identify the fractional ASA at which amino acids were exposed to the phospholipid environment. While there is no theoretical fractional ASA value that distinguishes between buried and exposed residues[220], visual inspection determined that a fractional ASA of 0.3 was a suitable threshold to systematically identify amino acids that were exposed to the membrane. Amino acid groups with a fractional ASA greater than 0.3 and a similar orientation with respect to one another were selected as candidates for mutagenesis. Amino acid candidates were only selected for mutagenesis if they were found in the TM region, which was defined by UniProt[219].

2.3 Cloning and Site-Directed Mutagenesis

The stop codon was removed from the AT1R cDNA construct (Origene Technologies) using a Phusion® High-Fidelity PCR Kit (New England Biolabs® Inc.). As an addition to the EcoRI cut site that was present upstream of the AT1R gene, an XhoI cut site was inserted downstream of the AT1R gene using polymerase chain reaction (PCR). The receptor was subcloned into the EcoRI-XhoI cut sites of a pcDNA 3.1(+) (Life Technologies) mammalian expression vector using T4 DNA Ligase (New England BioLabs® Inc.). The recombinant DNA was used as a template for mutagenesis. Mutants were developed using the QuikChange™ site-directed mutagenesis method that was designed by Stratagene (La Jolla, CA, USA). This protocol was modified to allow for the use of Phusion® High-Fidelity DNA Polymerase, which is manufactured by New England BioLabs® Inc.. Components of the reaction are outlined in Table 5, and reaction conditions are summarized in Table 6.

Table 5 Composition of mutagenesis reactions that were performed according to the Stratagene QuikChange™ mutagenesis protocol.

Components	Volume	Final Concentration
5X GC Buffer	10.0 µl	1X
10 mM dNTP Mixture	1.0 µl	200 µM each
Primer Mix (10 µM each)	2.5 µl	0.5 µM each
DMSO (100%)	1.5 µl	3%
WT AT1R pcDNA 3.1(+) (10 ng/µl)	5.0 µl	1.0 ng/µl
Phusion® High Fidelity DNA Polymerase	0.5 µl	1.0 unit
Double Processed Tissue Culture Water	29.5 µl	n/a

Table 6 Outline of reaction conditions that were used during site-directed mutagenesis with Phusion® High-Fidelity DNA Polymerase.

Step	Temperature	Time	Cycle Count
Initial Denaturation	98 °C	30 sec	1
Denaturation	98 °C	10 sec	35
Annealing	Variable	30 sec	
Extension	72 °C	3.75 min	
Final Extension	72 °C	10 min	1
Hold	4 °C	∞	1

Forward and reverse oligonucleotide primers were designed for three mutant receptors (C76S AT1R; L154,158A AT1R; L202,F206,I210A AT1R) using the online QuikChange™ Primer Design software that is provided by Agilent

Technologies (http://www.genomics.agilent.com/primerDesignProgram.jsp). The annealing temperature was determined for each pair of oligonucleotides using a web-based melting temperature (Tm) calculator designed by Thermo Fisher Scientific (http://www.thermoscientificbio.com/webtools/tmc). Successful mutagenesis was confirmed using the automated DNA sequencing service that is offered by Genewiz, Inc. (South Plainfield, NJ, USA). Receptors containing the desired amino acid substitutions were tagged with either GFP10 or Rluc2 at the C-terminal domain between the XhoI-XbaI cut sites. Four additional mutant receptors (I150,L154A AT1R; I151,L155,158A AT1R; L247,F251,I258A AT1R; I286,F293,L297A AT1R) were synthesized by Genewiz (South Plainfield, NJ), and tagged with either GFP10 or Rluc2 at the C-terminus as described above.

2.4 Cell Culture and Transfection

Human embryonic kidney (HEK) 293A cells were cultured in Dulbecco's Modified Eagle's Medium (DMEM) that was supplemented with 10 % (v/v) fetal bovine serum and 1% penicillin streptomycin. Cells were seeded in 6-well plates and incubated at 37 °C in a humidified environment of 5% CO_2. After 24 hours, when each culture reached approximately 75% confluence, the cells were subjected to polyethylenimine (PEI)-induced transfection. Transfection solutions were prepared such that there was a 3:1 ratio of PEI:DNA in each well. The transfection solution was removed after 24 hours and replaced with DMEM that was supplemented as described above. Following an additional 24 hour

incubation period, the supplemented medium was replaced with minimal DMEM. A 24 hour starvation period was completed in the presence of this minimal medium. All experiments were performed 72 hours post-transfection.

2.5 Receptor Expression

Cells were divided among the wells of a 6-well plate, and transfected with 1.0 μg of a specific AT1R-GFP10 construct. Following transfection, each well was harvested with 1 mL PBS (1X) and subjected to centrifugation (2.35×10^3 g). The resulting cell pellets were resuspended with 90 μL PBS (1X) and transferred to a 96-well plate. Overall receptor expression was quantified using fluorescence spectroscopy. The PerkinElmer EnVision 2104 Multilabel Reader was used to quantify GFP10 fluorescence (RFU) with an excitation filter set at 410 nm, and an emission filter set at 515 nm. Wallac EnVision Manager software was used to process the data output. These values were analyzed using GraphPad Prism.

2.6 Dose-Response Experiments

Ang II-induced β-arrestin1-*R*luc2 recruitment to each mutant and WT AT1R-GFP10 construct was examined using a dose-response experiment. Recruitment was quantified using BRET^2 at a fixed acceptor/donor ratio of 6.0. Cells were verified for successful transfection using fluorescence microscopy, and nine doses of human Ang II (Sigma-Aldrich Canada) were diluted using water to yield concentrations that ranged from 0 μM to 1 μM. These solutions were added to the corresponding wells of a 6-well plate, and stimulation took place over a 10 minute

period at 37 °C and 5% CO_2. Cells were harvested with 1 mL ice-cold PBS (1X) and subjected to centrifugation at 2.35 x 10^3 g. The resulting cell pellets were resuspended with 90 µL PBS (1X) and transferred to a 96-well plate. A 10 µL aliquot of coelenterazine 400a (50 µM) was added to each well to yield a final concentration of 5 µM per well. BRET2 was quantified using the PerkinElmer EnVision 2104 Multilabel Reader with emission filters set at 410 nm and 515 nm to observe donor and acceptor emission, respectively. Wallac EnVision Manager software was used to process BRET2 ratios (acceptor emission : donor emission). These values were analyzed using GraphPad Prism.

2.7 BRET^2 SATURATION EXPERIMENTS

BRET2 saturation experiments were performed using a recombinant human AT1R that was tagged with either a C-terminal GFP10 or a C-terminal Rluc2. The amount of transfected AT1R-Rluc2 (donor) was held constant at 1.00 µg/well while the amount of transfected AT1R-GFP2 (acceptor) ranged from 0.25 µg/well to 5.00 µg/well in a six-well plate. The cells were verified for successful transfection using fluorescence microscopy and harvested with 1 mL PBS (1X). Following centrifugation (2.35 x 10^3 g), cell pellets were resuspended with 90 µL PBS (1X) and transferred to a 96-well plate. A 10 µL aliquot of coelenterazine 400a (50 µM) was added to each well to yield a final concentration of 5 µM per well. BRET2 was quantified using the PerkinElmer EnVision 2104 Multilabel Reader with emission filters set at 410 nm and 515 nm to observe donor and acceptor emission, respectively. Wallac EnVision Manager software was used to

process BRET2 ratios (acceptor emission : donor emission). These values were analyzed using GraphPad Prism.

CHAPTER 3 RESULTS

3.1 A WORKING MODEL OF THE AT1R

The FASTA sequence for the AT1R was obtained from the UniProt database (UniProt ID: P30556)[219]. This sequence was entered into GOMoDo[189], and a series of 46 models were generated based on 23 GPCR templates. These models were assessed based on normalized DOPE[204] and GA341[205] scores. A low normalized DOPE score and high GA341 score is indicative of a high quality model. With a normalized DOPE score of 0.032 and a GA341 score of 0.929, the δ-opioid receptor (δOR; PDB ID: 4N6H)[216] was selected as the best template for AT1R modelling (Figure 5).

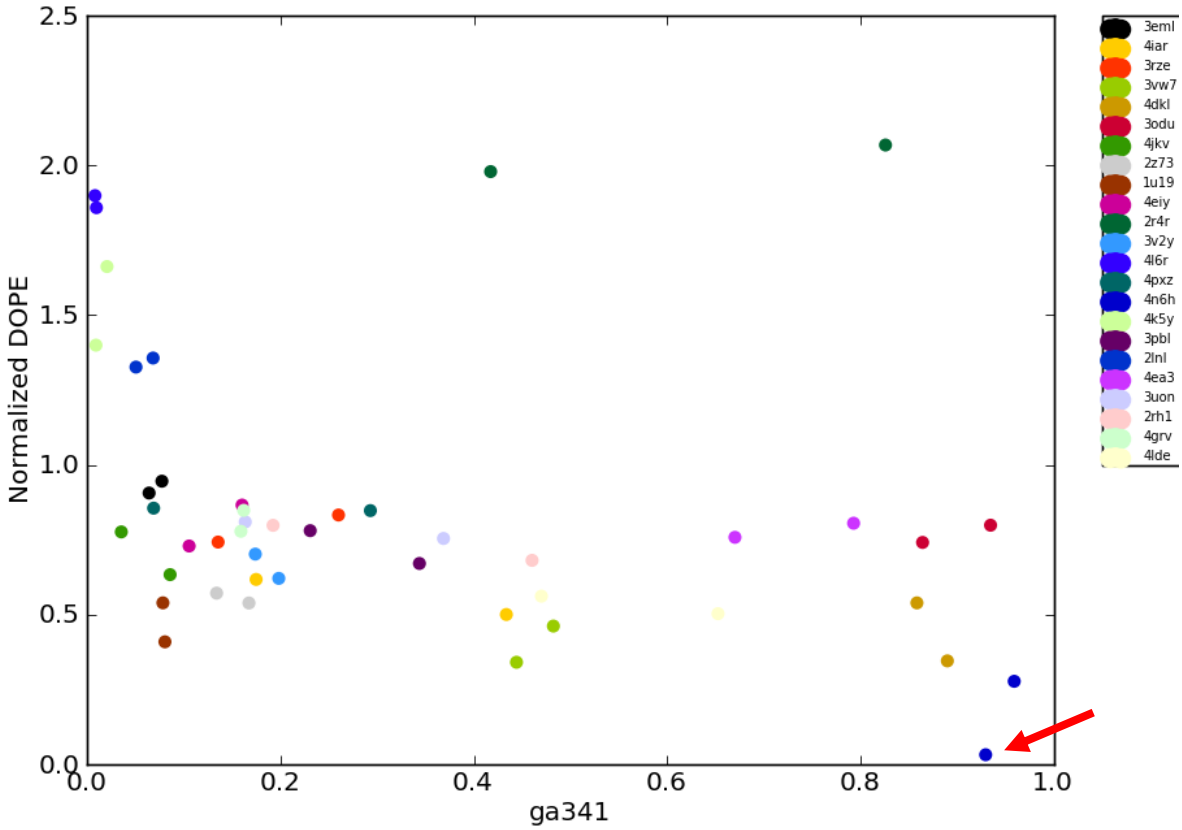

Figure 5 **Normalized DOPE score plotted as a function of the GA341 score for various models of the AT1R.** The side panel identifies each model by Protein Data Bank codes for the various GPCR templates used. Scores represent the quality of each model based on 1 of 23 GPCR templates with known structures. A low normalized DOPE score and a high GA341 score is indicative of a high quality model. The δOR (denoted by an arrow; PDB ID: 4N6H) was selected as the best template for modelling the AT1R. The model developed using this template received a normalized DOPE score of 0.032 and a GA341 score of 0.929. This graph was generated using GOMoDo.[189]

The PyMOL Molecular Graphics System (Version 1.7.6) was used to produce a visualization of the selected model (Figure 6A). A simple visual inspection shows an N-terminus, seven α-helical domains separated by six loops, and a C-terminus. These structural features are typical of a GPCR. *A R*amachandran plot

was *developed to supplement this data with a quantitative measure* (Figure 6B). Looking at the plot, there is a dense cluster of amino acids with ϕ angles of approximately -75° and ψ angles of approximately -25°. This backbone geometry is typical of α-helices, which are the distinguishing features of a GPCR. Very few amino acids were disallowed based on backbone geometry, suggesting that a suitable model was produced.

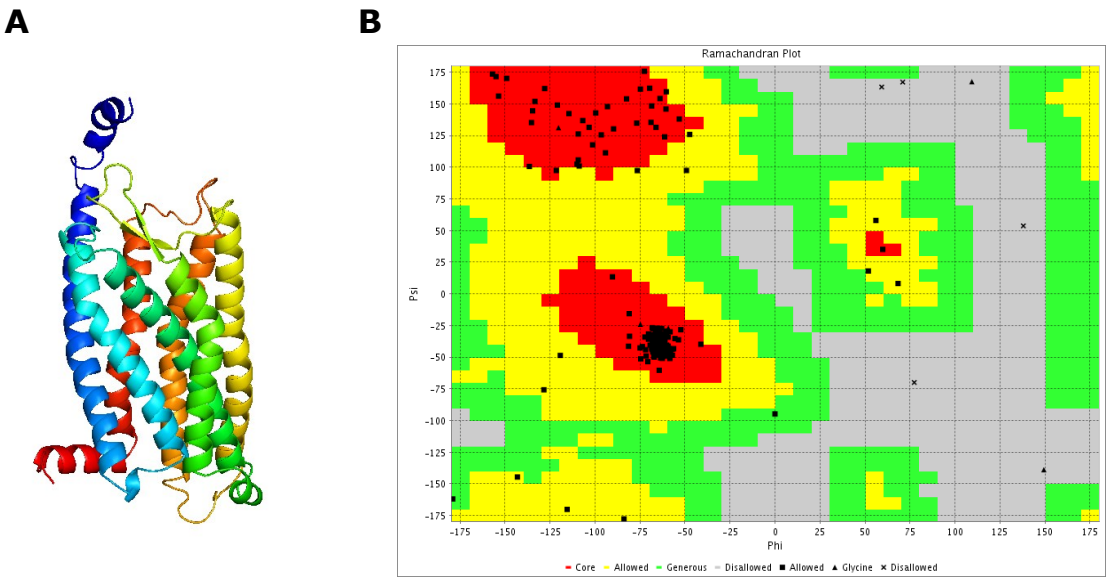

Figure 6 **A model of the AT1R was successfully developed using GOMoDo.** (A) Pymol was used to produce a visualization of the AT1R using PDB coordinates obtained from GOMoDo. GOMoDo produced this model using MODELLER, with the δORselected as a template. (B) A Ramachandran plot provides a graphical representation of the backbone dihedral angles for amino acid residues found in this model of the AT1R. The pattern depicted in this graph is typical of GPCRs. Most amino acids in the model have backbone dihedral angles that are found in α-helices while some have backbone dihedral angles that are typical of β-sheets. Very few amino acids were disallowed based on the geometry of their backbone.

3.2 Candidates Selected for Mutagenesis

In the absence of a crystal structure, TMs were defined using the UniProt database[219]. These domains were classified as follows: TMI (F28-V52); TMII (V65-Y87); TMIII (I103-I124); TMIV (L143-P162); TMV (I193-S214); TMVI (I241-L262); TMVII (I276-C296). VADAR was used to quantify the fractional ASA of amino acids within these regions. The visual representation of the model was inspected, and it was noted that amino acids that were exposed to the phospholipid environment generally had a fractional ASA greater than 0.3. Therefore, all amino acids with a fractional ASA greater than 0.3 were identified as candidates for mutagenesis. Those amino acids that were selected for mutagenesis either had the potential to form a covalent linkage or were highly hydrophobic.

3.2.1 Candidates in TMI

While 48% of the amino acids found in TMI have a fractional ASA greater than 0.3, none of these candidates were selected for mutagenesis. This decision was guided by data found in the literature that suggests other TMs have a more prominent role in class A GPCR dimerization[166,171,221]. Nonetheless, these candidates ought not to be ruled out as potential participants in homomer formation and have been noted for future studies. The fractional ASA for amino acids located in this region can be found in Figure 7A. Likewise, a visual representation confirming the exposure of these amino acids can be found in Figure 7B.

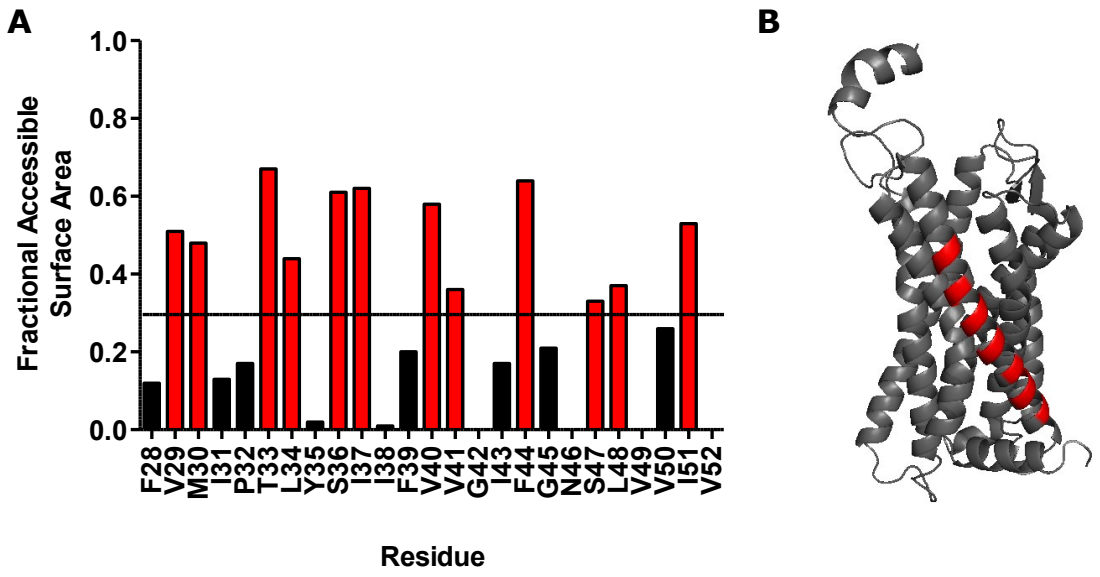

Figure 7 **TMI is highly exposed to the phospholipid bilayer, with 48% of amino acids in this region having a fractional ASA greater than 0.3.** (A) A bar graph summarizing the fractional ASA of amino acids found in TMI. Twelve of these amino acids have a factional ASA higher than 0.3 (red bars). (B) Visualization of these amino acids (red) confirms their exposure to the phospholipid environment.

3.2.2 Candidates in TMII

In terms of fractional ASA, amino acids found in TMII enjoy relatively low exposure to the phospholipid bilayer. Only 22% of amino acids found in TMII have a fractional ASA greater than 0.3 (Figure 8A). Given this, and the very few studies that have implicated TMII in dimerization[171], it was not the main focus of this study. However, there was an exposed cysteine found at position 76 with TMII. This residue was targeted for mutagenesis because of its potential to stabilize AT1R-AT1R interactions via disulphide bond formation. A visualization of C76 along with other exposed residues located in TMII can be found in Figure 8B. While L79 has a fractional ASA greater than 0.3, it was not considered to be a

candidate for mutagenesis because it is not exposed to the membrane environment in the visual representation of the model.

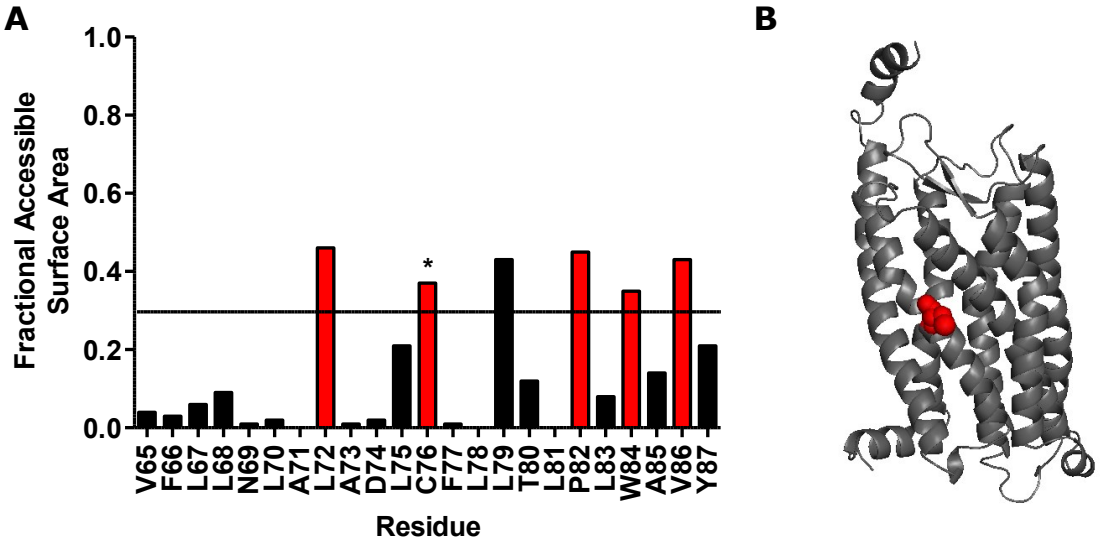

Figure 8 **Amino acids in TMII have little exposure to the phospholipid bilayer as only 22% of these residues have a fractional ASA greater than 0.3.** (A) A bar graph summarizing the fractional ASA of amino acids found within TMII. Amino acids with a fractional ASA higher than 0.3 are highlighted by red bars. The amino acid that was selected for mutagenesis (C76) is denoted by an asterisk. (B) A visual depiction of the model highlights this candidate as red spheres.

3.2.3 Candidates in TMIII

TMIII has the highest buried surface area among all TMs. Only 9% of amino acids in this region have a fractional ASA that exceeds 0.3. Figure 9A provides a graphical representation of the fractional ASA of amino acids located in TMIII. Visualization of the receptor (Figure 9B) shows that only two exposed residues are found in TMIII and, due to the conformation of this domain, these amino

acids have two distinct orientations. The first, I103, is oriented in the direction of TMII, and the second, I124, is oriented in the direction of TMIV and V. Despite being implicated in dimerization of CXCR4[166], TMIII was not the focus of this study given its relatively low exposure to the phospholipid bilayer.

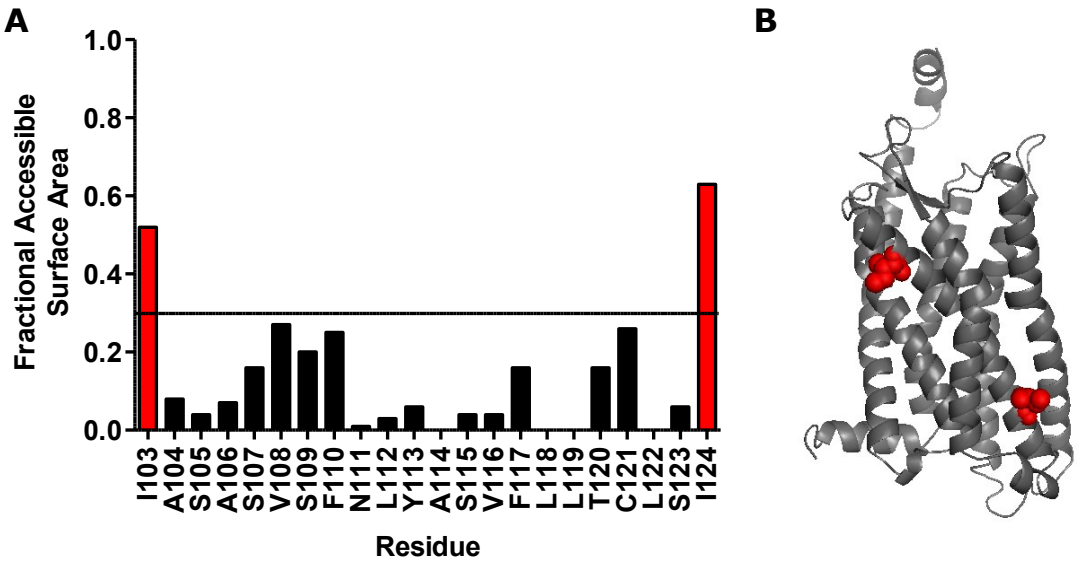

Figure 9 **TMIII has the highest buried surface area of all AT1R TM domains.** (A) Graphical representation of fractional ASA for all amino acids found in TMIII. Amino acids with a fractional ASA that exceeds 0.3 are labelled red. (B) A visual representation of the AT1R shows only two amino acids with an fractional ASA greater than 0.3.

3.2.4 Candidates in TMIV

TMIV is one of the most noteworthy regions of the AT1R when it comes to dimerization. While there is a lack of direct evidence to guide studies surrounding AT1R dimerization, a molecular dynamics simulation of the δOR has suggested that TMIV plays an integral role in this phenomenon[221]. Given the structural

similarities that have led to the use of the δOR as a template for AT1R modelling, we focused on this region for mutagenesis. As shown in Figure 10A, 60% of the amino acids found in TMIV have an accessible surface area that exceeds 0.3. Three combinations of five amino acids in this domain were selected for mutagenesis. Combination selection was based on the orientation of each amino acid side chain in respect to one another. This approach was used to characterize the exact nature of the potential interface at TMIV as it has been proposed that this region acts as a "hinge" in δOR dimers[221].

Looking at a visual representation of the model (Figure 10B), there are two possible orientations that the amino acids within TMIV can face. The first is in the direction of TMIII (green), and the second is in the direction of TMV (blue). An isoleucine at position 150 and a leucine at position 154 were selected to represent the TMIII orientation (Figure 10C), while an isoleucine at position 151 and two leucine residues at positions 155 and 158 were chosen to represent the TMV orientation (Figure 10D). One mutant construct was designed to incorporate an amino acid from each orientation. A leucine at position 154 was selected to represent the TMV orientation, and another at position 158 was selected to represent the TMIII orientation (Figure 10E).

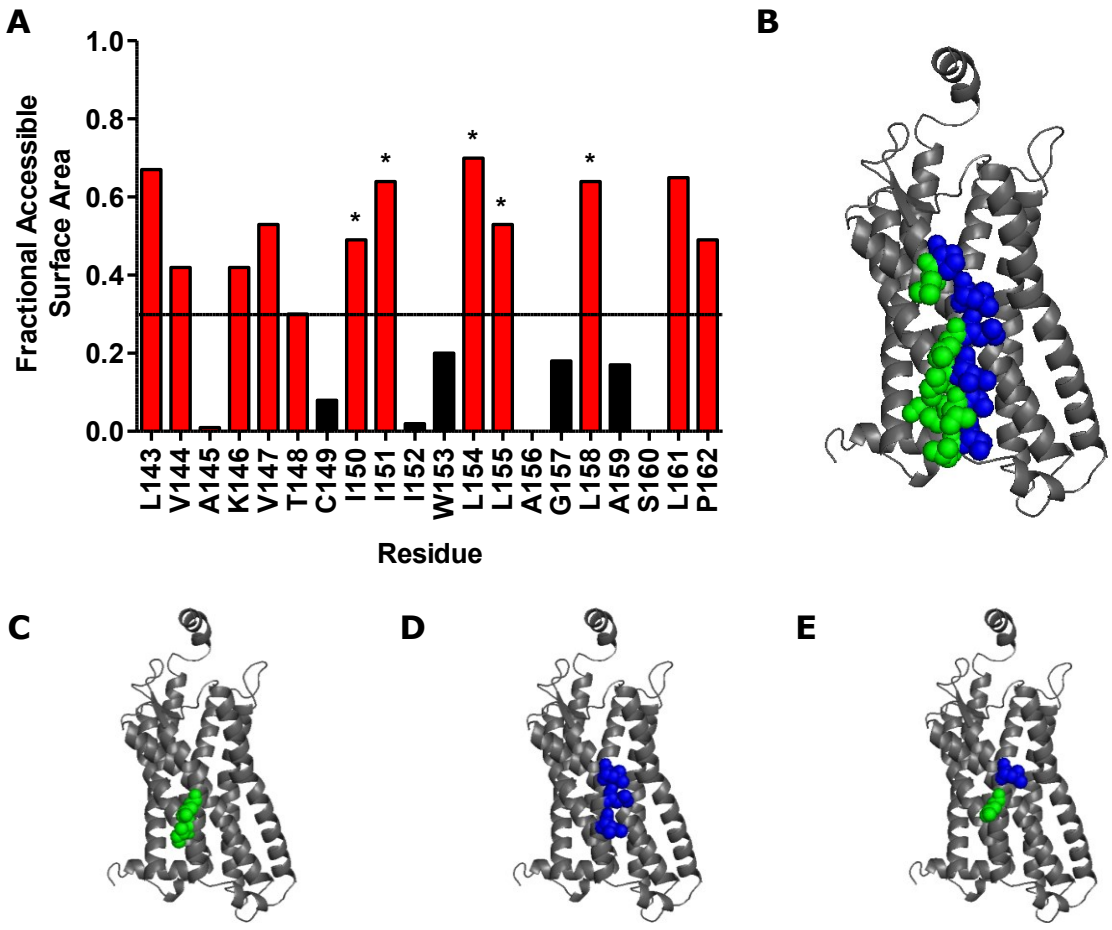

Figure 10 **TMIV is highly accessible to the phospholipid environment, with 60% of amino acids in this region exceeding a fractional ASA of 0.3.** (A) Bar graph summarizing the fractional ASA of amino acids found within TMIV. Amino acids with a fractional ASA greater than 0.3 are identified by red bars, and those that were selected for mutagenesis are denoted by an asterisk. (B) Visualization of amino acids with a fractional ASA greater than 0.3. Amino acids that were considered to be oriented towards TMIII are labelled green, and those that were considered to be oriented towards TMV are labelled blue. (C) A combination consisting of I150 and L154 were selected to represent the TMIII orientation (green). (D) A combination comprised of I151, L155, and L158 were selected to represent the TMV orientation (blue). (E) A final combination of L154 (blue) and L158 (green) was selected to represent the TMIII and V orientations simultaneously.

3.2.5 Candidates in TMV

Similar to TMIV, a molecular dynamics simulation has suggested that TMV may participate in dimerization of the δ-opioid receptor[221]. Furthermore, TMV has been shown to provide an interaction interface for dimers of the β1AR[222], the M3R[146], and CXCR4[166]. Accordingly, TMV was selected as an area of interest for mutagenesis. Looking at amino acid exposure to in this region, 59% were shown to have a fractional ASA greater than 0.3 (Figure 11A). Three of these amino acids were selected for mutagenesis based on their hydrophobicity and their deep location within the TM. These include L202, F206, and I210. A visual representation of these amino acids can be found in Figure 11B.

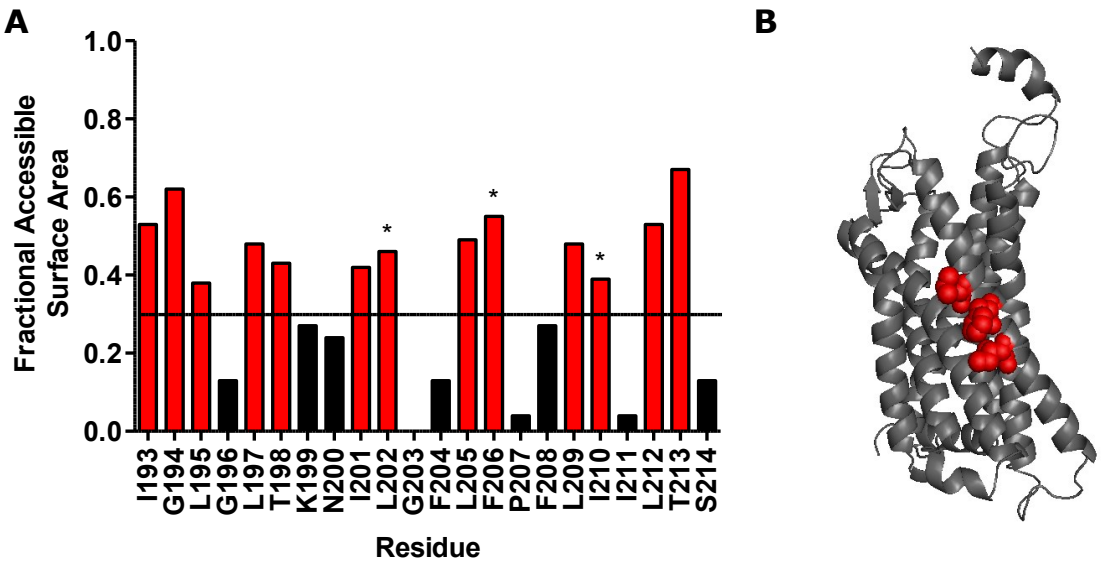

Figure 11 **TMV is another region with high exposure to the phospholipid environment.** (A) A bar graph shows that, of the 22 amino acids found in this TM, 13 have a fractional ASA that exceeds 0.3. Amino acids with a fractional ASA greater than 0.3 are identified by red bars, and those that were selected for mutagenesis are denoted by an asterisk. (B) L202, F206, and I210, which were selected for mutagenesis, are depicted as red spheres in this visual representation of the AT1R.

3.2.6 Candidates in TMVI

TMVI has been shown to form an asymmetrical interface with TMV in a dimeric crystal structure of the μ-opioid receptor (μOR)[171]. For this reason, it was not ruled out as a potential interaction interface among AT1R homomers. Among the 22 amino acids that make up TMVI, 27% have a fractional ASA greater than 0.3. These values are summarized in Figure 12A. While a threonine at position 260 was shown to have a fractional ASA that exceeds the 0.3 threshold, visual inspection of the model determined that this amino acid was oriented towards the interior of the TM bundle. Therefore, it was not deemed to be a suitable

candidate for mutagenesis. Three amino acids were selected for mutagenesis given their location deep within the TM and their symmetry with a series of hydrophobic amino acids within TMVII. These amino acids include L247, F251, and I258, which are visualized in Figure 12B.

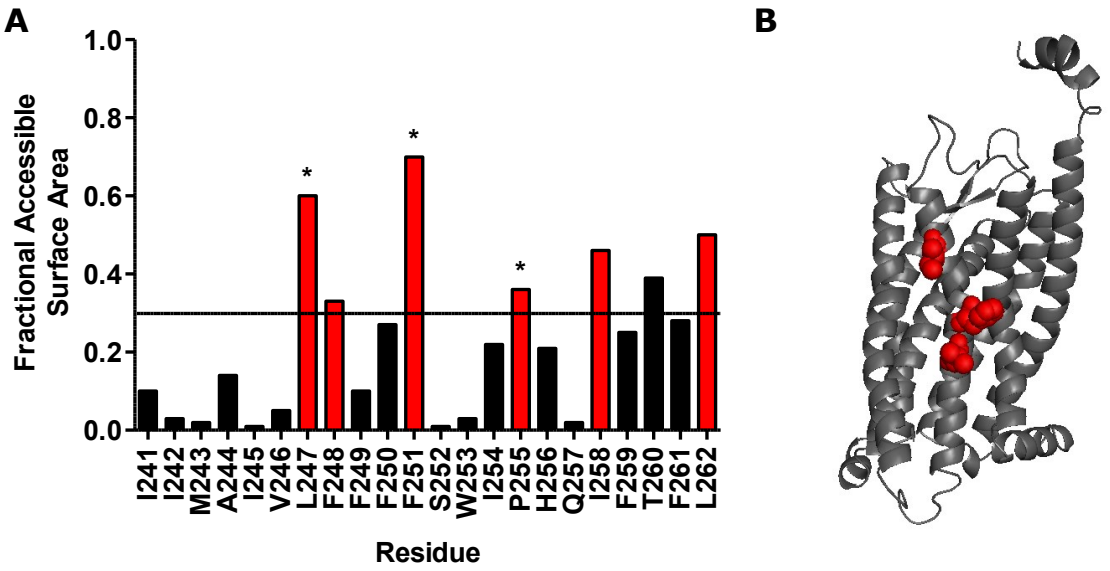

Figure 12 Approximately 27% of amino acids in TMVI are exposed to the phospholipid bilayer. (A) Fractional ASA values for each amino acid found in TMVI are plotted in this bar graph. Those amino acids with a fractional ASA greater than 0.3 are identified by a red bar. Amino acids that were selected for mutagenesis are denoted by an asterisk. (B) A visualization of the AT1R shows the amino acids in TMVI that were selected for mutagenesis (red spheres). These amino acids are L247, F251, and I258.

3.2.7 Candidates in TMVII

A third of all amino acids found in TMVII have a fractional ASA larger than 0.3. A summary of these values can be found in the bar graph in Figure 13A. While L297 does not reside within TMVII as defined by UniProt, it does belong to TMIV

according to the visual representation of the model (Figure 13B). Given this information, and the symmetrical location of L247 (TMVI) and L297 (TMVII), this amino acid was selected for mutagenesis. In addition, I286 and F293 were selected for mutagenesis given the symmetry observed between these hydrophobic amino acids and those found in TMVI.

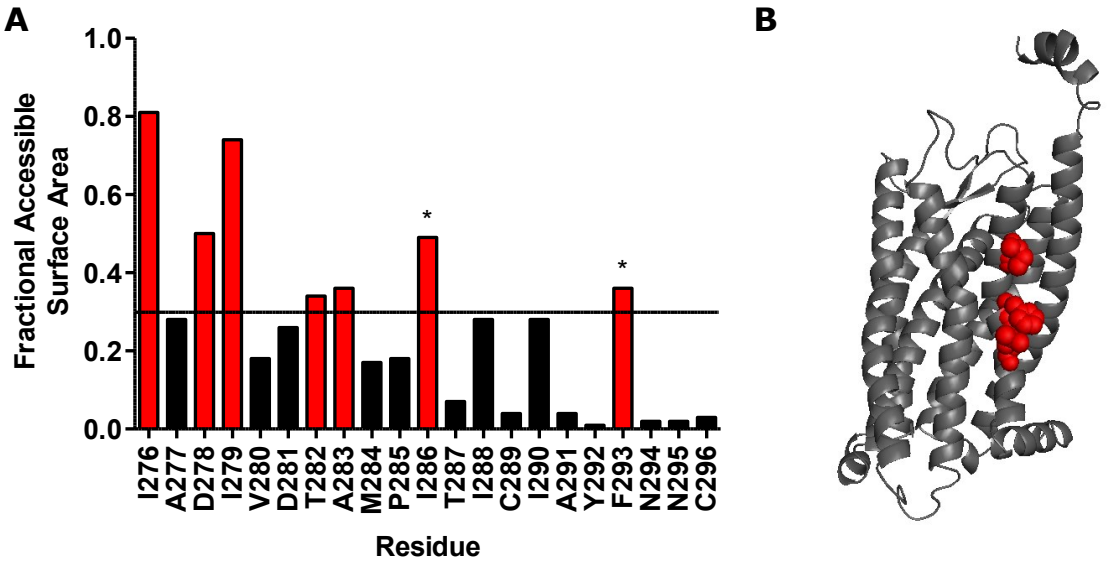

Figure 13 **A third of the amino acids in TMVII have a fractional ASA that exceeds the threshold of 0.3.** (A) A graphical representation of these amino acids and their corresponding fractional ASA values can be found in this bar graph. Amino acids with a fractional ASA larger than 0.3 are noted by red bars, and those that were selected for mutagenesis are denoted by an asterisk. (B) A visual representation of the AT1R recapitulates that I286, F293, and L297 are exposed to the membrane environement

3.2.8 Summary

Various amino acids were selected for mutagenesis based largely on type and fractional ASA. TMs IV and V had the largest percentage of residues with a fractional ASA larger than 0.3, suggesting that these TMs enjoy the most exposure to the phospholipid bilayer. While two amino acids were initially identified as candidates for mutagenesis based on fractional ASA, visual inspection of the model excluded these residues due to their orientation in respect to the phospholipid bilayer. A summary of all amino acids that were selected for mutagenesis can be found in Table 7.

Table 7 Summary of amino acids that were selected for mutagenesis along with their corresponding transmembrane domains

Transmembrane Region	Candidates Selected for Mutagenesis
I	N/A
II	C76S
III	N/A
IV	I150, I151, L154, L155, L158
V	L202, F206, I210
VI	L247, F251, I258
VII	I286, F293, L297

3.3 Receptor Function and Expression

In order to assess the overall expression of each GFP10-tagged AT1R mutant, GFP10 fluorescence was measured (Figure 14). Fluorescence is represented as net relative fluorescence units (RFU), with background fluorescence of the pcDNA control subtracted from each value. There was no significant fluctuation in GFP10 fluorescence when each mutant was compared to the WT receptor ($p > 0.05$; two-tailed, unpaired t-test).

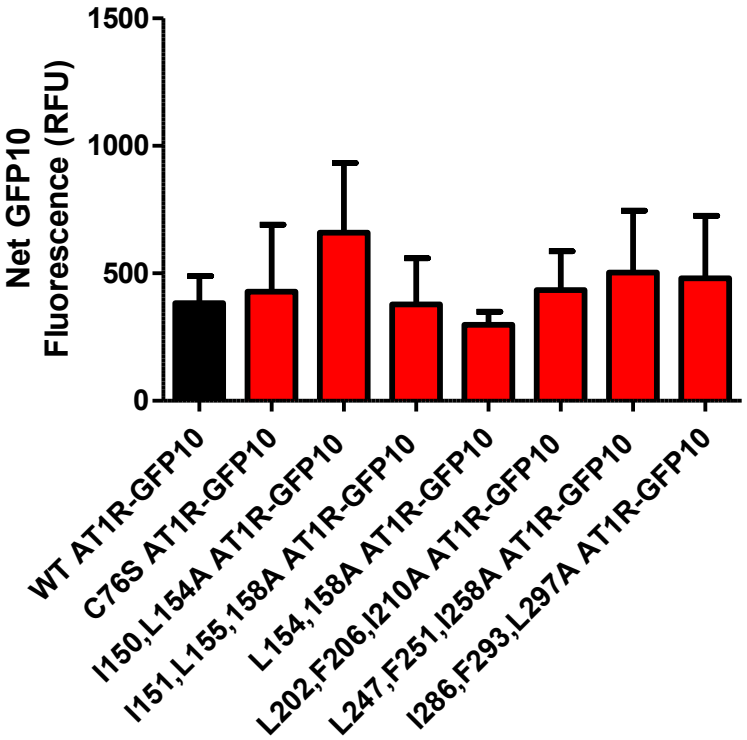

Figure 14 Overall expression is similar among GFP10-tagged receptors. Net GFP10 fluorescence (RFU) does not vary significantly between HEK293A cells expressing the WT AT1R-GFP10 and mutant AT1R-GFP10 constructs (n = 3; $p > 0.05$; two-tailed, unpaired t-test). Net fluorescence is defined as total fluorescence minus fluorescence of the pcDNA control. Data is presented as the mean ± standard error (S.E.).

In addition to receptor expression, it was important to establish whether or not each receptor construct was responsive to Ang II. Responsiveness to Ang II, which is an extracellular ligand, would indicate that the receptor is expressed at the membrane and that it is functional. To determine this, BRET^2 was used to quantify Ang II-induced β-arrestin1-*R*luc2 recruitment to each GPF10-tagged receptor. Interestingly, the dose-response parameters (E_{Min}, $logEC_{50}$, E_{max}) for

each AT1R mutant were identical to that of the WT receptor (Table 8; $p > 0.05$; two-tailed, unpaired t-test). A graphical representation of these results can be found in Figures 15-19.

Table 8 Dose-response parameters suggest that each AT1R mutant is similar to the WT receptor in terms of ability to recruit β-arrestin1. Values are represented as the mean ± S.E. and are each compared to the WT receptor ($n = 3$; $p > 0.05$; two-tailed, unpaired t-test).

Receptor Construct	E_{Min} (% Max)	$logEC_{50}$	E_{Max} (% Max)
WT AT1R-GFP10	79.68 ± 1.81	0.74 ± 0.22	99.99 ± 2.30
C76S AT1R-GFP10	84.47 ± 1.06	0.88 ± 0.17	99.99 ± 1.45
I150,L154A AT1R-GFP10	77.52 ± 1.20	0.48 ± 0.13	99.99 ± 1.30
I151,L154,158A AT1R-GFP10	78.94 ± 1.02	0.91 ± 0.12	100.00 ± 1.41
L154,158A AT1R-GFP10	75.19 ± 1.23	0.92 ± 0.13	100.00 ± 1.80
L202,F206,I210A AT1R-GFP10	79.96 ± 1.25	0.87 ± 0.16	100.00 ± 1.69
L247,F251,I258A AT1R-GFP10	82.82 ± 1.07	0.71 ± 0.15	100.00 ± 1.35
I286,F293,L297A AT1R-GFP10	82.86 ± 1.11	0.81 ± 0.16	100.00 ± 1.46

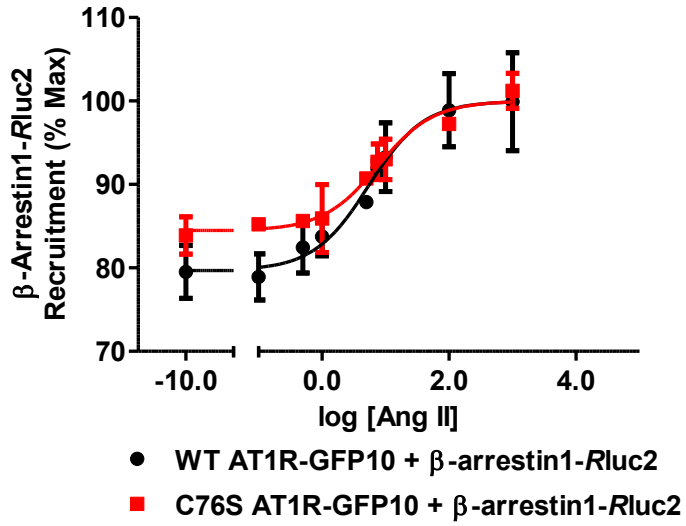

Figure 15 Dose-response profiles suggest that the C76S AT1R-GFP10 construct is similar to the WT receptor in terms of its ability to recruit β-arrestin1. BRET^2 was used to quantify Ang II-induced β-arrestin1-*R*luc2 recruitment to each GFP10-tagged receptor. Recruitment was examined in the presence of nine concentrations of Ang II, which ranged from 0 μM to 1 μM. Values are represented as the mean ± S.E.

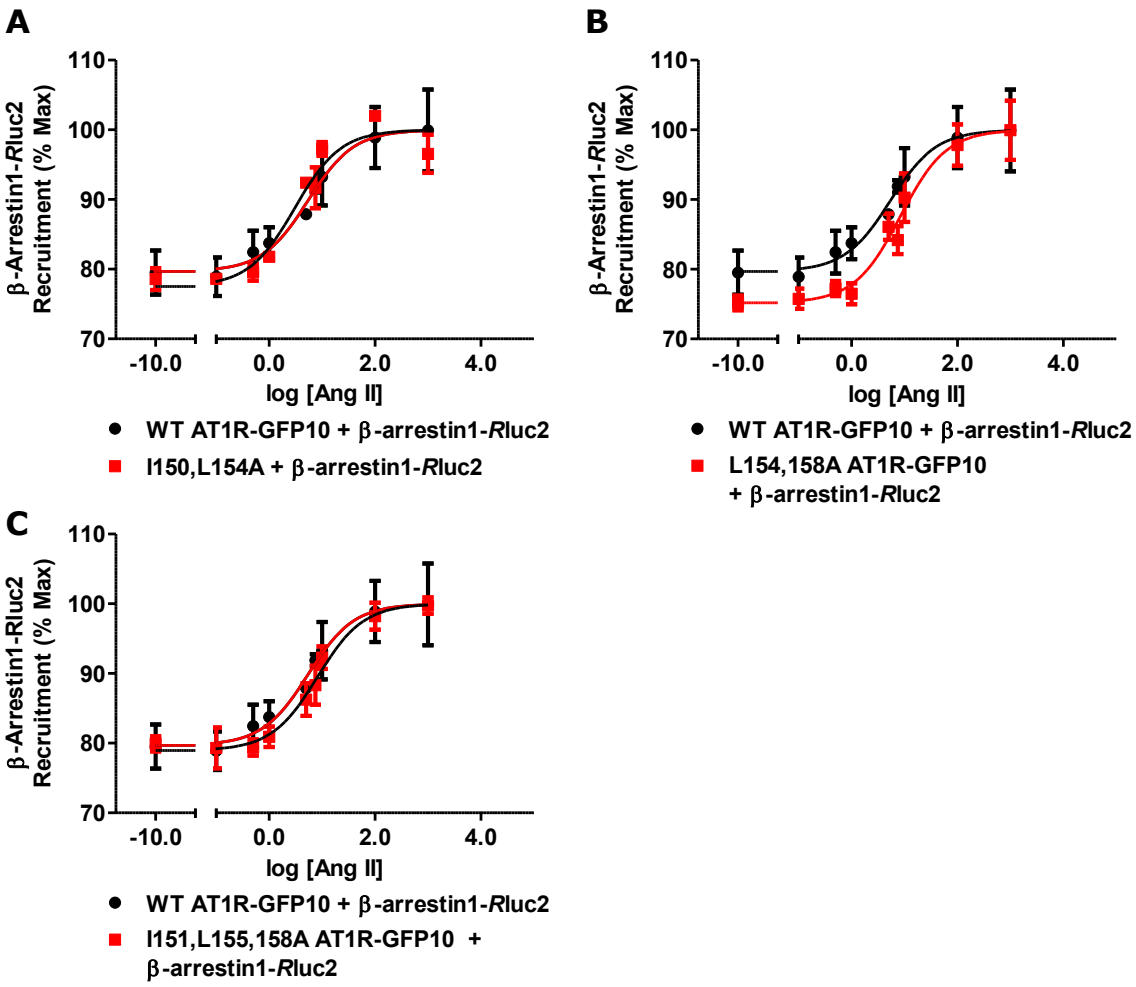

Figure 16 **Dose-response profiles suggest that each combination of mutants in TMIV is similar to the WT receptor in terms of its ability to recruit β-arrestin1.** BRET² was used to quantify Ang II-induced β-arrestin1-*R*luc2 recruitment to each GFP10-tagged receptor. Recruitment was examined in the presence of nine concentrations of Ang II, which ranged from 0 μM to 1 μM. Dose-response profiles were generated for the (A) I150,L154A, (B) L154,158A, and (C) I151,L155,158A AT1R-GFP10 constructs. Values are represented as the mean ± S.E.

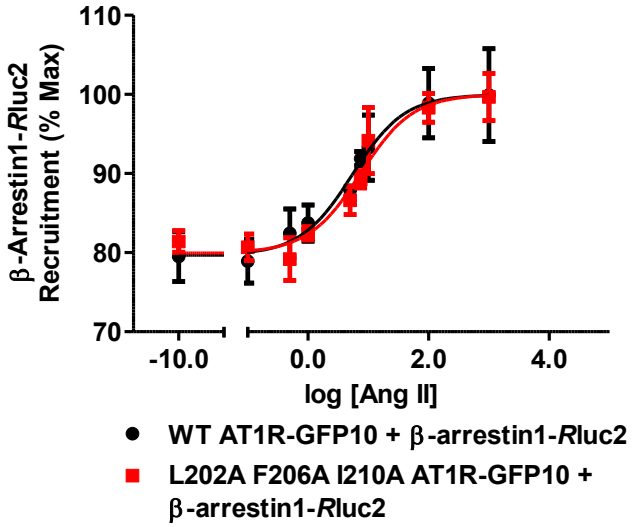

Figure 17 **Dose-response profiles suggest that the L202,F206,I210A AT1R-GFP10 contruct is similar to the WT receptor in terms of its ability to recruit β-arrestin1.** BRET^2 was used to quantify Ang II-induced β-arrestin1-*R*luc2 recruitment to each GFP10-tagged receptor. Recruitment was examined in the presence of nine concentrations of Ang II, which ranged from 0 μM to 1 μM. Values are represented as the mean ± S.E.

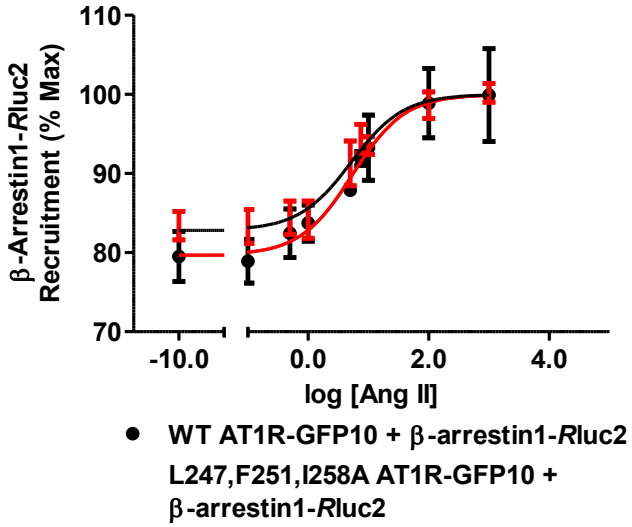

Figure 18 **Dose-response profiles suggest that the L247,F251,I258A AT1R-GFP10 construct is similar to the WT receptor in terms of their ability to recruit β-arrestin1.** BRET^2 was used to quantify Ang II-induced β-arrestin1-*R*luc2 recruitment to each GFP10-tagged receptor. Recruitment was examined in the presence of nine concentrations of Ang II, which ranged from 0 μM to 1 μM. Values are represented as the mean ± S.E.

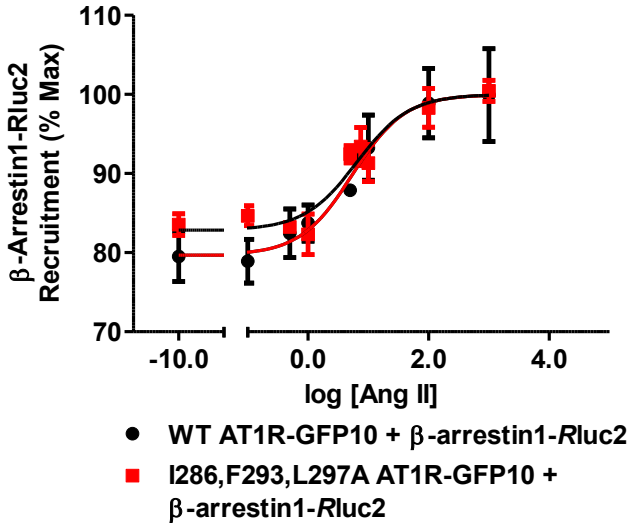

Figure 19 **Dose-response profiles suggest that the I286,F293,L297A AT1R-GFP10 construct is similar to the WT receptor in terms of its ability to recruit β-arrestin1.** BRET² was used to quantify Ang II-induced β-arrestin1-*R*luc2 recruitment to each GFP10-tagged receptor. Recruitment was examined in the presence of nine concentrations of Ang II, which ranged from 0 μM to 1 μM. Values are represented as the mean ± S.E.

3.4 BRET² Saturation Experiments

A series of BRET² saturation experiments were designed in order to quantify the affinity between the WT *R*luc2-tagged receptor and each GFP10-tagged AT1R construct. As described in the Materials and Methods, the level of WT AT1R-*R*luc2 pcDNA was held constant at a transfection rate of 1.00 μg/well in a six-well plate. The level of WT or mutant AT1R-GFP10 increased from 0.25-5.00 μg/well, which yielded 12 acceptor/donor ratios in total. Using GraphPad Prism 5.0, a non-linear regression (one-phase decay) was performed, and the $BRET_{50}$ and $BRET_{Max}$ values were established for each receptor pairing. These two parameters are useful because $BRET_{50}$ is inversely proportional to receptor-receptor affinity,

and $BRET_{Max}$ is representative of the proximity of each tag, which makes it useful in identifying conformational changes that arise as a result of dimerization or mutagenesis.

3.4.1 Mutations in TMII

C76S was the first mutation to be examined in terms of its effect on AT1R homomer formation. Using a $BRET^2$ saturation experiment (Figure 20A), it was shown that titration of either the WT or mutant AT1R-GFP10 construct was sufficient to produce a saturable curve in the presence of the WT AT1R-*R*luc2 construct. Looking at the negative control (i.e. hERG-GFP10 paired with WT AT1R-*R*luc2), a non-saturable trend is observed. This indicates that, unlike the negative control, both the WT and mutant receptor constructs form a specific interaction with WT receptors. Nonetheless, the C76S substitution was shown to have no effect on $BRET_{50}$ (Figure 20B) or $BRET_{Max}$ (Figure 20C) ($n = 6$; $p > 0.05$; two-tailed, unpaired t-test). This indicates that the C76S mutation has no effect on AT1R-AT1R affinity or conformation when compared to the WT receptor.

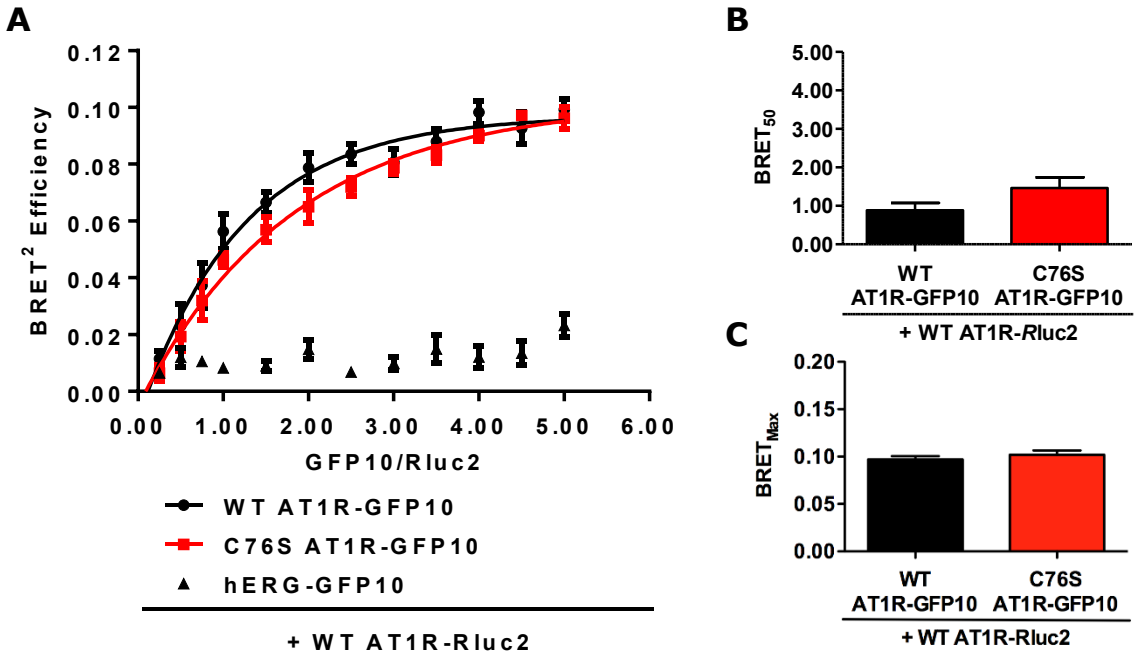

Figure 20 **The C76S mutation has no effect on AT1R-AT1R affinity.** (A) BRET² saturation experiments were designed such that HEK 293A cells were transiently transfected with a fixed concentration of AT1R-*R*luc2 and increasing concentrations of WT or C76S AT1R-GFP10. BRET² efficiency ([BRET² Ratio – Background] / Positive Control) is plotted as a function of the ratio of GFP10/*R*luc2. Six replicates were performed for the WT and mutant receptors while three replicates were performed for the negative control (hERG-GFP10). Mean and S.E. are plotted for (B) $BRET_{50}$ values that were calculated using GraphPad Prism 5.0. There was no significant difference in $BRET_{50}$ between the WT and mutant receptors (n = 6; $p > 0.05$; two-tailed, unpaired t-test).

3.4.2 Mutations in TMIV

As discussed above, TMIV was one of the main regions of interest for this study. I150,L154A AT1R-GFP10 was the first mutant to be characterized. As discussed previously, these residues were oriented towards the putative TMIII interface. Similar to the other mutants, this construct has no effect on the overall specificity of the interaction. In pairing this GFP10-tagged mutant with the WT AT1R-*R*luc2

construct, a saturable curve was produced (Figure 21A). Mutation of these residues did, however, lead to an increase in $BRET_{50}$ (Figure 21B) (n= 6; $p < 0.05$; two-tailed, unpaired t-test) and, by extension, a reduction in AT1R-AT1R affinity. These mutation did not affect the $BRET_{Max}$ value (Figure 21C) (n = 6; $p > 0.05$; two-tailed, unpaired t-test).

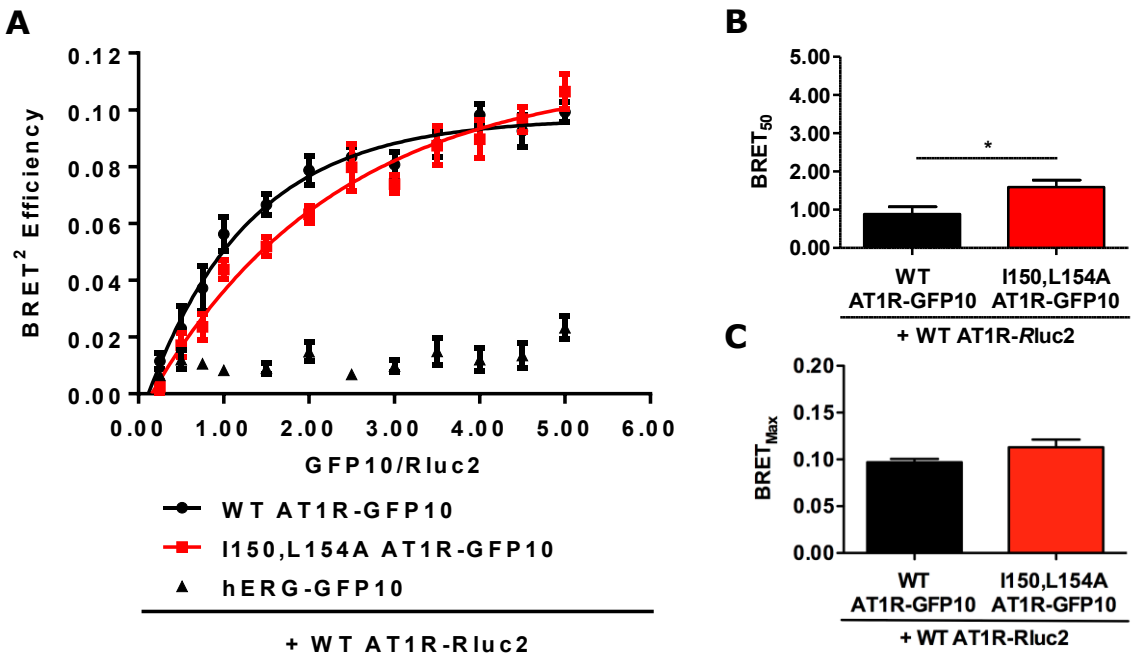

Figure 21 **The I150,L154A substitutions result in decreased AT1R-AT1R affinity.** (A) BRET² saturation experiments were designed such that HEK 293A cells were transiently transfected with a fixed concentration of AT1R-*R*luc2 and increasing concentrations of WT or mutant AT1R-GFP10. BRET² efficiency ([BRET² Ratio – Background] / Positive Control) is plotted as a function of the ratio of GFP10/*R*luc2. Six replicates were performed for the WT and mutant receptors, while three replicates were performed for the negative control (hERG-GFP10). Mean and S.E. are plotted for (B) $BRET_{50}$ and (D) $BRET_{Max}$ values that were calculated using GraphPad Prism 5.0. The I150L154A mutations result in a significant increase in $BRET_{50}$ (n = 6; *$p < 0.05$; two-tailed, unpaired t-test), but no change in $BRET_{Max}$ (n = 6; $p > 0.05$) when compared to the WT AT1R.

The I151,L155,158A mutant was the next construct to be characterized. As mentioned above, these amino acid residues were found in TMIV but oriented towards TMV. A saturable $BRET^2$ profile was also observed with this mutant (Figure 22A), suggesting that it had no effect on the specificity of the receptor-receptor interaction. However, this mutant did lead to an approximate 2-fold increase in the $BRET_{50}$ value when compared to the WT receptor (Figure 22B) ($n = 6$; $p < 0.05$; two-tailed, unpaired t-test). This suggests that mutation of these residues, the largest number mutated in TMIV, leads to a significant reduction in AT1R-AT1R affinity. Mutation of these residues had no effect on $BRET_{Max}$ (Figure 22C) ($n = 6$; $p > 0.05$; two-tailed, unpaired t-test).

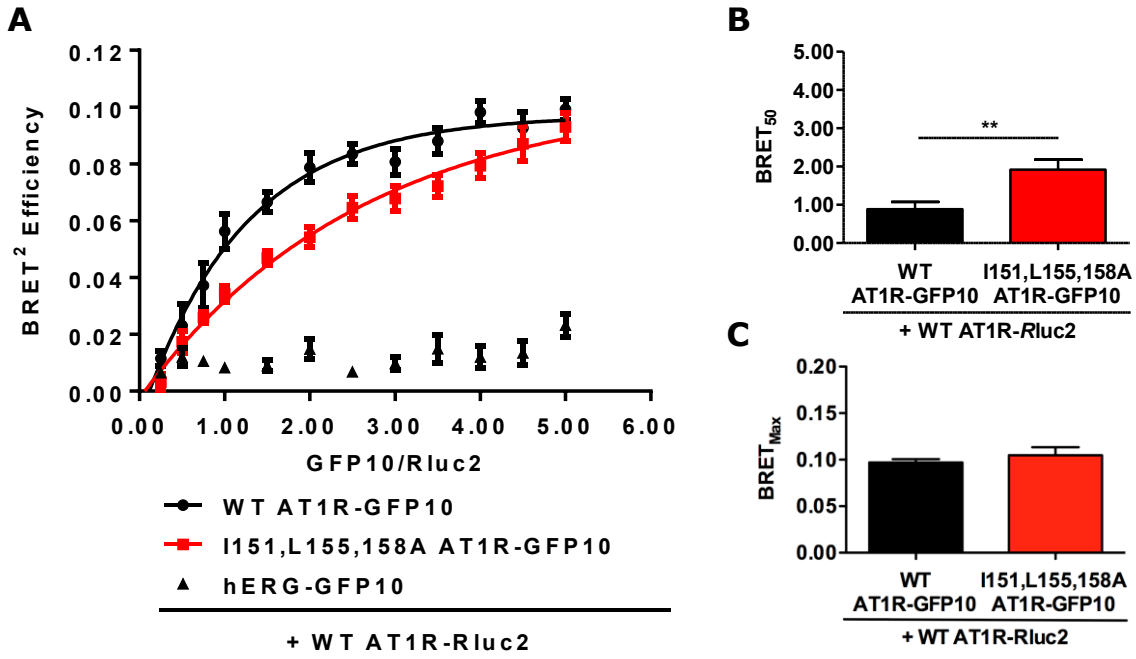

Figure 22 **The I151,L155,158A mutation decreases AT1R-AT1R affinity.** (A) BRET² saturation experiments were designed such that HEK 293A cells were transiently transfected with a fixed concentration of AT1R-*R*luc2 and increasing concentrations of WT or mutant AT1R-GFP10. BRET² efficiency values ([BRET² Ratio - Background] / Positive Control) are plotted as a function of the ratio of GFP10/*R*luc2. Six replicates were performed for the wild-type and mutant receptors, while three replicates were performed for the negative control (hERG-GFP10). Mean and S.E. are plotted for (B) $BRET_{50}$ and (C) $BRET_{Max}$ values that were calculated using GraphPad Prism 5.0. The I151,L155,158A mutation results in a significant increase in $BRET_{50}$ ($n = 6$; $^{**}p < 0.01$; two-tailed, unpaired t-test) but no change in $BRET_{Max}$ ($n = 6$; $p > 0.05$).

L154 and L158 were the last series of amino acids to be examined in the TMIV. These amino acids were selected because each side chain has a distinct orientation. L154 is oriented toward TMV and L158 is oriented towards TMIII. Substitution of both of these amino acids with an alanine residue produced a saturable BRET² curve (Figure 23A). These substitutions also resulted in a significant increase in $BRET_{50}$ (Figure 23B) ($n = 6$; $p < 0.05$; two-tailed, unpaired

t-test). $BRET_{Max}$, on the other hand, was not affected (Figure 23C) (n = 6; p > 0.05; two-tailed, unpaired t-test).

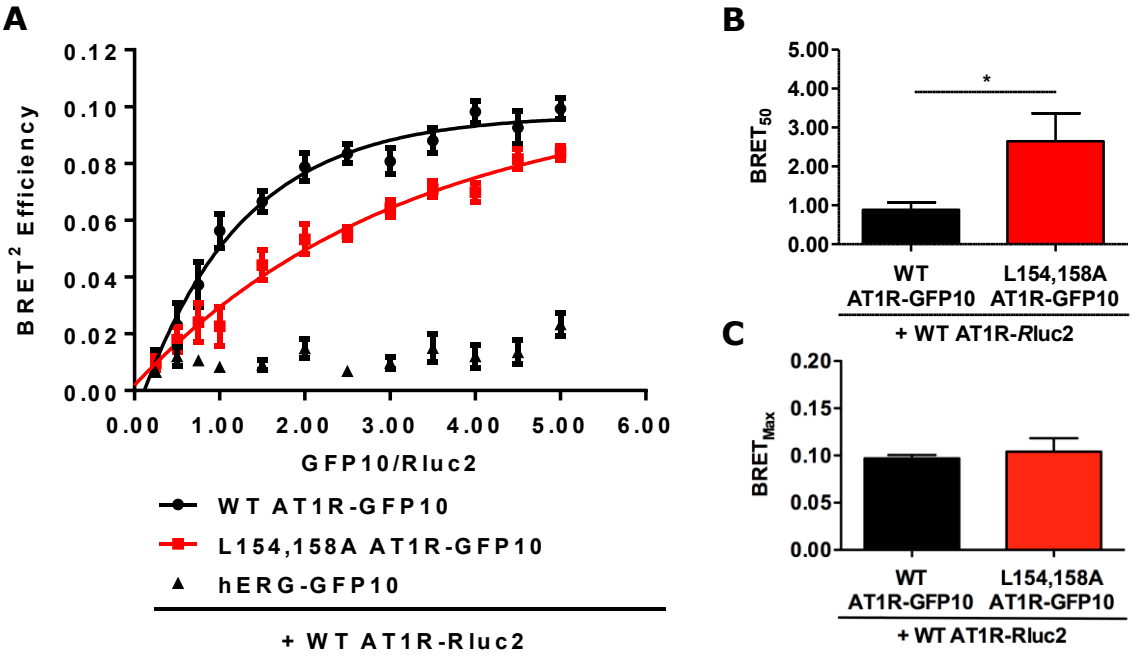

Figure 23 **The L154,158A mutation decreases AT1R-AT1R affinity.** (A) $BRET^2$ saturation experiments were designed such that HEK 293A cells were transiently transfected with a fixed concentration of AT1R-*R*luc2 and increasing concentrations of WT or mutant AT1R-GFP10. $BRET^2$ efficiency values ([$BRET^2$ Ratio - Background] / Positive Control) are plotted as a function of the ratio of GFP10/*R*luc2. Six replicates were performed for the wild-type and mutant receptors, while three replicates were performed for the negative control (hERG-GFP10). Mean and S.E. are plotted for (B) $BRET_{50}$ and (C) $BRET_{Max}$ values that were calculated using GraphPad Prism 5.0. The L154,158A mutation results in a significant increase in $BRET_{50}$ (n = 6; *p < 0.05; two-tailed, unpaired t-test) but no change in $BRET_{Max}$ (n = 6; p > 0.05).

3.4.3 Mutations in TMV

TMV is another area of interest when it comes to AT1R homomer formation. The L202,F206,I210A AT1R-GFP10 construct was shown to produce a saturable

curve (Figure 24A) and, therefore, interact specifically with the WT AT1R-*R*luc2 construct. This mutant was also shown to produce a significant increase in $BRET_{50}$ (Figure 24B) ($n = 6$; $p < 0.05$; two-tailed, unpaired t-test). However, it yielded no change in the $BRET_{Max}$ value when compared to the WT receptor (Figure 24C) ($n = 6$; $p > 0.05$; two-tailed unpaired t-test).

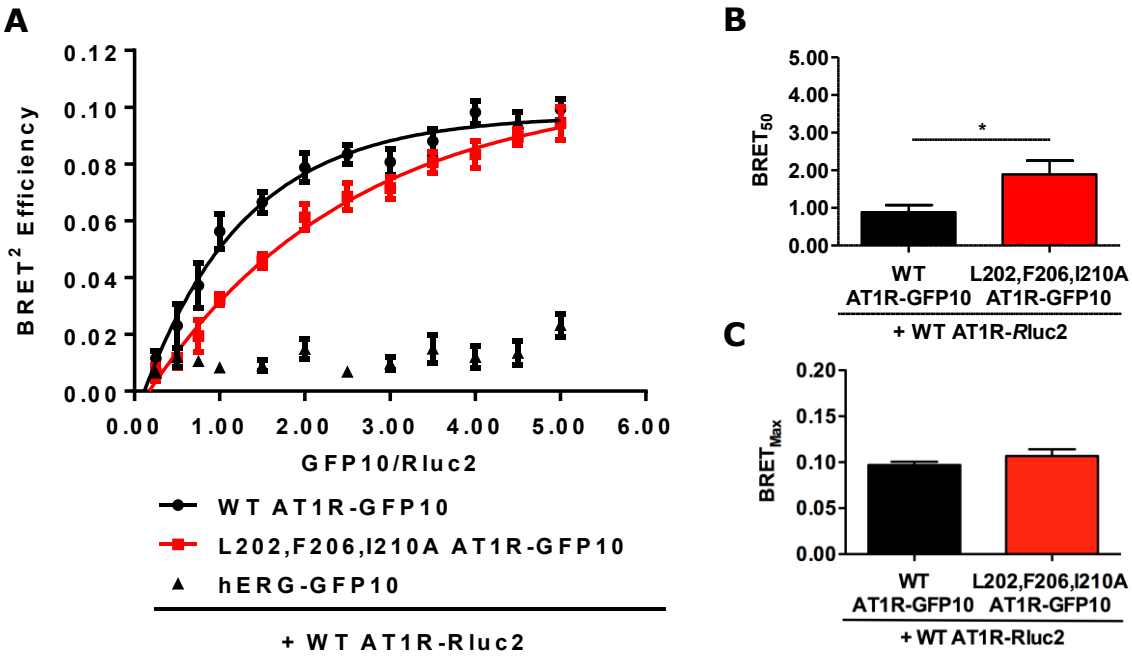

Figure 24 **The L202,F206,I210A mutation decreases AT1R-AT1R affinity.** (A) BRET saturation experiments were designed such that HEK 293A cells were transiently transfected with a fixed concentration of AT1R-*R*luc2 and increasing concentrations of WT or mutant AT1R-GFP10. $BRET^2$ efficiency values ([$BRET^2$ Ratio - Background] / Positive Control) are plotted as a function of GFP10/*R*luc2 ratios. Six replicates were performed for the wild-type and mutant receptors, while three replicates were performed for the negative control (hERG-GFP10). Mean and S.E. are plotted for (B) $BRET_{50}$ and (C) $BRET_{Max}$ values that were calculated using GraphPad Prism 5.0. The L202,F206,I210A mutation results in a significant increase in $BRET_{50}$ ($n = 6$; $^*p < 0.05$; two-tailed, unpaired t-test) and no change in $BRET_{Max}$ ($n = 6$; $p > 0.05$).

3.4.4 Mutations in TMVI

The next area of interest was TMVI. In this domain, L247, F251, and I258 were mutated to three alanine residues in order to reduce hydrophobicity at this region. Nonetheless, a saturable, thus, specific interaction did occur between the mutant and WT AT1R constructs (Figure 25A). Mutation of these amino acids was sufficient to increase $BRET_{50}$ (Figure 25B) ($n = 6$; $p < 0.05$; two-tailed, unpaired t-test) and, therefore, decrease affinity between the two receptors. $BRET_{Max}$ was not perturbed by this series of substitutions (Figure 25C).

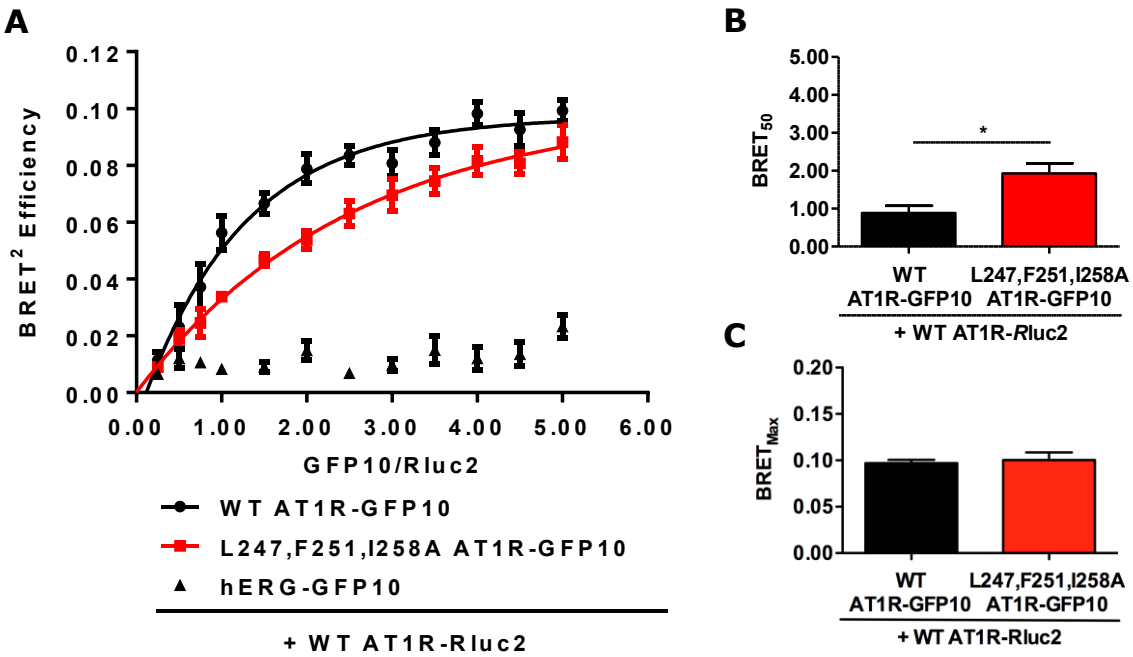

Figure 25 **The L247,F251,I258A mutation decreases AT1R-AT1R affinity.** (A) BRET² saturation experiments were designed such that HEK 293A cells were transiently transfected with a fixed concentration of AT1R-*R*luc2 and increasing concentrations of WT or mutant AT1R-GFP10. BRET² efficiency values ([BRET² Ratio - Background] / Positive Control) are plotted as a function of GFP10/*R*luc2 ratios. Six replicates were performed for the wild-type and mutant receptors, while three replicates were performed for the negative control (hERG-GFP10). Mean and S.E. are plotted for (B) $BRET_{50}$ and (C) $BRET_{Max}$ values that were calculated using GraphPad Prism 5.0. The L247,F251,I258A mutation results in a significant increase in $BRET_{50}$ ($n = 6$; $^*p < 0.05$; two-tailed, unpaired t-test) but no change in $BRET_{Max}$ ($n= 6$; $p > 0.05$).

3.4.5 Mutations in TMVI

Mutation of I286,F293, and L297 in TMVI was shown to produce a saturable curve (Figure 26A). While the $BRET_{50}$ value was significantly larger for the mutant when compared to the WT construct (Figure 26B) ($n = 6$; $p < 0.05$; two-tailed, unpaired t-test), the $BRET_{Max}$ value for this curve was unchanged (Figure

26C) ($n = 6$; $p > 0.05$; two-tailed, unpaired t-test),. Looking at the curve itself, however, there did appear to be a shift in the saturation point. While not significant, this may be related to the fact that the GFP10 tag is found at the C-terminus of the receptor. Given the direct connection between TMVII and the C-terminus, mutation of this region is very likely to disrupt the orientation of the tag, thus, affect BRET.

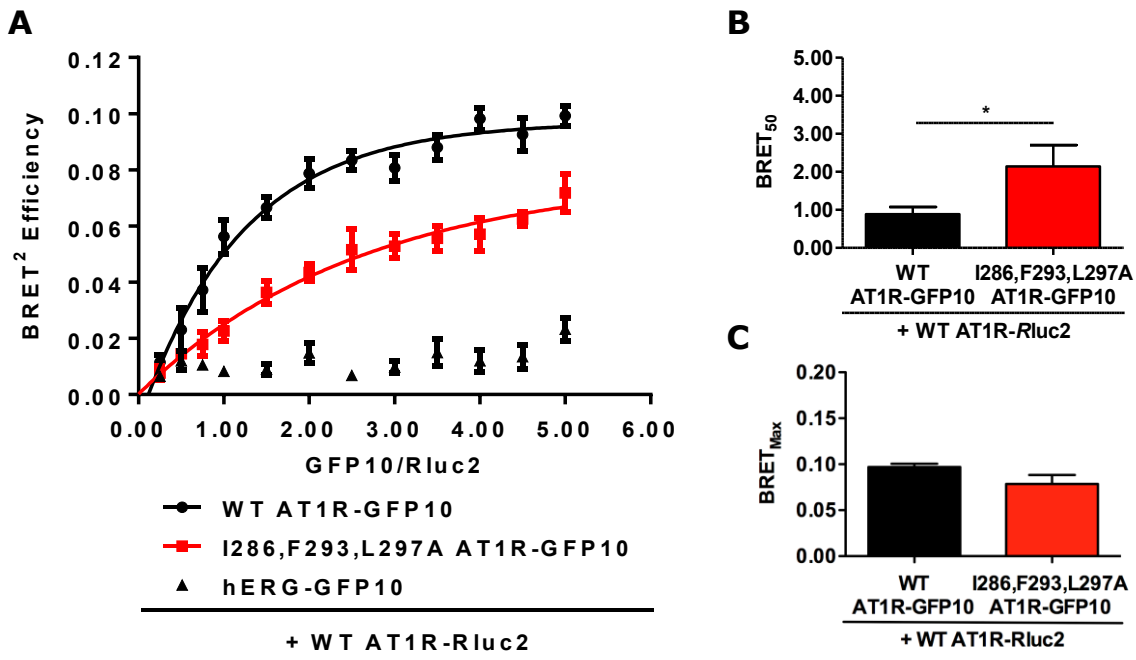

Figure 26 **The I286,F293,L297A mutations decrease AT1R-AT1R affinity.** (A) BRET² saturation experiments were designed such that HEK 293A cells were transiently transfected with a fixed concentration of AT1R-*R*luc2 and increasing concentrations of WT or mutant AT1R-GFP10. BRET² efficiency values ([BRET² Ratio - Background] / Positive Control) are plotted as a function of the ratio of GFP10/*R*luc2. Six replicates were performed for the wild-type and mutant receptors, while three replicates were performed for the negative control (hERG-GFP10). Mean and S.E. are plotted for (B) $BRET_{50}$ and (C) $BRET_{Max}$ values that were calculated using GraphPad Prism 5.0. The I286,F293,L297A mutations result in a significant increase in $BRET_{50}$ ($n = 6$; $^*p < 0.05$; two-tailed, unpaired t-test) but no change in $BRET_{Max}$ ($n = 6$; $p > 0.05$).

3.4.6 Summary

With the exception of TMII, mutations in all TMs that were examined herein produced an increase in $BRET_{50}$. The most dramatic increase in $BRET_{50}$ was seen with the I151,L155,158A (TMIV) construct. Despite this, no mutations produced a complete ablation of BRET and, therefore, they did not result in the complete

disruption of the AT1R homomer interface. Furthermore, there were no significant shifts in $BRET_{Max}$, suggesting that none of the mutations disrupted receptor conformation in such a way that would displace GFP10. A summary of the BRET parameters for each receptor can be found in Table 9 below.

Table 9 **Summary of $BRET_{50}$ and $BRET_{Max}$ values derived from $BRET^2$ saturation experiments performed for each mutant AT1R construct.** Values are represented as the mean ± S.E. and are each compared to the WT receptor (n = 3; * $p < 0.05$; ** $p < 0.005$; two-tailed, unpaired t-test).

$BRET^2$ Acceptor	**$BRET_{50}$**	**$BRET_{Max}$**
WT AT1R-GFP10	0.885 ± 0.193	0.097 ± 0.004
C76S AT1R-GFP10	1.462 ± 0.280	0.102 ± 0.005
I150,L154A AT1R-GFP10	1.589 ± 0.184*	0.113 ± 0.008
I151,L155,158A AT1R-GFP10	1.922 ± 0.258**	0.105 ± 0.009
L154,158A AT1R-GFP10	2.648 ± 0.716*	0.104 ± 0.014
L202,F206,I210A AT1R-GFP10	1.894 ± 0.359*	0.107 ± 0.007
L247A,F251,I258A AT1R-GFP10	1.928 ± 0.269*	0.100 ± 0.008
I286,F293,L297A AT1R-GFP10	2.141 ± 0.563*	0.078 ± 0.010

CHAPTER 4 DISCUSSION

4.1 GENERAL OVERVIEW

Members of the GPCR superfamily make up one of the largest classes of drug targets. Some examples of diseases that are treated using GPCR-based therapies include schizophrenia, depression, Parkinson's disease, obstructive pulmonary disease, benign prostatic hyperplasia, congestive heart failure, and hypertension[223]. Despite this, we know very few details about GPCR structure. The limited body of knowledge that does exist has demonstrated that our original understanding of these receptors was oversimplified. We now know that, unlike their name suggests, GPCRs can signal independent of heterotrimeric G proteins, and they can also form quaternary complexes with unique pharmacological properties. These insights have fuelled growth in the field of GPCR research and have demonstrated that these receptors will have a prominent role in disease treatment for years to come.

While GPCRs have a central role in disease treatment, the current approach to drug design is limited largely by the need to mimic endogenous ligands. Without key structural data, progress in the field has been slow. Currently, only 25 high resolution crystal structures exist for GPCRs, representing approximately 3% of all 800 GPCRs known to humans. This shortcoming is exacerbated when receptor dimers and oligomers are included. Indeed, only a handful of crystal structures exist for receptor dimers. These include the μOR[171], the κ-opioid receptor[170], the

β_1-adrenergic receptor[222], and CXCR4[166]. While there is a lack of structural data, there is a considerable body of knowledge surrounding the physiological consequences of GPCR dimerization[55]. These consequences have been outlined in Table 1.

As a means to define the physiological relevance of GPCR dimerization, the International Union of Basic and Clinical Pharmacology (IUPHAR) established three criteria for assessing GPCR dimers. Two of these three criteria must be met in order for a GPCR dimer to be deemed physiologically relevant. These criteria include expression of the dimer in native tissues or primary cells, dimer-specific qualities such as unique signaling or ligand binding properties, and *in vivo* validation of the dimer in animal models[224]. Numerous studies have examined GPCRs in the scope of these criteria, and several GPCR dimers can now be considered physiologically relevant.

The pharmacological potential of GPCR dimers is highlighted by the fact that some of these structures have been shown to have distinct ligand binding properties. The earliest studies to demonstrate this looked at dimerization-induced alterations in radioligand binding affinity and dissociation constants. These efforts challenged the traditional paradigm of a single, independent GPCR binding a single ligand. In one study, the δOR and μOR were shown to form heterodimers in native tissues. Interestingly, ligand binding at one receptor within the heterodimeric complex was also shown to influence ligand binding at the adjacent receptor. Specifically, administration of δOR antagonists was shown

to increase μOR affinity for morphine and DAMGO[101]. This phenomenon was identified as positive cooperativity. In a more recent study, negative cooperativity was observed among heteromers of the dopamine $D2_L$ receptor and the neurotensin receptor 1. With negative cooperativity, the dopamine $D2_L$ receptor showed a 34-fold decrease in agonist affinity following administration of neurotensin[117]. Aside from ligand affinity, dimerization has also been shown to influence ligand selectivity. Coexpression of the δ- and κ–opioid receptors has been shown to decrease receptor affinity for selective agonists and antagonists, but increase receptor affinity for partially selective agonists and antagonists[64]. Evidently, the therapeutic potential of GPCR complexes is underappreciated.

While ligand binding can be influenced by GPCR dimerization, a complete switch in signaling can also occur as a result of this phenomenon. In fact, dimerization of the dopamine D1 and D2 receptors has been shown to yield a complete switch in G protein coupling. When expressed alone, the D1R couples $G\alpha_s$, and the D2R couples $G\alpha_i$. Heterodimerization of these receptors, however, has been shown to result ligand-stimulated $G\alpha_{q/11}$ coupling. This leads to the subsequent activation phospholipase C and a dramatic increase in intracellular calcium release[108]. In another example, heterodimerization of the cannabinoid receptor type 1 (CB1R) and D2R has been shown to result in a G protein switch. When expressed alone, the CB1R is coupled to $G\alpha_i$ and inhibits cAMP production via adenylyl cyclase. However, coactivation of the D2R and the CB1R results in $G\alpha_s$ coupling and an increase in cAMP levels[92]. Other signaling switches that arise following heterodimerization include a switch from G protein signaling to β-arrestin-

mediated signaling[102]. This has obvious consequences for GPCR pharmacology and, again, provides a potential avenue for drug development.

GPCR dimerization also has important implications for receptor trafficking. Indeed, receptor-receptor interactions have been shown to affect cell surface expression, receptor maturation, and ligand-induced internalization among GPCRs[55]. The α_{1D}-adrenergic receptor, for example, has limited activity when expressed alone because it is not transported to the cell surface efficiently[225]. However, heterodimerization of the α_{1D}-adrenergic receptor with the α_{1B}-adrenergic receptor has been shown to increase α_{1D}-adrenergic receptor expression at the cell surface by a factor of 10[78]. This suggests that the α_{1B}-adrenergic receptor acts as a chaperone, and it is essential for α_{1D}-adrenergic receptor function. In addition to this, receptor dimerization can lead to ligand-induced cointernalization. Stimulation of the δOR has been shown to decrease cell surface expression of both the δOR and the μOR subtypes[226]. While this has implications for the use of morphine as an analgesic, it also highlights the previously unrecognized consequences of GPCR dimerization.

In addition to the altered trafficking patterns observed among GPCR dimers, the magnitude of receptor signaling can also change as a result of receptor-receptor interactions. Indeed, signaling via either one or two receptors within a dimeric complex can be increased or decreased when compared to signaling of the respective monomeric constituents. Morphine, which is a μOR agonist, was shown to inhibit norepinephrine-induced α_{2A}-adrenergic receptor signaling in

cells coexpressing the μ-opioid and α_{2A}-adrenergic receptors. Specifically, α_{2A}-adrenergic receptor-mediated $G\alpha_i$ activation and ERK1/2 phosphorylation were reduced in the presence of morphine[84]. By contrast, Ang II-mediated AT1R signaling was shown to be increased with coexpression of the B2R in vascular smooth muscle cells. This increase was observed even in the absence of bradykinin, and it has been shown to result in preeclampsia[85] and experimental hypertension[218]. The AT1R-B2R complex is of great interest because specific targeting or disruption of this dimer may have therapeutic benefits for individuals suffering with hypertension and related cardiovascular disease. It was also recently demonstrated that the AT1R forms functional heteromers with the D2R in the rat striatum. Selective blockade of the AT1R in cotransfected cells was shown to block dopaminergic signaling, suggesting that drug therapies targeting the RAAS may have off-target effects in the central nervous system[87]. In light of these findings, we sought a better understanding of the structural context of these interactions with the goal of identifying the TM regions that are involved in AT1R homomer formation.

4.2 GOMoDo Can Be Used to Develop an Accurate Model of the AT1R

Given the obstacles associated with elucidating three-dimensional GPCR structure experimentally, many groups have turned to computational methods for modelling GPCR structure. Traditionally, this approach required expert computer programming skills and was computationally taxing; however, the

emergence of several web-based platforms has provided a low-cost, user-friendly means for novice researchers to model GPCRs. Here, we used GOMoDo to develop a three-dimensional model of the AT1R in the absence of a published crystal structure. This modelling was essential for the identification of amino acids that were exposed to the phospholipid bilayer and, thus, had the potential to participate in AT1R homomer formation. Using this approach, the δOR was selected as the best template for AT1R modelling as it had a low DOPE score and a high GA341 score (Figure 5).

After this model was generated, a crystal structure was published for the AT1R (PDB ID: 4YAY)[186]. Interestingly, the model that was based on the crystal structure of the δOR was highly similar to the solved crystal structure for the AT1R. Using the GPCRDB superimposition tool[16], it was determined that there is a RMSD of 2.1 Å between the α-carbon atoms of each structure. This value is considerably smaller than the 2.9 Å resolution of the crystal structure[186]. Therefore, it was concluded that GOMoDo produced an adequate model of the AT1R. By visual comparison alone, it was evident that the model was accurate as all amino acids that were selected for mutagenesis were exposed to the membrane environment in both the model (Figure 27A) and the crystal structure (Figure 27B). This finding is significant because it validates the selection of candidates for mutagenesis, and it indicates that GOMoDo can be used for similar applications in the future. This is a novel finding as GOMoDo has not yet been used for the examination of GPCR homomerization.

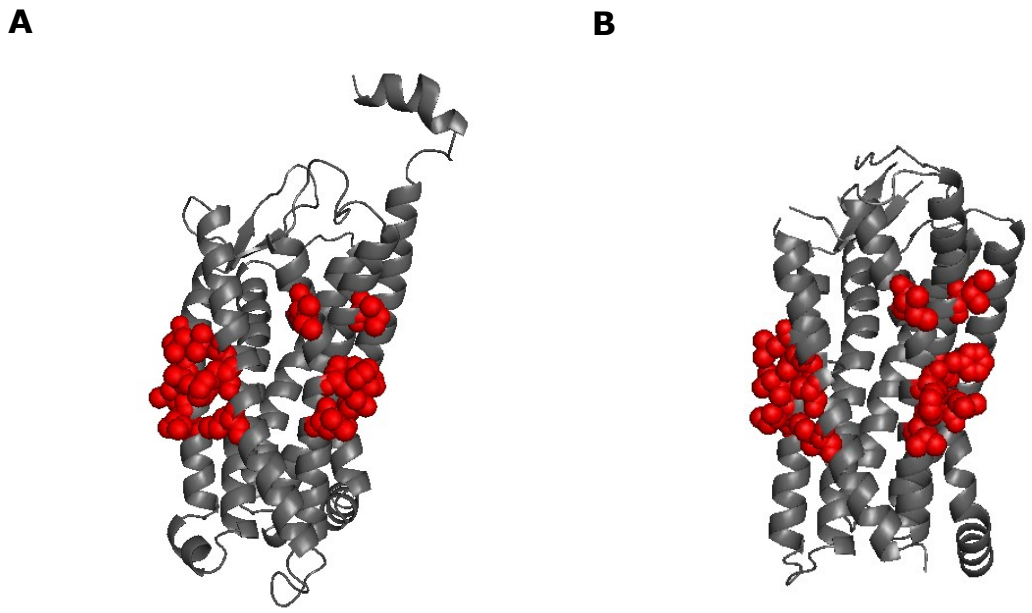

Figure 27 All amino acids that were selected for mutagenesis are exposed in both the model and the crystal structure. (A) A visual representation of the AT1R produced using GOMoDo shows that all mutated amino acids (red spheres) are exposed to the membrane environment. (B) The AT1R crystal structure (PDB ID: 4YAY)[186] shows a similar pattern, with each selected amino acid (red spheres) appearing to be exposed to the membrane environment. Using the GPCRDB superimposition tool[16], it was determined that there was a RMSD of 2.1 Å between the α-carbon backbone of the model and that of the crystal structure.

Although GOMoDo was capable of developing an accurate model of the AT1R, there are some caveats to consider when using this program. When looking at the adhesion family, for instance, there are no complete crystal structures available to use as templates for modeling. Therefore, users may have difficulty using GOMoDo to model receptors within this family. In fact, 21 of the 25 crystal structures available for GPCRs belong to the rhodopsin-like family. This presents some challenges for those looking to use GOMoDo to model receptors outside of

this class. The scoring parameters of the AT1R model presented herein may be used as a positive control for suitable modeling; however, the usefulness of GOMoDo is still limited by the availability of suitable templates for GPCR modeling.

4.3 Hydrophobic Residues Within TMs IV, V, VI, and VII Participate in AT1R Homomerization

Despite the emergence of a three-dimensional structure for the AT1R monomer[186], very little is known about the three-dimensional structure of multimeric AT1R complexes. Based on the data that exists for other multimeric class A GPCRs, we hypothesized that the AT1R forms homomeric interactions via hydrophobic residues within TMs IV, V, VI, and VII. Indeed, different combinations of these domains have been shown to participate in dimerization of the μOR[171], the β1AR,[222] the M3R[146], and CXCR4[166]. There is, however, some variation in the specific nature of these interactions.

When CXCR4 is bound to a small molecule antagonist known as IT1t, dimer association was shown to be driven by hydrophobic interactions between amino acids at the extracellular end of TMs V and VI[166]. However, when CXCR4 dimers are bound to a cyclic peptide known as CVX15, receptors were shown to interact via another interface at the intracellular side of TMIII, TMIV, and ICL2. Binding of this bulky peptide was shown to induce a conformational change in the extracellular region of TMV and promote contact between the intracellular regions of opposing receptors[166]. It has been speculated that this conformational

change alters ligand affinity at the adjacent receptor, and this may provide a mechanistic model for the positive and negative cooperativity that can be observed among ligands that target other GPCR dimers. The presence of the E/DRY motif on TMIII is also notable because, aside from mediating ligand-induced receptor activation, this motif may provide a mechanism by which ligand binding influences the dimer interface and vice versa. Indeed, when CXCR4 interacts with C-C chemokine receptor type 2 or type 5, negative binding cooperativity has been observed between their ligands[227-229]. Nonetheless, the structural details of CXCR4 dimerization appear to be unique. This suggests that the mechanisms of dimerization can vary within a single GPCR family, and this phenomenon merits further investigation with the AT1R.

Although a crystal structure does not yet exist for the δOR dimer, there has been some recent effort to characterize the interaction interface between these receptors. Using a molecular dynamics simulation, it was shown that TMs IV and V contribute to a putative interface among δOR dimers[221]. This finding is highly relevant to the current study as the δOR was selected as the best template for AT1R modelling (Figure 5). Accordingly, substitution of hydrophobic amino acids within TMIV (I150,L154A, I151,L155,158A, and L154,158A) and TMV (L202,F206,I210A) led to significant changes in the $BRET^2$ saturation profile for each receptor (Figures 21-24). Specifically, each mutant produced a significant increase in $BRET_{50}$, which suggests that reduced hydrophobicity at these regions is associated with decreased AT1R-AT1R affinity. Nonetheless, each of these

mutants was responsive to Ang II (Figures 16 & 17), which suggests that they are functional and expressed at the membrane.

The μOR (PDB ID: 4DK1) is also among the small number of GPCRs with a known quaternary structure[171]. Coincidentally, it was identified as the second best template for AT1R modelling via GOMoDo (Figure 5). Given this, the dimer interface of the μOR was also thought to be an accurate predictor of the AT1R dimer interface. Similar to CXCR4, the μOR has an asymmetrical dimer interface at TMs V and VI. Different from CXCR4, however, this interface is tightly packed because it does not rely solely on amino acids within the extracellular region of these domains. In addition, two discrete interaction interfaces can be found at TMI, TMII, and helix VIII within μOR dimers[171]. This interface is loosely packed when compared to the TMV/VI interface and it was, therefore, assumed to make less of a contribution to receptor-receptor affinity. As result, our focus was directed to the TMV/VI interface. Interestingly, the $BRET^2$ saturation curves found in Figures 24 and 25 demonstrate that mutation of a series of hydrophobic amino acids in TMV (L202,F206,I210) and TMVI (L247,F251,I258) is sufficient to reduce AT1R-AT1R affinity. Similar to the constructs discussed above, there receptor were responsive to Ang II (Figures 17 & 18) and, thus, assumed to be functional.

Data to implicate TMVII in GPCR dimerization is limited, but some studies have suggested that it is involved in this phenomenon among certain GPCRs. Specifically, Ng *et al.* (1996) demonstrated that a peptide segment designed to

mimic TMVII of the D2R was sufficient to disrupt D2R dimerization[230]. Likewise, a more recent study has indicated that injection of this peptide segment into rate brain leads to selective blockade of D2R activity[231]. Together, this evidence suggests that, through dimerization, TMVII has a role in GPCR inhibition, which lends support to the notion that GPCR dimers are druggable targets. The data presented herein demonstrates that mutation of hydrophobic amino acids found in this region (I286,F293,L297A) results in a decrease in receptor-receptor affinity (Figure 26). Further characterization of this construct with regards to its effect on receptor activity would be an interesting avenue for future studies.

While the results contained in this study are consistent with information found in the literature, this study does not provide information concerned with the overall geometry of these interactions. Do TMs V and VI form discrete interaction interfaces, or do both TMs form a single, asymmetrical interface? Looking at CXCR4 and the μOR, the latter scenario appears to be most likely. However, this becomes complicated when data available for the β1AR is considered[222]. With this receptor, TMs IV and V have been shown to form a single interface. While each of these TMs appear to contribute to AT1R-AT1R affinity, the exact nature of this interaction remains unknown. Do TMs IV and V form a single, asymmetrical interface in lieu of TMs V and VI? Do separate interfaces exist within AT1R homomers at all? Additional studies are required to answer these questions, but theoretical information provides some insight on this topic.

4.4 Does the AT1R Exist as a Dimer or Higher Order Oligomer?

In producing a $BRET_{50}$ value, BRET saturation experiments can be used to determine the relative affinity of GPCR-GPCR complexes. By extension, BRET saturation experiments can also be used to track the shift from tetramer to trimer, trimer to dimer, and dimer to monomer (Figure 28)[232]. Receptor homodimers, for example, have a theoretical $BRET_{50}$ value of 1. In the current study, the $BRET_{50}$ value obtained for WT AT1R-AT1R complex was 0.885 ± 0.193 (Table 9). There is no significant difference between this value and the theoretical $BRET_{50}$ value of 1 for receptor homodimers ($p > 0.05$; two-tailed, unpaired t-test). Based on this alone, it would appear that the AT1R does not form high order oligomers. However, it is important to note that there is no significant difference between the theoretical $BRET_{50}$ value for trimers[232] and the experimental $BRET_{50}$ value of 0.885 ± 0.193 ($p > 0.05$; two-tailed, unpaired t-test). This suggests that, while sensitive enough to detect increases in $BRET_{50}$ on that magnitude of 50% or more, the $BRET^2$ saturation experiments presented here were not suitable for detecting changes smaller than this.

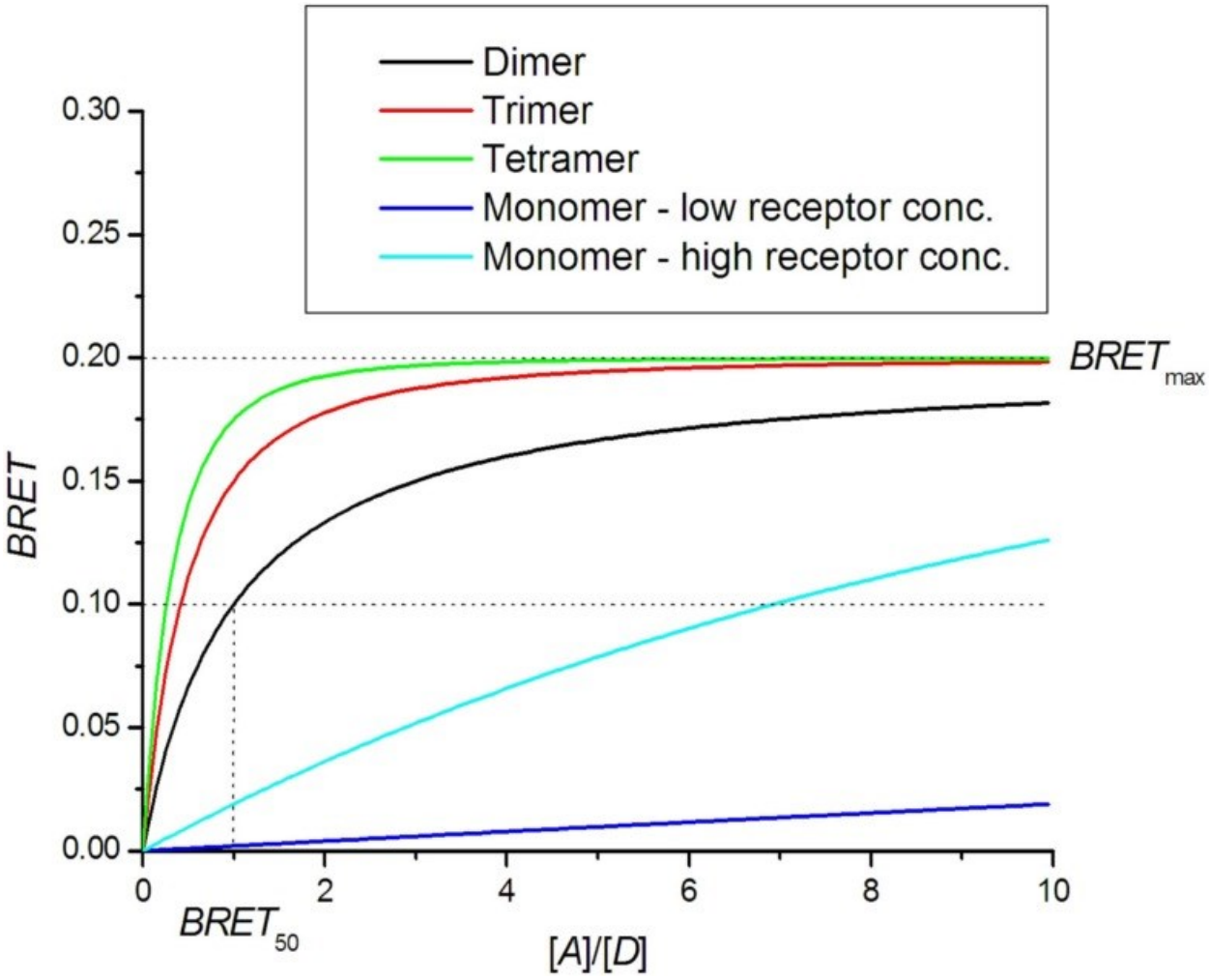

Figure 28 Theoretical BRET saturation curves that describe oligomer formation[232]. BRET ratio is plotted as a function of acceptor/donor ratios ([A]/[D]). $BRET_{50}$ is the represented as the ratio at which the saturation curve reaches half of the maximal BRET response ($BRET_{max}$). High order complexes reach $BRET_{max}$ faster and have lower $BRET_{50}$ values. This material has been reproduced under the terms of the Creative Commons Attribution License (http://creativecommons.org/licenses/by/3.0/legalcode). Copyright © 2012 Drinovec, Kubale, Nøhr Larsen and Vrecl.

4.5 Future Work

Given some evidence to suggest that TMs I and III have a role in dimerization among certain GPCRs[166,171], we hope to examine these regions in the context of

AT1R homomers. Furthermore, we hope to characterize the exact nature of the interfaces that have already been examined by looking at different combinations of mutations across different TMs. Because $BRET_{50}$ was increased in the presence of almost every series of mutations with the exception of C76S, we propose that certain combinations of mutations from different TMs will lead to a further reduction and perhaps a complete ablation of BRET. For example, if TMs V and VI happen to make up a single, asymmetrical interface, a combination of mutations in both of these regions should have no further effect on BRET. However, if these TMs make up two discreet interfaces, a combination of mutations in both regions should lead to a further reduction and possibly a complete disruption of BRET. While this would help distinguish between discreet interfaces, it would also provide a glimpse at the overall geometry of AT1R homomers. Specifically, it will tell us whether or not the AT1R exists as a dimer or a high order oligomer. In the future, we hope to use this data to guide studies that examine AT1R heteromers. With the existence of AT1R-B2R heteromers that have been implicated in preeclampsia[85] and experimental hypertension[218], these structures would be the next logical target for future studies.

4.6 Conclusions

The AT1R has had a central role in cardiovascular disease treatment for decades[207]. However, the realization that this GPCR forms homomeric and heteromeric complexes has complicated our understanding AT1R pharmacology. While the AT1R is known to form complexes with a handful of other GPCRs, its

interactions with the B2R and the AT2R are perhaps the most notable[59,85,218]. Formation of these complexes has been shown to have profound effects on AT1R pharmacology and cardiovascular physiology. With is mind, we set out to examine the AT1R homomer interface with the intent of applying this data to future studies focused on AT1R heteromers. To our knowledge, this is the first time GOMoDo has been used for the characterization of a GPCR homomer interface. The recent publication of a crystal structure for the AT1R[186] has validated this approach. In addition to developing an adequate model of the AT1R, our data demonstrates that AT1R-AT1R affinity is reduced by mutation of hydrophobic amino acids within TMs IV, V, VI, and VII. This work provides the first glimpse at AT1R homomer structure, and it serves as a foundation for the development of compounds that target multimeric AT1R complexes.

REFERENCES

1. Fredriksson R, Lagerstrom MC, Lundin LG, Schioth HB. The G-protein-coupled receptors in the human genome form five main families. Phylogenetic analysis, paralogon groups, and fingerprints. *Mol Pharmacol*. 2003;63(6):1256-1272.

2. Venter JC, Adams MD, Myers EW, et al. The sequence of the human genome. *Science (New York, N.Y.)*. 2001;291(5507):1304-1351.

3. Lander ES, Linton LM, Birren B, et al. Initial sequencing and analysis of the human genome. *Nature*. 2001;409(6822):860-921.

4. Schoneberg T, Hofreiter M, Schulz A, Rompler H. Learning from the past: evolution of GPCR functions. *Trends Pharmacol Sci*. 2007;28(3):117-121.

5. Koutalos Y, Ebrey TG. Recent progress in vertebrate photoreception. *Photochemistry and photobiology*. 1986;44(6):809-817.

6. Barnes PJ. Beta-adrenergic receptors and their regulation. *American journal of respiratory and critical care medicine*. 1995;152(3):838-860.

7. Bridges TM, Lindsley CW. G-protein-coupled receptors: from classical modes of modulation to allosteric mechanisms. *ACS Chem Biol*. 2008;3(9):530-541.

8. Ellis C. The state of GPCR research in 2004. *Nat Rev Drug Discov*. 2004;3(7):575, 577-626.

9. Barnett AH, Bain SC, Bouter P, et al. Angiotensin-receptor blockade versus converting-enzyme inhibition in type 2 diabetes and nephropathy. *N Engl J Med*. 2004;351(19):1952-1961.

10. Squire IB, Barnett DB. The rational use of beta-adrenoceptor blockers in the treatment of heart failure. The changing face of an old therapy. *Br J Clin Pharmacol*. 2000;49(1):1-9.

11. Ram FS, Sestini P. Regular inhaled short acting beta2 agonists for the management of stable chronic obstructive pulmonary disease: Cochrane systematic review and meta-analysis. *Thorax*. 2003;58(7):580-584.

12. Seeman P, Niznik HB. Dopamine receptors and transporters in Parkinson's disease and schizophrenia. *FASEB J*. 1990;4(10):2737-2744.

13. Ritter SL, Hall RA. Fine-tuning of GPCR activity by receptor-interacting proteins. *Nat Rev Mol Cell Biol*. 2009;10(12):819-830.

14. Schiöth HB, Fredriksson R. The GRAFS classification system of G-protein coupled receptors in comparative perspective. *General and Comparative Endocrinology*. 2005;142(1–2):94-101.

15. Kolakowski LF, Jr. GCRDb: a G-protein-coupled receptor database. *Receptors Channels*. 1994;2(1):1-7.

16. Horn F, Bettler E, Oliveira L, Campagne F, Cohen FE, Vriend G. GPCRDB information system for G protein-coupled receptors. *Nucleic Acids Research*. 2003;31(1):294-297.

17. Fridmanis D, Fredriksson R, Kapa I, Schiöth HB, Klovins J. Formation of new genes explains lower intron density in mammalian Rhodopsin G protein-coupled receptors. *Molecular Phylogenetics and Evolution*. 2007;43(3):864-880.

18. Cardoso JC, Pinto VC, Vieira FA, Clark MS, Power DM. Evolution of secretin family GPCR members in the metazoa. *BMC Evol Biol*. 2006;6:108.

19. Das SS, Banker GA. The role of protein interaction motifs in regulating the polarity and clustering of the metabotropic glutamate receptor mGluR1a. *J Neurosci*. 2006;26(31):8115-8125.

20. Foord SM, Jupe S, Holbrook J. Bioinformatics and type II G-protein-coupled receptors. *Biochem Soc Trans*. 2002;30(4):473-479.

21. Krishnan A, Almen MS, Fredriksson R, Schioth HB. The origin of GPCRs: identification of mammalian like Rhodopsin, Adhesion, Glutamate and Frizzled GPCRs in fungi. *PLoS One*. 2012;7(1):e29817.

22. Rosenbaum DM, Rasmussen SGF, Kobilka BK. The structure and function of G-protein-coupled receptors. *Nature*. 2009;459(7245):356-363.

23. Peeters MC, van Westen GJ, Li Q, AP IJ. Importance of the extracellular loops in G protein-coupled receptors for ligand recognition and receptor activation. *Trends Pharmacol Sci*. 2011;32(1):35-42.

24. Massotte D, Kieffer B. Structure—Function Relationships in G Protein-Coupled Receptors. In: Devi L, ed. *The G Protein-Coupled Receptors Handbook*: Humana Press; 2005:3-31.

25. Wheatley M, Wootten D, Conner MT, et al. Lifting the lid on GPCRs: the role of extracellular loops. *Br J Pharmacol*. 2012;165(6):1688-1703.

26. Kristiansen K. Molecular mechanisms of ligand binding, signaling, and regulation within the superfamily of G-protein-coupled receptors: molecular modeling and mutagenesis approaches to receptor structure and function. *Pharmacol Ther*. 2004;103(1):21-80.

27. Okada T, Sugihara M, Bondar AN, Elstner M, Entel P, Buss V. The retinal conformation and its environment in rhodopsin in light of a new 2.2 A crystal structure. *J Mol Biol*. 2004;342(2):571-583.

28. Li J, Edwards PC, Burghammer M, Villa C, Schertler GF. Structure of bovine rhodopsin in a trigonal crystal form. *J Mol Biol*. 2004;343(5):1409-1438.

29. Vogel R, Mahalingam M, Ludeke S, Huber T, Siebert F, Sakmar TP. Functional role of the "ionic lock"--an interhelical hydrogen-bond network in family A heptahelical receptors. *J Mol Biol*. 2008;380(4):648-655.

30. Ballesteros JA, Jensen AD, Liapakis G, et al. Activation of the beta 2-adrenergic receptor involves disruption of an ionic lock between the cytoplasmic ends of transmembrane segments 3 and 6. *J Biol Chem*. 2001;276(31):29171-29177.

31. Rasmussen SG, Jensen AD, Liapakis G, Ghanouni P, Javitch JA, Gether U. Mutation of a highly conserved aspartic acid in the beta2 adrenergic receptor: constitutive activation, structural instability, and conformational rearrangement of transmembrane segment 6. *Mol Pharmacol.* 1999;56(1):175-184.

32. Fritze O, Filipek S, Kuksa V, Palczewski K, Hofmann KP, Ernst OP. Role of the conserved NPxxY(x)(5,6)F motif in the rhodopsin ground state and during activation. *Proceedings of the National Academy of Sciences of the United States of America.* 2003;100(5):2290-2295.

33. Barak LS, Menard L, Ferguson SS, Colapietro AM, Caron MG. The conserved seven-transmembrane sequence NP(X)2,3Y of the G-protein-coupled receptor superfamily regulates multiple properties of the beta 2-adrenergic receptor. *Biochemistry.* 1995;34(47):15407-15414.

34. Borroto-Escuela DO, Romero-Fernandez W, Garcia-Negredo G, et al. Dissecting the conserved NPxxY motif of the M3 muscarinic acetylcholine receptor: critical role of Asp-7.49 for receptor signaling and multiprotein complex formation. *Cell Physiol Biochem.* 2011;28(5):1009-1022.

35. Urizar E, Claeysen S, Deupí X, et al. An Activation Switch in the Rhodopsin Family of G Protein-coupled Receptors: THE THYROTROPIN RECEPTOR. *Journal of Biological Chemistry.* 2005;280(17):17135-17141.

36. Okada T, Fujiyoshi Y, Silow M, Navarro J, Landau EM, Shichida Y. Functional role of internal water molecules in rhodopsin revealed by X-ray crystallography. *Proc Natl Acad Sci U S A.* 2002;99(9):5982-5987.

37. Pardo L, Deupi X, Dolker N, Lopez-Rodriguez ML, Campillo M. The role of internal water molecules in the structure and function of the rhodopsin family of G protein-coupled receptors. *Chembiochem.* 2007;8(1):19-24.

38. Ullrich A, Schlessinger J. Signal transduction by receptors with tyrosine kinase activity. *Cell.* 1990;61(2):203-212.

39. Maggio R, Vogel Z, Wess J. Coexpression studies with mutant muscarinic/adrenergic receptors provide evidence for intermolecular "cross-talk" between G-protein-linked receptors. *Proceedings of the National Academy of Sciences of the United States of America.* 1993;90(7):3103-3107.

40. Hill SJ. G-protein-coupled receptors: past, present and future. *British journal of pharmacology*. 2006;147 Suppl 1:S27-37.

41. Limbird LE, Meyts PD, Lefkowitz RJ. Beta-adrenergic receptors: evidence for negative cooperativity. *Biochem Biophys Res Commun*. 1975;64(4):1160-1168.

42. Mattera R, Pitts BJ, Entman ML, Birnbaumer L. Guanine nucleotide regulation of a mammalian myocardial muscarinic receptor system. Evidence for homo- and heterotropic cooperativity in ligand binding analyzed by computer-assisted curve fitting. *J Biol Chem*. 1985;260(12):7410-7421.

43. Potter LT, Ballesteros LA, Bichajian LH, et al. Evidence of paired M2 muscarinic receptors. *Mol Pharmacol*. 1991;39(2):211-221.

44. Venter JC, Schaber JS, U'Prichard DC, Fraser CM. Molecular size of the human platelet alpha 2-adrenergic receptor as determined by radiation inactivation. *Biochem Biophys Res Commun*. 1983;116(3):1070-1075.

45. Conn PM, Venter JC. Radiation inactivation (target size analysis) of the gonadotropin-releasing hormone receptor: evidence for a high molecular weight complex. *Endocrinology*. 1985;116(4):1324-1326.

46. Lilly L, Fraser CM, Jung CY, Seeman P, Venter JC. Molecular size of the canine and human brain D2 dopamine receptor as determined by radiation inactivation. *Mol Pharmacol*. 1983;24(1):10-14.

47. AbdAlla S, Lother H, Quitterer U. AT1-receptor heterodimers show enhanced G-protein activation and altered receptor sequestration. *Nature*. 2000;407(6800):94-98.

48. Rogers TB. High affinity angiotensin II receptors in myocardial sarcolemmal membranes. Characterization of receptors and covalent linkage of 125I-angiotensin II to a membrane component of 116,000 daltons. *J Biol Chem*. 1984;259(13):8106-8114.

49. Kroeger K, Pfleger KG, Eidne K. Biophysical and Biochemical Methods to Study GPCR Oligomerization. In: Devi L, ed. *The G Protein-Coupled Receptors Handbook*: Humana Press; 2005:217-241.

50. Salahpour A, Angers S, Bouvier M. Functional significance of oligomerization of G-protein-coupled receptors. *Trends in endocrinology and metabolism: TEM*. 2000;11(5):163-168.

51. Hebert TE, Moffett S, Morello JP, et al. A peptide derived from a beta2-adrenergic receptor transmembrane domain inhibits both receptor dimerization and activation. *J Biol Chem*. 1996;271(27):16384-16392.

52. Kaupmann K, Malitschek B, Schuler V, et al. GABA(B)-receptor subtypes assemble into functional heteromeric complexes. *Nature*. 1998;396(6712):683-687.

53. White JH, Wise A, Main MJ, et al. Heterodimerization is required for the formation of a functional GABA(B) receptor. *Nature*. 1998;396(6712):679-682.

54. Jones KA, Borowsky B, Tamm JA, et al. GABA(B) receptors function as a heteromeric assembly of the subunits GABA(B)R1 and GABA(B)R2. *Nature*. 1998;396(6712):674-679.

55. Hiller C, Kuhhorn J, Gmeiner P. Class A G-protein-coupled receptor (GPCR) dimers and bivalent ligands. *J Med Chem*. 2013;56(17):6542-6559.

56. Gurevich VV, Gurevich EV. How and why do GPCRs dimerize? *Trends in pharmacological sciences*. 2008;29(5):234-240.

57. Milligan G. G protein-coupled receptor dimerization: function and ligand pharmacology. *Molecular pharmacology*. 2004;66(1):1-7.

58. Barki-Harrington L, Luttrell LM, Rockman HA. Dual inhibition of beta-adrenergic and angiotensin II receptors by a single antagonist: a functional role for receptor-receptor interaction in vivo. *Circulation*. 2003;108(13):1611-1618.

59. AbdAlla S, Lother H, Abdel-tawab AM, Quitterer U. The angiotensin II AT2 receptor is an AT1 receptor antagonist. *J Biol Chem*. 2001;276(43):39721-39726.

60. Pfeiffer M, Koch T, Schroder H, et al. Homo- and heterodimerization of somatostatin receptor subtypes. Inactivation of sst(3) receptor function by heterodimerization with sst(2A). *J Biol Chem*. 2001;276(17):14027-14036.

61. Gines S, Hillion J, Torvinen M, et al. Dopamine D1 and adenosine A1 receptors form functionally interacting heteromeric complexes. *Proc Natl Acad Sci U S A*. 2000;97(15):8606-8611.

62. Zhu CC, Cook LB, Hinkle PM. Dimerization and phosphorylation of thyrotropin-releasing hormone receptors are modulated by agonist stimulation. *J Biol Chem*. 2002;277(31):28228-28237.

63. Cvejic S, Devi LA. Dimerization of the delta opioid receptor: implication for a role in receptor internalization. *J Biol Chem*. 1997;272(43):26959-26964.

64. Jordan BA, Devi LA. G-protein-coupled receptor heterodimerization modulates receptor function. *Nature*. 1999;399(6737):697-700.

65. Berglund MM, Schober DA, Esterman MA, Gehlert DR. Neuropeptide Y Y4 receptor homodimers dissociate upon agonist stimulation. *J Pharmacol Exp Ther*. 2003;307(3):1120-1126.

66. Lukasiewicz S, Polit A, Kedracka-Krok S, Wedzony K, Mackowiak M, Dziedzicka-Wasylewska M. Hetero-dimerization of serotonin 5-HT(2A) and dopamine D(2) receptors. *Biochim Biophys Acta*. 2010;1803(12):1347-1358.

67. Albizu L, Holloway T, Gonzalez-Maeso J, Sealfon SC. Functional crosstalk and heteromerization of serotonin 5-HT2A and dopamine D2 receptors. *Neuropharmacology*. 2011;61(4):770-777.

68. Ciruela F, Casado V, Rodrigues RJ, et al. Presynaptic control of striatal glutamatergic neurotransmission by adenosine A1-A2A receptor heteromers. *J Neurosci*. 2006;26(7):2080-2087.

69. Romano FD, MacDonald SG, Dobson JG, Jr. Adenosine receptor coupling to adenylate cyclase of rat ventricular myocyte membranes. *Am J Physiol*. 1989;257(4 Pt 2):H1088-1095.

70. Gerwins P, Nordstedt C, Fredholm BB. Characterization of adenosine A1 receptors in intact DDT1 MF-2 smooth muscle cells. *Mol Pharmacol.* 1990;38(5):660-666.

71. Carriba P, Ortiz O, Patkar K, et al. Striatal adenosine A2A and cannabinoid CB1 receptors form functional heteromeric complexes that mediate the motor effects of cannabinoids. *Neuropsychopharmacology.* 2007;32(11):2249-2259.

72. Hillion J, Canals M, Torvinen M, et al. Coaggregation, cointernalization, and codesensitization of adenosine A2A receptors and dopamine D2 receptors. *J Biol Chem.* 2002;277(20):18091-18097.

73. Canals M, Burgueno J, Marcellino D, et al. Homodimerization of adenosine A2A receptors: qualitative and quantitative assessment by fluorescence and bioluminescence energy transfer. *J Neurochem.* 2004;88(3):726-734.

74. Kamiya T, Saitoh O, Yoshioka K, Nakata H. Oligomerization of adenosine A2A and dopamine D2 receptors in living cells. *Biochem Biophys Res Commun.* 2003;306(2):544-549.

75. Tanganelli S, Sandager Nielsen K, Ferraro L, et al. Striatal plasticity at the network level. Focus on adenosine A2A and D2 interactions in models of Parkinson's Disease. *Parkinsonism Relat Disord.* 2004;10(5):273-280.

76. Fuxe K, Agnati LF, Jacobsen K, et al. Receptor heteromerization in adenosine A2A receptor signaling: relevance for striatal function and Parkinson's disease. *Neurology.* 2003;61(11 Suppl 6):S19-23.

77. Fuxe K, Ferre S, Canals M, et al. Adenosine A2A and dopamine D2 heteromeric receptor complexes and their function. *J Mol Neurosci.* 2005;26(2-3):209-220.

78. Uberti MA, Hall RA, Minneman KP. Subtype-specific dimerization of alpha 1-adrenoceptors: effects on receptor expression and pharmacological properties. *Mol Pharmacol.* 2003;64(6):1379-1390.

79. Stanasila L, Perez JB, Vogel H, Cotecchia S. Oligomerization of the alpha 1a- and alpha 1b-adrenergic receptor subtypes. Potential implications in receptor internalization. *J Biol Chem*. 2003;278(41):40239-40251.

80. Carrillo JJ, Pediani J, Milligan G. Dimers of class A G protein-coupled receptors function via agonist-mediated trans-activation of associated G proteins. *J Biol Chem*. 2003;278(43):42578-42587.

81. Hague C, Uberti MA, Chen Z, Hall RA, Minneman KP. Cell surface expression of alpha1D-adrenergic receptors is controlled by heterodimerization with alpha1B-adrenergic receptors. *J Biol Chem*. 2004;279(15):15541-15549.

82. Hague C, Lee SE, Chen Z, Prinster SC, Hall RA, Minneman KP. Heterodimers of alpha1B- and alpha1D-adrenergic receptors form a single functional entity. *Mol Pharmacol*. 2006;69(1):45-55.

83. Xu J, He J, Castleberry AM, Balasubramanian S, Lau AG, Hall RA. Heterodimerization of alpha 2A- and beta 1-adrenergic receptors. *J Biol Chem*. 2003;278(12):10770-10777.

84. Vilardaga JP, Nikolaev VO, Lorenz K, Ferrandon S, Zhuang Z, Lohse MJ. Conformational cross-talk between alpha2A-adrenergic and mu-opioid receptors controls cell signaling. *Nat Chem Biol*. 2008;4(2):126-131.

85. AbdAlla S, Lother H, el Massiery A, Quitterer U. Increased AT(1) receptor heterodimers in preeclampsia mediate enhanced angiotensin II responsiveness. *Nat Med*. 2001;7(9):1003-1009.

86. Hansen JL, Hansen JT, Speerschneider T, et al. Lack of evidence for AT1R/B2R heterodimerization in COS-7, HEK293, and NIH3T3 cells: how common is the AT1R/B2R heterodimer? *J Biol Chem*. 2009;284(3):1831-1839.

87. Martinez-Pinilla E, Rodriguez-Perez AI, Navarro G, et al. Dopamine D and angiotensin II type 1 receptors form functional heteromers in rat striatum. *Biochem Pharmacol*. 2015.

88. Rozenfeld R, Gupta A, Gagnidze K, et al. AT1R-CB(1)R heteromerization reveals a new mechanism for the pathogenic properties of angiotensin II. *EMBO J*. 2011;30(12):2350-2363.

89. Zhu WZ, Chakir K, Zhang S, et al. Heterodimerization of beta1- and beta2-adrenergic receptor subtypes optimizes beta-adrenergic modulation of cardiac contractility. *Circ Res*. 2005;97(3):244-251.

90. Jordan BA, Trapaidze N, Gomes I, Nivarthi R, Devi LA. Oligomerization of opioid receptors with beta 2-adrenergic receptors: a role in trafficking and mitogen-activated protein kinase activation. *Proc Natl Acad Sci U S A*. 2001;98(1):343-348.

91. Wrzal PK, Devost D, Petrin D, et al. Allosteric interactions between the oxytocin receptor and the beta2-adrenergic receptor in the modulation of ERK1/2 activation are mediated by heterodimerization. *Cell Signal*. 2012;24(1):342-350.

92. Jarrahian A, Watts VJ, Barker EL. D2 dopamine receptors modulate Galpha-subunit coupling of the CB1 cannabinoid receptor. *J Pharmacol Exp Ther*. 2004;308(3):880-886.

93. Marcellino D, Carriba P, Filip M, et al. Antagonistic cannabinoid CB1/dopamine D2 receptor interactions in striatal CB1/D2 heteromers. A combined neurochemical and behavioral analysis. *Neuropharmacology*. 2008;54(5):815-823.

94. Kearn CS, Blake-Palmer K, Daniel E, Mackie K, Glass M. Concurrent stimulation of cannabinoid CB1 and dopamine D2 receptors enhances heterodimer formation: a mechanism for receptor cross-talk? *Mol Pharmacol*. 2005;67(5):1697-1704.

95. Rozenfeld R, Bushlin I, Gomes I, et al. Receptor Heteromerization Expands the Repertoire of Cannabinoid Signaling in Rodent Neurons. *PLoS ONE*. 2012;7(1):e29239.

96. Rios C, Gomes I, Devi LA. mu opioid and CB1 cannabinoid receptor interactions: reciprocal inhibition of receptor signaling and neuritogenesis. *Br J Pharmacol*. 2006;148(4):387-395.

97. Springael JY, Le Minh PN, Urizar E, Costagliola S, Vassart G, Parmentier M. Allosteric modulation of binding properties between units of chemokine receptor homo- and hetero-oligomers. *Mol Pharmacol.* 2006;69(5):1652-1661.

98. El-Asmar L, Springael JY, Ballet S, Andrieu EU, Vassart G, Parmentier M. Evidence for negative binding cooperativity within CCR5-CCR2b heterodimers. *Mol Pharmacol.* 2005;67(2):460-469.

99. Chen C, Li J, Bot G, Szabo I, Rogers TJ, Liu-Chen LY. Heterodimerization and cross-desensitization between the mu-opioid receptor and the chemokine CCR5 receptor. *Eur J Pharmacol.* 2004;483(2-3):175-186.

100. Parenty G, Appelbe S, Milligan G. CXCR2 chemokine receptor antagonism enhances DOP opioid receptor function via allosteric regulation of the CXCR2-DOP receptor heterodimer. *Biochem J.* 2008;412(2):245-256.

101. Gomes I, Gupta A, Filipovska J, Szeto HH, Pintar JE, Devi LA. A role for heterodimerization of mu and delta opiate receptors in enhancing morphine analgesia. *Proc Natl Acad Sci U S A.* 2004;101(14):5135-5139.

102. Rozenfeld R, Devi LA. Receptor heterodimerization leads to a switch in signaling: beta-arrestin2-mediated ERK activation by mu-delta opioid receptor heterodimers. *FASEB J.* 2007;21(10):2455-2465.

103. Hasbi A, Nguyen T, Fan T, et al. Trafficking of preassembled opioid mu-delta heterooligomer-Gz signaling complexes to the plasma membrane: coregulation by agonists. *Biochemistry.* 2007;46(45):12997-13009.

104. George SR, Fan T, Xie Z, et al. Oligomerization of mu- and delta-opioid receptors. Generation of novel functional properties. *J Biol Chem.* 2000;275(34):26128-26135.

105. Gomes I, Ijzerman AP, Ye K, Maillet EL, Devi LA. G protein-coupled receptor heteromerization: a role in allosteric modulation of ligand binding. *Mol Pharmacol.* 2011;79(6):1044-1052.

106. van Rijn RM, Harvey JH, Brissett DI, DeFriel JN, Whistler JL. Novel screening assay for the selective detection of G-protein-coupled receptor heteromer signaling. *J Pharmacol Exp Ther.* 2013;344(1):179-188.

107. Urizar E, Yano H, Kolster R, Gales C, Lambert N, Javitch JA. CODA-RET reveals functional selectivity as a result of GPCR heteromerization. *Nat Chem Biol.* 2011;7(9):624-630.

108. Rashid AJ, So CH, Kong MM, et al. D1-D2 dopamine receptor heterooligomers with unique pharmacology are coupled to rapid activation of Gq/11 in the striatum. *Proc Natl Acad Sci U S A.* 2007;104(2):654-659.

109. So CH, Varghese G, Curley KJ, et al. D1 and D2 dopamine receptors form heterooligomers and cointernalize after selective activation of either receptor. *Mol Pharmacol.* 2005;68(3):568-578.

110. Marcellino D, Ferre S, Casado V, et al. Identification of dopamine D1-D3 receptor heteromers. Indications for a role of synergistic D1-D3 receptor interactions in the striatum. *J Biol Chem.* 2008;283(38):26016-26025.

111. Fiorentini C, Busi C, Gorruso E, Gotti C, Spano P, Missale C. Reciprocal regulation of dopamine D1 and D3 receptor function and trafficking by heterodimerization. *Mol Pharmacol.* 2008;74(1):59-69.

112. Ferrada C, Ferre S, Casado V, et al. Interactions between histamine H3 and dopamine D2 receptors and the implications for striatal function. *Neuropharmacology.* 2008;55(2):190-197.

113. Han Y, Moreira IS, Urizar E, Weinstein H, Javitch JA. Allosteric communication between protomers of dopamine class A GPCR dimers modulates activation. *Nat Chem Biol.* 2009;5(9):688-695.

114. Scarselli M, Novi F, Schallmach E, et al. D2/D3 dopamine receptor heterodimers exhibit unique functional properties. *J Biol Chem.* 2001;276(32):30308-30314.

115. Maggio R, Scarselli M, Novi F, Millan MJ, Corsini GU. Potent activation of dopamine D3/D2 heterodimers by the antiparkinsonian agents, S32504, pramipexole and ropinirole. *J Neurochem.* 2003;87(3):631-641.

116. Rocheville M, Lange DC, Kumar U, Patel SC, Patel RC, Patel YC. Receptors for dopamine and somatostatin: formation of hetero-oligomers with enhanced functional activity. *Science.* 2000;288(5463):154-157.

117. Koschatzky S, Tschammer N, Gmeiner P. Cross-receptor interactions between dopamine D2L and neurotensin NTS1 receptors modulate binding affinities of dopaminergics. *ACS Chem Neurosci.* 2011;2(6):308-316.

118. Pfeiffer M, Koch T, Schroder H, Laugsch M, Hollt V, Schulz S. Heterodimerization of somatostatin and opioid receptors cross-modulates phosphorylation, internalization, and desensitization. *J Biol Chem.* 2002;277(22):19762-19772.

119. Rocheville M, Lange DC, Kumar U, Sasi R, Patel RC, Patel YC. Subtypes of the somatostatin receptor assemble as functional homo- and heterodimers. *J Biol Chem.* 2000;275(11):7862-7869.

120. Terrillon S, Barberis C, Bouvier M. Heterodimerization of V1a and V2 vasopressin receptors determines the interaction with beta-arrestin and their trafficking patterns. *Proc Natl Acad Sci U S A.* 2004;101(6):1548-1553.

121. Skieterska K, Duchou J, Lintermans B, Van Craenenbroeck K. Detection of G protein-coupled receptor (GPCR) dimerization by coimmunoprecipitation. *Methods Cell Biol.* 2013;117:323-340.

122. Park PS, Wells JW. Oligomeric potential of the M2 muscarinic cholinergic receptor. *J Neurochem.* 2004;90(3):537-548.

123. Gomes I, Jordan BA, Gupta A, Rios C, Trapaidze N, Devi LA. G protein coupled receptor dimerization: implications in modulating receptor function. *J Mol Med (Berl).* 2001;79(5-6):226-242.

124. Rios CD, Jordan BA, Gomes I, Devi LA. G-protein-coupled receptor dimerization: modulation of receptor function. *Pharmacol Ther.* 2001;92(2-3):71-87.

125. Angers S, Salahpour A, Bouvier M. Dimerization: an emerging concept for G protein-coupled receptor ontogeny and function. *Annu Rev Pharmacol Toxicol.* 2002;42:409-435.

126. Berthouze M, Ayoub M, Russo O, et al. Constitutive dimerization of human serotonin 5-HT4 receptors in living cells. *FEBS Lett*. 2005;579(14):2973-2980.

127. Ciruela F, Casado V, Mallol J, Canela EI, Lluis C, Franco R. Immunological identification of A1 adenosine receptors in brain cortex. *J Neurosci Res*. 1995;42(6):818-828.

128. Dorsch S, Klotz KN, Engelhardt S, Lohse MJ, Bunemann M. Analysis of receptor oligomerization by FRAP microscopy. *Nat Methods*. 2009;6(3):225-230.

129. Mercier JF, Salahpour A, Angers S, Breit A, Bouvier M. Quantitative assessment of beta 1- and beta 2-adrenergic receptor homo- and heterodimerization by bioluminescence resonance energy transfer. *J Biol Chem*. 2002;277(47):44925-44931.

130. Bai M, Trivedi S, Brown EM. Dimerization of the extracellular calcium-sensing receptor (CaR) on the cell surface of CaR-transfected HEK293 cells. *J Biol Chem*. 1998;273(36):23605-23610.

131. Ward DT, Brown EM, Harris HW. Disulfide bonds in the extracellular calcium-polyvalent cation-sensing receptor correlate with dimer formation and its response to divalent cations in vitro. *J Biol Chem*. 1998;273(23):14476-14483.

132. Rodriguez-Frade JM, Vila-Coro AJ, de Ana AM, Albar JP, Martinez AC, Mellado M. The chemokine monocyte chemoattractant protein-1 induces functional responses through dimerization of its receptor CCR2. *Proc Natl Acad Sci U S A*. 1999;96(7):3628-3633.

133. Vila-Coro AJ, Mellado M, Martín de Ana A, et al. HIV-1 infection through the CCR5 receptor is blocked by receptor dimerization. *Proceedings of the National Academy of Sciences of the United States of America*. 2000;97(7):3388-3393.

134. Wilson S, Wilkinson G, Milligan G. The CXCR1 and CXCR2 receptors form constitutive homo- and heterodimers selectively and with equal apparent affinities. *J Biol Chem*. 2005;280(31):28663-28674.

135. Trettel F, Di Bartolomeo S, Lauro C, Catalano M, Ciotti MT, Limatola C. Ligand-independent CXCR2 dimerization. *J Biol Chem*. 2003;278(42):40980-40988.

136. Gomes I, Filipovska J, Jordan BA, Devi LA. Oligomerization of opioid receptors. *Methods*. 2002;27(4):358-365.

137. George SR, Lee SP, Varghese G, et al. A transmembrane domain-derived peptide inhibits D1 dopamine receptor function without affecting receptor oligomerization. *J Biol Chem*. 1998;273(46):30244-30248.

138. Lee SP, So CH, Rashid AJ, et al. Dopamine D1 and D2 Receptor Co-activation Generates a Novel Phospholipase C-mediated Calcium Signal. *Journal of Biological Chemistry*. 2004;279(34):35671-35678.

139. Lee SP, O'Dowd BF, Ng GY, et al. Inhibition of cell surface expression by mutant receptors demonstrates that D2 dopamine receptors exist as oligomers in the cell. *Mol Pharmacol*. 2000;58(1):120-128.

140. Ng GY, O'Dowd BF, Caron M, Dennis M, Brann MR, George SR. Phosphorylation and palmitoylation of the human D2L dopamine receptor in Sf9 cells. *J Neurochem*. 1994;63(5):1589-1595.

141. Nimchinsky EA, Hof PR, Janssen WG, Morrison JH, Schmauss C. Expression of dopamine D3 receptor dimers and tetramers in brain and in transfected cells. *J Biol Chem*. 1997;272(46):29229-29237.

142. Wang D, Sun X, Bohn LM, Sadee W. Opioid receptor homo- and heterodimerization in living cells by quantitative bioluminescence resonance energy transfer. *Mol Pharmacol*. 2005;67(6):2173-2184.

143. Ayoub MA, Couturier C, Lucas-Meunier E, et al. Monitoring of ligand-independent dimerization and ligand-induced conformational changes of melatonin receptors in living cells by bioluminescence resonance energy transfer. *J Biol Chem*. 2002;277(24):21522-21528.

144. Robbins MJ, Ciruela F, Rhodes A, McIlhinney RA. Characterization of the dimerization of metabotropic glutamate receptors using an N-terminal truncation of mGluR1alpha. *J Neurochem*. 1999;72(6):2539-2547.

145. Romano C, Yang WL, O'Malley KL. Metabotropic glutamate receptor 5 is a disulfide-linked dimer. *J Biol Chem*. 1996;271(45):28612-28616.

146. Hu J, Thor D, Zhou Y, et al. Structural aspects of M(3) muscarinic acetylcholine receptor dimer formation and activation. *FASEB J*. 2012;26(2):604-616.

147. Terrillon S, Durroux T, Mouillac B, et al. Oxytocin and vasopressin V1a and V2 receptors form constitutive homo- and heterodimers during biosynthesis. *Mol Endocrinol*. 2003;17(4):677-691.

148. Ban T, Kosugi S, Kohn LD. Specific antibody to the thyrotropin receptor identifies multiple receptor forms in membranes of cells transfected with wild-type receptor complementary deoxyribonucleic acid: characterization of their relevance to receptor synthesis, processing, structure, and function. *Endocrinology*. 1992;131(2):815-829.

149. Szidonya L, Cserzo M, Hunyady L. Dimerization and oligomerization of G-protein-coupled receptors: debated structures with established and emerging functions. *J Endocrinol*. 2008;196(3):435-453.

150. Salim K, Fenton T, Bacha J, et al. Oligomerization of G-protein-coupled receptors shown by selective co-immunoprecipitation. *J Biol Chem*. 2002;277(18):15482-15485.

151. Chabre M, le Maire M. Monomeric G-protein-coupled receptor as a functional unit. *Biochemistry*. 2005;44(27):9395-9403.

152. Breton B, Lagace M, Bouvier M. Combining resonance energy transfer methods reveals a complex between the alpha2A-adrenergic receptor, Galphai1beta1gamma2, and GRK2. *FASEB J*. 2010;24(12):4733-4743.

153. Eidne KA, Kroeger KM, Hanyaloglu AC. Applications of novel resonance energy transfer techniques to study dynamic hormone receptor interactions in living cells. *Trends Endocrinol Metab*. 2002;13(10):415-421.

154. Ward RJ, Milligan G. Structural and biophysical characterisation of G protein-coupled receptor ligand binding using resonance energy transfer and fluorescent labelling techniques. *Biochim Biophys Acta*. 2014;1838(1 Pt A):3-14.

155. Zheng Y, Akgun E, Harikumar KG, et al. Induced association of mu opioid (MOP) and type 2 cholecystokinin (CCK2) receptors by novel bivalent ligands. *J Med Chem*. 2009;52(2):247-258.

156. Pollok BA, Heim R. Using GFP in FRET-based applications. *Trends Cell Biol*. 1999;9(2):57-60.

157. Förster T. Zwischenmolekulare Energiewanderung und Fluoreszenz. *Annalen der Physik*. 1948;437(1-2):55-75.

158. Palczewski K, Kumasaka T, Hori T, et al. Crystal structure of rhodopsin: A G protein-coupled receptor. *Science*. 2000;289(5480):739-745.

159. Okada T, Le Trong I, Fox BA, Behnke CA, Stenkamp RE, Palczewski K. X-Ray diffraction analysis of three-dimensional crystals of bovine rhodopsin obtained from mixed micelles. *J Struct Biol*. 2000;130(1):73-80.

160. Xu Y, Piston DW, Johnson CH. A bioluminescence resonance energy transfer (BRET) system: application to interacting circadian clock proteins. *Proc Natl Acad Sci U S A*. 1999;96(1):151-156.

161. Krebs A, Villa C, Edwards PC, Schertler GF. Characterisation of an improved two-dimensional p22121 crystal from bovine rhodopsin. *J Mol Biol*. 1998;282(5):991-1003.

162. Schertler GFX, Villa C, Henderson R. Projection structure of rhodopsin. *Nature*. 1993;362(6422):770-772.

163. Cherezov V, Rosenbaum DM, Hanson MA, et al. High-resolution crystal structure of an engineered human beta2-adrenergic G protein-coupled receptor. *Science*. 2007;318(5854):1258-1265.

164. Jaakola V-P, Griffith MT, Hanson MA, et al. The 2.6 Å Crystal Structure of a Human A(2A) Adenosine Receptor Bound to an Antagonist. *Science (New York, N.Y.)*. 2008;322(5905):1211-1217.

165. Warne T, Serrano-Vega MJ, Baker JG, et al. Structure of a beta1-adrenergic G-protein-coupled receptor. *Nature*. 2008;454(7203):486-491.

166. Wu B, Chien EY, Mol CD, et al. Structures of the CXCR4 chemokine GPCR with small-molecule and cyclic peptide antagonists. *Science*. 2010;330(6007):1066-1071.

167. Chien EY, Liu W, Zhao Q, et al. Structure of the human dopamine D3 receptor in complex with a D2/D3 selective antagonist. *Science*. 2010;330(6007):1091-1095.

168. Shimamura T, Shiroishi M, Weyand S, et al. Structure of the human histamine H1 receptor complex with doxepin. *Nature*. 2011;475(7354):65-70.

169. Granier S, Manglik A, Kruse AC, et al. Structure of the delta-opioid receptor bound to naltrindole. *Nature*. 2012;485(7398):400-404.

170. Wu H, Wacker D, Katritch V, et al. Structure of the human kappa opioid receptor in complex with JDTic. *Nature*. 2012;485(7398):327-332.

171. Manglik A, Kruse AC, Kobilka TS, et al. Crystal structure of the [micro]-opioid receptor bound to a morphinan antagonist. *Nature*. 2012;485(7398):321-326.

172. Haga K, Kruse AC, Asada H, et al. Structure of the human M(2) muscarinic acetylcholine receptor bound to an antagonist. *Nature*. 2012;482(7386):547-551.

173. Kruse AC, Hu J, Pan AC, et al. Structure and dynamics of the M3 muscarinic acetylcholine receptor. *Nature*. 2012;482(7386):552-556.

174. White JF, Noinaj N, Shibata Y, et al. Structure of the agonist-bound neurotensin receptor. *Nature*. 2012;490(7421):508-513.

175. Thompson AA, Liu W, Chun E, et al. Structure of the nociceptin/orphanin FQ receptor in complex with a peptide mimetic. *Nature*. 2012;485(7398):395-399.

176. Zhang C, Srinivasan Y, Arlow DH, et al. High-resolution crystal structure of human protease-activated receptor 1. *Nature*. 2012;492(7429):387-392.

177. Hanson MA, Roth CB, Jo E, et al. Crystal structure of a lipid G protein-coupled receptor. *Science*. 2012;335(6070):851-855.

178. Wang C, Jiang Y, Ma J, et al. Structural basis for molecular recognition at serotonin receptors. *Science*. 2013;340(6132):610-614.

179. Wacker D, Wang C, Katritch V, et al. Structural features for functional selectivity at serotonin receptors. *Science*. 2013;340(6132):615-619.

180. Tan Q, Zhu Y, Li J, et al. Structure of the CCR5 chemokine receptor-HIV entry inhibitor maraviroc complex. *Science*. 2013;341(6152):1387-1390.

181. Hollenstein K, Kean J, Bortolato A, et al. Structure of class B GPCR corticotropin-releasing factor receptor 1. *Nature*. 2013;499(7459):438-443.

182. Siu FY, He M, de Graaf C, et al. Structure of the human glucagon class B G-protein-coupled receptor. *Nature*. 2013;499(7459):444-449.

183. Wang C, Wu H, Katritch V, et al. Structure of the human smoothened receptor bound to an antitumour agent. *Nature*. 2013;497(7449):338-343.

184. Wu H, Wang C, Gregory KJ, et al. Structure of a class C GPCR metabotropic glutamate receptor 1 bound to an allosteric modulator. *Science*. 2014;344(6179):58-64.

185. Zhang K, Zhang J, Gao ZG, et al. Structure of the human P2Y12 receptor in complex with an antithrombotic drug. *Nature*. 2014;509(7498):115-118.

186. Zhang H, Unal H, Gati C, et al. Structure of the Angiotensin Receptor Revealed by Serial Femtosecond Crystallography. *Cell*. 2015.

187. Ghosh E, Kumari P, Jaiman D, Shukla AK. Methodological advances: the unsung heroes of the GPCR structural revolution. *Nat Rev Mol Cell Biol*. 2015;16(2):69-81.

188. Li YY, Hou TJ, Goddard WA, 3rd. Computational modeling of structure-function of g protein-coupled receptors with applications for drug design. *Current medicinal chemistry*. 2010;17(12):1167-1180.

189. Sandal M, Duy TP, Cona M, et al. GOMoDo: A GPCRs online modeling and docking webserver. *PloS one*. 2013;8(9):e74092.

190. Soding J. Protein homology detection by HMM-HMM comparison. *Bioinformatics*. 2005;21(7):951-960.

191. Soding J, Biegert A, Lupas AN. The HHpred interactive server for protein homology detection and structure prediction. *Nucleic acids research*. 2005;33(Web Server issue):W244-248.

192. Altschul SF, Gish W, Miller W, Myers EW, Lipman DJ. Basic local alignment search tool. *Journal of molecular biology*. 1990;215(3):403-410.

193. Altschul SF, Madden TL, Schaffer AA, et al. Gapped BLAST and PSI-BLAST: a new generation of protein database search programs. *Nucleic acids research*. 1997;25(17):3389-3402.

194. Eswar N, Webb B, Marti-Renom MA, et al. Comparative protein structure modeling using MODELLER. *Current protocols in protein science / editorial board, John E. Coligan ... [et al.]*. 2007;Chapter 2:Unit 2.9.

195. Marti-Renom MA, Stuart AC, Fiser A, Sanchez R, Melo F, Sali A. Comparative protein structure modeling of genes and genomes. *Annual review of biophysics and biomolecular structure*. 2000;29:291-325.

196. Sali A, Blundell TL. Comparative protein modelling by satisfaction of spatial restraints. *Journal of molecular biology*. 1993;234(3):779-815.

197. Fiser A, Do RK, Sali A. Modeling of loops in protein structures. *Protein science : a publication of the Protein Society*. 2000;9(9):1753-1773.

198. Trott O, Olson AJ. AutoDock Vina: improving the speed and accuracy of docking with a new scoring function, efficient optimization, and multithreading. *Journal of computational chemistry*. 2010;31(2):455-461.

199. Dominguez C, Boelens R, Bonvin AM. HADDOCK: a protein-protein docking approach based on biochemical or biophysical information. *Journal of the American Chemical Society*. 2003;125(7):1731-1737.

200. de Vries SJ, van Dijk AD, Krzeminski M, et al. HADDOCK versus HADDOCK: new features and performance of HADDOCK2.0 on the CAPRI targets. *Proteins*. 2007;69(4):726-733.

201. van Dijk AD, Bonvin AM. Solvated docking: introducing water into the modelling of biomolecular complexes. *Bioinformatics (Oxford, England)*. 2006;22(19):2340-2347.

202. Willard L, Ranjan A, Zhang H, et al. VADAR: a web server for quantitative evaluation of protein structure quality. *Nucleic Acids Res*. 2003;31(13):3316-3319.

203. Li J, Deng X, Eickholt J, Cheng J. Designing and benchmarking the MULTICOM protein structure prediction system. *BMC Struct Biol*. 2013;13:2.

204. Shen MY, Sali A. Statistical potential for assessment and prediction of protein structures. *Protein Sci*. 2006;15(11):2507-2524.

205. John B, Sali A. Comparative protein structure modeling by iterative alignment, model building and model assessment. *Nucleic acids research*. 2003;31(14):3982-3992.

206. Melo F, Sanchez R, Sali A. Statistical potentials for fold assessment. *Protein Sci*. 2002;11(2):430-448.

207. Atlas SA. The renin-angiotensin aldosterone system: pathophysiological role and pharmacologic inhibition. *J Manag Care Pharm*. 2007;13(8 Suppl B):9-20.

208. Brown MJ. Direct renin inhibition — a new way of targeting the renin system. *Journal of Renin-Angiotensin-Aldosterone System*. 2006;7(2 suppl):S7-S11.

209. Morgan L, Broughton Pipkin F, Kalsheker N. Angiotensinogen: molecular biology, biochemistry and physiology. *Int J Biochem Cell Biol*. 1996;28(11):1211-1222.

210. Zaman MA, Oparil S, Calhoun DA. Drugs targeting the renin-angiotensin-aldosterone system. *Nat Rev Drug Discov*. 2002;1(8):621-636.

211. Lonn EM, Yusuf S, Jha P, et al. Emerging role of angiotensin-converting enzyme inhibitors in cardiac and vascular protection. *Circulation*. 1994;90(4):2056-2069.

212. Thompson AA, Liu W, Chun E, et al. Structure of the Nociceptin/Orphanin FQ Receptor in Complex with a Peptide Mimetic. *Nature*. 2012;485(7398):395-399.

213. Unal H, Jagannathan R, Bhatnagar A, Tirupula K, Desnoyer R, Karnik SS. Long range effect of mutations on specific conformational changes in the extracellular loop 2 of angiotensin II type 1 receptor. *J Biol Chem*. 2013;288(1):540-551.

214. Balakumar P, Jagadeesh G. Structural determinants for binding, activation, and functional selectivity of the angiotensin AT1 receptor. *J Mol Endocrinol*. 2014;53(2):R71-92.

215. Katritch V, Fenalti G, Abola EE, Roth BL, Cherezov V, Stevens RC. Allosteric sodium in class A GPCR signaling. *Trends in Biochemical Sciences*. 2014;39(5):233-244.

216. Fenalti G, Giguere PM, Katritch V, et al. Molecular control of delta-opioid receptor signalling. *Nature*. 2014;506(7487):191-196.

217. Ricchiuti V, Lapointe N, Pojoga L, et al. Dietary sodium intake regulates angiotensin II type 1, mineralocorticoid receptor, and associated signaling proteins in heart. *J Endocrinol*. 2011;211(1):47-54.

218. AbdAlla S, Abdel-Baset A, Lother H, el Massiery A, Quitterer U. Mesangial AT1/B2 receptor heterodimers contribute to angiotensin II hyperresponsiveness in experimental hypertension. *J Mol Neurosci*. 2005;26(2-3):185-192.

219. UniProt: a hub for protein information. *Nucleic Acids Res*. 2015;43(Database issue):D204-212.

220. Chen H, Zhou H-X. Prediction of solvent accessibility and sites of deleterious mutations from protein sequence. *Nucleic Acids Research*. 2005;33(10):3193-3199.

221. Johnston JM, Aburi M, Provasi D, et al. Making Structural Sense of Dimerization Interfaces of Delta Opioid Receptor Homodimers. *Biochemistry*. 2011;50(10):1682-1690.

222. Huang J, Chen S, Zhang JJ, Huang XY. Crystal structure of oligomeric beta1-adrenergic G protein-coupled receptors in ligand-free basal state. *Nat Struct Mol Biol*. 2013;20(4):419-425.

223. Insel PA, Tang CM, Hahntow I, Michel MC. Impact of GPCRs in clinical medicine: monogenic diseases, genetic variants and drug targets. *Biochim Biophys Acta*. 2007;1768(4):994-1005.

224. Pin JP, Neubig R, Bouvier M, et al. International Union of Basic and Clinical Pharmacology. LXVII. Recommendations for the recognition and nomenclature of G protein-coupled receptor heteromultimers. *Pharmacol Rev*. 2007;59(1):5-13.

225. Chalothorn D, McCune DF, Edelmann SE, Garcia-Cazarin ML, Tsujimoto G, Piascik MT. Differences in the cellular localization and agonist-mediated internalization properties of the alpha(1)-adrenoceptor subtypes. *Mol Pharmacol*. 2002;61(5):1008-1016.

226. He SQ, Zhang ZN, Guan JS, et al. Facilitation of mu-opioid receptor activity by preventing delta-opioid receptor-mediated codegradation. *Neuron*. 2011;69(1):120-131.

227. Sohy D, Yano H, de Nadai P, et al. Hetero-oligomerization of CCR2, CCR5, and CXCR4 and the Protean Effects of "Selective" Antagonists. *Journal of Biological Chemistry*. 2009;284(45):31270-31279.

228. Wang J, He L, Combs CA, Roderiquez G, Norcross MA. Dimerization of CXCR4 in living malignant cells: control of cell migration by a synthetic peptide that reduces homologous CXCR4 interactions. *Molecular Cancer Therapeutics*. 2006;5(10):2474-2483.

229. Sohy D, Parmentier M, Springael J-Y. Allosteric Transinhibition by Specific Antagonists in CCR2/CXCR4 Heterodimers. *Journal of Biological Chemistry*. 2007;282(41):30062-30069.

230. Ng GYK, O'Dowd BF, Lee SP, et al. Dopamine D2 Receptor Dimers and Receptor-Blocking Peptides. *Biochemical and Biophysical Research Communications*. 1996;227(1):200-204.

231. George SR, Ng GYK, Lee SP, et al. Blockade of G Protein-Coupled Receptors and the Dopamine Transporter by a Transmembrane Domain Peptide: Novel Strategy for Functional Inhibition of Membrane Proteins in Vivo. *Journal of Pharmacology and Experimental Therapeutics*. 2003;307(2):481-489.

232. Drinovec L, Kubale V, Nøhr Larsen J, Vrecl M. Mathematical Models for Quantitative Assessment of Bioluminescence Resonance Energy Transfer: Application to Seven Transmembrane Receptors Oligomerization. *Frontiers in Endocrinology*. 2012;3:104.

APPENDIX I COPYRIGHT PERMISSION FOR FIGURE 1

NATURE PUBLISHING GROUP LICENSE TERMS AND CONDITIONS

Jun 24, 2015

This is an Agreement between Brent M Young ("You") and Nature Publishing Group ("Nature Publishing Group"). It consists of your order details, the terms and conditions provided by Nature Publishing Group, and the payment terms and conditions.

All payments must be made in full to CCC. For payment instructions, please see information listed at the bottom of this form.

License Number	3627721020077
License date	May 14, 2015
Licensed Content Publisher	Nature Publishing Group
Licensed Content Publication	Nature Reviews Molecular Cell Biology
Licensed Content Title	Fine-tuning of GPCR activity by receptor-interacting proteins
Licensed Content Author	Stefanie L. Ritter and Randy A. Hall
Licensed Content Date	Dec 1, 2009
Volume number	10
Issue number	12
Type of Use	reuse in a dissertation / thesis
Requestor type	academic/educational
Format	print and electronic
Portion	figures/tables/illustrations
Number of figures/tables/illustrations	1
High-res required	no
Figures	Box 1
Author of this NPG article	no
Your reference number	None
Title of your thesis / dissertation	Transmembrane domains IV, V and VI participate in human angiotensin II type 1 receptor homomerization
Expected completion date	Jun 2015
Estimated size (number of pages)	100
Total	**0.00 CAD**
Terms and Conditions	

Terms and Conditions for Permissions

Nature Publishing Group hereby grants you a non-exclusive license to reproduce this material for this purpose, and for no other use,subject to the conditions below:

1. NPG warrants that it has, to the best of its knowledge, the rights to license reuse of this material. However, you should ensure that the material you are requesting is original to Nature Publishing Group and does not carry the copyright of another entity (as credited in the published version). If the credit line on any part of the material you have requested indicates that it was reprinted or adapted by NPG with permission from another source, then you should also seek permission from that source to reuse the material.

2. Permission granted free of charge for material in print is also usually granted for any electronic version of that work, provided that the material is incidental to the work as a whole and that the electronic version is essentially

equivalent to, or substitutes for, the print version.Where print permission has been granted for a fee, separate permission must be obtained for any additional, electronic re-use (unless, as in the case of a full paper, this has already been accounted for during your initial request in the calculation of a print run).NB: In all cases, web-based use of full-text articles must be authorized separately through the 'Use on a Web Site' option when requesting permission.

3. Permission granted for a first edition does not apply to second and subsequent editions and for editions in other languages (except for signatories to the STM Permissions Guidelines, or where the first edition permission was granted for free).

4. Nature Publishing Group's permission must be acknowledged next to the figure, table or abstract in print. In electronic form, this acknowledgement must be visible at the same time as the figure/table/abstract, and must be hyperlinked to the journal's homepage.

5. The credit line should read:
   Reprinted by permission from Macmillan Publishers Ltd: [JOURNAL NAME] (reference citation), copyright (year of publication)
   For AOP papers, the credit line should read:
   Reprinted by permission from Macmillan Publishers Ltd: [JOURNAL NAME], advance online publication, day month year (doi: 10.1038/sj.[JOURNAL ACRONYM].XXXXX)

   Note: For republication from the *British Journal of Cancer*, the following credit lines apply.
   Reprinted by permission from Macmillan Publishers Ltd on behalf of Cancer Research UK: [JOURNAL NAME] (reference citation), copyright (year of publication)For AOP papers, the credit line should read:
   Reprinted by permission from Macmillan Publishers Ltd on behalf of Cancer Research UK: [JOURNAL NAME], advance online publication, day month year (doi: 10.1038/sj.[JOURNAL ACRONYM].XXXXX)

6. Adaptations of single figures do not require NPG approval. However, the adaptation should be credited as follows:

   Adapted by permission from Macmillan Publishers Ltd: [JOURNAL NAME] (reference citation), copyright (year of publication)

   Note: For adaptation from the *British Journal of Cancer*, the following credit line applies.
   Adapted by permission from Macmillan Publishers Ltd on behalf of Cancer Research UK: [JOURNAL NAME] (reference citation), copyright (year of publication)

7. Translations of 401 words up to a whole article require NPG approval. Please visit http://www.macmillanmedicalcommunications.com for more information.Translations of up to a 400 words do not require NPG approval. The translation should be credited as follows:

   Translated by permission from Macmillan Publishers Ltd: [JOURNAL NAME] (reference citation), copyright (year of publication).

   Note: For translation from the *British Journal of Cancer*, the following credit line applies.
   Translated by permission from Macmillan Publishers Ltd on behalf of Cancer Research UK: [JOURNAL NAME] (reference citation), copyright (year of publication)

We are certain that all parties will benefit from this agreement and wish you the best in the use of this material. Thank you.
Special Terms:
v1.1

APPENDIX II COPYRIGHT PERMISSION FOR FIGURE 2

RE: Copyright Permission - Thesis (Young)

JournalForms <JournalForms@faseb.org>

Fri 5/15/2015 12:10 PM

Inbox

To:Brent Young <Brent.Young@Dal.Ca>;

Cc:Mooneyhan, Cody <cmooneyhan@faseb.org>;

Good Morning Dr. Young,

Permission is granted to use the figure as outlined below.

Thank you,
Journal Forms Staff
FASEB Office of Publications
9650 Rockville Pike
Bethesda, Maryland 20814
Fax (240) 407-4430
E-mail journalforms@faseb.org<mailto:journalforms@faseb.org>
Web www.FASEB.org<http://www.faseb.org/>

From: Brent Young [Brent.Young@Dal.Ca]
Sent: Friday, May 15, 2015 10:45 AM
To: JournalForms
Subject: Copyright Permission - Thesis

1. Brent M Young
2. Figure 1A
3. Breton B, Lagace M, Bouvier M. Combining resonance energy transfer methods reveals a complex between the alpha2A-adrenergic receptor, Galphai1beta1gamma2, and GRK2. FASEB J. 2010;24(12):4733-4743. DOI:10.1096/fj.10-164061. http://www.fasebj.org/content/24/12/4733.full
4. Thesis - MSc
5. Dalhousie University - Department of Pharmacology - http://medicine.dal.ca/departments/department-sites/pharmacology.html

APPENDIX III COPYRIGHT PERMISSION FOR FIGURE 3

NATURE PUBLISHING GROUP LICENSE TERMS AND CONDITIONS

Jun 24, 2015

This is an Agreement between Brent M Young ("You") and Nature Publishing Group ("Nature Publishing Group"). It consists of your order details, the terms and conditions provided by Nature Publishing Group, and the payment terms and conditions.

All payments must be made in full to CCC. For payment instructions, please see information listed at the bottom of this form.

License Number	3640271306786
License date	Jun 01, 2015
Licensed Content Publisher	Nature Publishing Group
Licensed Content Publication	Nature Reviews Drug Discovery
Licensed Content Title	Drugs targeting the renin|[ndash]|angiotensin|[ndash]|aldosterone system
Licensed Content Author	Mohammad Amin Zaman,Suzanne OparilandDavid A. Calhoun
Licensed Content Date	Aug 1, 2002
Volume number	1
Issue number	8
Type of Use	reuse in a dissertation / thesis
Requestor type	academic/educational
Format	print and electronic
Portion	figures/tables/illustrations
Number of figures/tables/illustrations	1
High-res required	no
Figures	Figure 1
Author of this NPG article	no
Your reference number	None
Title of your thesis / dissertation	Transmembrane domains IV, V and VI participate in human angiotensin II type 1 receptor homomerization
Expected completion date	Jun 2015
Estimated size (number of pages)	100
Total	**0.00 CAD**
Terms and Conditions	

Terms and Conditions for Permissions

Nature Publishing Group hereby grants you a non-exclusive license to reproduce this material for this purpose, and for no other use,subject to the conditions below:

1. NPG warrants that it has, to the best of its knowledge, the rights to license reuse of this material. However, you should ensure that the material you are requesting is original to Nature Publishing Group and does not carry the copyright of another entity (as credited in the published version). If the credit line on any part of the material you have requested indicates that it was reprinted or adapted by NPG with permission from another source, then you should also seek permission from that source to reuse the material.

2. Permission granted free of charge for material in print is also usually granted for any electronic version of that work, provided that the material is incidental to the work as a whole and that the electronic version is essentially

equivalent to, or substitutes for, the print version.Where print permission has been granted for a fee, separate permission must be obtained for any additional, electronic re-use (unless, as in the case of a full paper, this has already been accounted for during your initial request in the calculation of a print run).NB: In all cases, web-based use of full-text articles must be authorized separately through the 'Use on a Web Site' option when requesting permission.

3. Permission granted for a first edition does not apply to second and subsequent editions and for editions in other languages (except for signatories to the STM Permissions Guidelines, or where the first edition permission was granted for free).

4. Nature Publishing Group's permission must be acknowledged next to the figure, table or abstract in print. In electronic form, this acknowledgement must be visible at the same time as the figure/table/abstract, and must be hyperlinked to the journal's homepage.

5. The credit line should read:
   Reprinted by permission from Macmillan Publishers Ltd: [JOURNAL NAME] (reference citation), copyright (year of publication)
   For AOP papers, the credit line should read:
   Reprinted by permission from Macmillan Publishers Ltd: [JOURNAL NAME], advance online publication, day month year (doi: 10.1038/sj.[JOURNAL ACRONYM].XXXXX)

   Note: For republication from the *British Journal of Cancer*, the following credit lines apply.
   Reprinted by permission from Macmillan Publishers Ltd on behalf of Cancer Research UK: [JOURNAL NAME] (reference citation), copyright (year of publication)For AOP papers, the credit line should read:
   Reprinted by permission from Macmillan Publishers Ltd on behalf of Cancer Research UK: [JOURNAL NAME], advance online publication, day month year (doi: 10.1038/sj.[JOURNAL ACRONYM].XXXXX)

6. Adaptations of single figures do not require NPG approval. However, the adaptation should be credited as follows:

   Adapted by permission from Macmillan Publishers Ltd: [JOURNAL NAME] (reference citation), copyright (year of publication)

   Note: For adaptation from the *British Journal of Cancer*, the following credit line applies.
   Adapted by permission from Macmillan Publishers Ltd on behalf of Cancer Research UK: [JOURNAL NAME] (reference citation), copyright (year of publication)

7. Translations of 401 words up to a whole article require NPG approval. Please visit http://www.macmillanmedicalcommunications.com for more information.Translations of up to a 400 words do not require NPG approval. The translation should be credited as follows:

   Translated by permission from Macmillan Publishers Ltd: [JOURNAL NAME] (reference citation), copyright (year of publication).

   Note: For translation from the *British Journal of Cancer*, the following credit line applies.
   Translated by permission from Macmillan Publishers Ltd on behalf of Cancer Research UK: [JOURNAL NAME] (reference citation), copyright (year of publication)

We are certain that all parties will benefit from this agreement and wish you the best in the use of this material. Thank you.
Special Terms:
v1.1

APPENDIX IV COPYRIGHT PERMISSION FOR FIGURE 4

NATURE PUBLISHING GROUP LICENSE TERMS AND CONDITIONS

Jun 24, 2015

This is an Agreement between Brent M Young ("You") and Nature Publishing Group ("Nature Publishing Group"). It consists of your order details, the terms and conditions provided by Nature Publishing Group, and the payment terms and conditions.

All payments must be made in full to CCC. For payment instructions, please see information listed at the bottom of this form.

License Number	3640270786187
License date	Jun 01, 2015
Licensed Content Publisher	Nature Publishing Group
Licensed Content Publication	Nature Reviews Drug Discovery
Licensed Content Title	Drugs targeting the renin|[ndash]|angiotensin|[ndash]|aldosterone system
Licensed Content Author	Mohammad Amin Zaman,Suzanne OparilandDavid A. Calhoun
Licensed Content Date	Aug 1, 2002
Volume number	1
Issue number	8
Type of Use	reuse in a dissertation / thesis
Requestor type	academic/educational
Format	print and electronic
Portion	figures/tables/illustrations
Number of figures/tables/illustrations	1
High-res required	no
Figures	Figure 3
Author of this NPG article	no
Your reference number	None
Title of your thesis / dissertation	Transmembrane domains IV, V and VI participate in human angiotensin II type 1 receptor homomerization
Expected completion date	Jun 2015
Estimated size (number of pages)	100
Total	**0.00 CAD**
Terms and Conditions	

Terms and Conditions for Permissions

Nature Publishing Group hereby grants you a non-exclusive license to reproduce this material for this purpose, and for no other use,subject to the conditions below:

1. NPG warrants that it has, to the best of its knowledge, the rights to license reuse of this material. However, you should ensure that the material you are requesting is original to Nature Publishing Group and does not carry the copyright of another entity (as credited in the published version). If the credit line on any part of the material you have requested indicates that it was reprinted or adapted by NPG with permission from another source, then you should also seek permission from that source to reuse the material.

2. Permission granted free of charge for material in print is also usually granted for any electronic version of that work, provided that the material is incidental to the work as a whole and that the electronic version is essentially

equivalent to, or substitutes for, the print version.Where print permission has been granted for a fee, separate permission must be obtained for any additional, electronic re-use (unless, as in the case of a full paper, this has already been accounted for during your initial request in the calculation of a print run).NB: In all cases, web-based use of full-text articles must be authorized separately through the 'Use on a Web Site' option when requesting permission.

3. Permission granted for a first edition does not apply to second and subsequent editions and for editions in other languages (except for signatories to the STM Permissions Guidelines, or where the first edition permission was granted for free).

4. Nature Publishing Group's permission must be acknowledged next to the figure, table or abstract in print. In electronic form, this acknowledgement must be visible at the same time as the figure/table/abstract, and must be hyperlinked to the journal's homepage.

5. The credit line should read:
   Reprinted by permission from Macmillan Publishers Ltd: [JOURNAL NAME] (reference citation), copyright (year of publication)
   For AOP papers, the credit line should read:
   Reprinted by permission from Macmillan Publishers Ltd: [JOURNAL NAME], advance online publication, day month year (doi: 10.1038/sj.[JOURNAL ACRONYM].XXXXX)

   Note: For republication from the *British Journal of Cancer*, the following credit lines apply.
   Reprinted by permission from Macmillan Publishers Ltd on behalf of Cancer Research UK: [JOURNAL NAME] (reference citation), copyright (year of publication)For AOP papers, the credit line should read:
   Reprinted by permission from Macmillan Publishers Ltd on behalf of Cancer Research UK: [JOURNAL NAME], advance online publication, day month year (doi: 10.1038/sj.[JOURNAL ACRONYM].XXXXX)

6. Adaptations of single figures do not require NPG approval. However, the adaptation should be credited as follows:

   Adapted by permission from Macmillan Publishers Ltd: [JOURNAL NAME] (reference citation), copyright (year of publication)

   Note: For adaptation from the *British Journal of Cancer*, the following credit line applies.
   Adapted by permission from Macmillan Publishers Ltd on behalf of Cancer Research UK: [JOURNAL NAME] (reference citation), copyright (year of publication)

7. Translations of 401 words up to a whole article require NPG approval. Please visit http://www.macmillanmedicalcommunications.com for more information.Translations of up to a 400 words do not require NPG approval. The translation should be credited as follows:

   Translated by permission from Macmillan Publishers Ltd: [JOURNAL NAME] (reference citation), copyright (year of publication).

   Note: For translation from the *British Journal of Cancer*, the following credit line applies.
   Translated by permission from Macmillan Publishers Ltd on behalf of Cancer Research UK: [JOURNAL NAME] (reference citation), copyright (year of publication)

We are certain that all parties will benefit from this agreement and wish you the best in the use of this material. Thank you.
Special Terms:
v1.1

APPENDIX V COPYRIGHT PERMISSION FOR FIGURE 28

Creative Commons Legal Code

Attribution 3.0 Unported

CREATIVE COMMONS CORPORATION IS NOT A LAW FIRM AND DOES NOT PROVIDE LEGAL SERVICES. DISTRIBUTION OF THIS LICENSE DOES NOT CREATE AN ATTORNEY-CLIENT RELATIONSHIP. CREATIVE COMMONS PROVIDES THIS INFORMATION ON AN "AS-IS" BASIS. CREATIVE COMMONS MAKES NO WARRANTIES REGARDING THE INFORMATION PROVIDED, AND DISCLAIMS LIABILITY FOR DAMAGES RESULTING FROM ITS USE.

License

THE WORK (AS DEFINED BELOW) IS PROVIDED UNDER THE TERMS OF THIS CREATIVE COMMONS PUBLIC LICENSE ("CCPL" OR "LICENSE"). THE WORK IS PROTECTED BY COPYRIGHT AND/OR OTHER APPLICABLE LAW. ANY USE OF THE WORK OTHER THAN AS AUTHORIZED UNDER THIS LICENSE OR COPYRIGHT LAW IS PROHIBITED.

BY EXERCISING ANY RIGHTS TO THE WORK PROVIDED HERE, YOU ACCEPT AND AGREE TO BE BOUND BY THE TERMS OF THIS LICENSE. TO THE EXTENT THIS LICENSE MAY BE CONSIDERED TO BE A CONTRACT, THE LICENSOR GRANTS YOU THE RIGHTS CONTAINED HERE IN CONSIDERATION OF YOUR ACCEPTANCE OF SUCH TERMS AND CONDITIONS.

1. Definitions

a. **"Adaptation"** means a work based upon the Work, or upon the Work and other pre-existing works, such as a translation, adaptation, derivative work, arrangement of music or other alterations of a literary or artistic work, or phonogram or performance and includes cinematographic adaptations or any other form in which the Work may be recast, transformed, or adapted including in any form recognizably derived from the original, except that a work that constitutes a Collection will not be considered an Adaptation for the purpose of this License. For the avoidance of doubt, where the Work is a musical work, performance or phonogram, the synchronization of the Work in timed-relation with a moving image ("synching") will be considered an Adaptation for the purpose of this License.
b. **"Collection"** means a collection of literary or artistic works, such as encyclopedias and anthologies, or performances, phonograms or broadcasts, or other works or subject matter other than works listed in Section 1(f) below, which, by reason of the selection and arrangement of their contents, constitute intellectual creations, in which the Work is included in its entirety in unmodified form along with one or more other contributions, each constituting separate and independent works in themselves, which together are assembled into a collective whole. A work that constitutes a Collection will not be considered an Adaptation (as defined above) for the purposes of this License.
c. **"Distribute"** means to make available to the public the original and copies of the Work or Adaptation, as appropriate, through sale or other transfer of ownership.
d. **"Licensor"** means the individual, individuals, entity or entities that offer(s) the Work under the terms of this License.
e. **"Original Author"** means, in the case of a literary or artistic work, the individual, individuals, entity or entities who created the Work or if no individual or entity can be identified, the publisher; and in addition (i) in the case of a performance the actors, singers, musicians, dancers, and other persons who act, sing, deliver, declaim, play in, interpret or otherwise perform literary or artistic works or expressions of folklore; (ii) in the case of a phonogram the producer being the person or legal entity

who first fixes the sounds of a performance or other sounds; and, (iii) in the case of broadcasts, the organization that transmits the broadcast.

f. **"Work"** means the literary and/or artistic work offered under the terms of this License including without limitation any production in the literary, scientific and artistic domain, whatever may be the mode or form of its expression including digital form, such as a book, pamphlet and other writing; a lecture, address, sermon or other work of the same nature; a dramatic or dramatico-musical work; a choreographic work or entertainment in dumb show; a musical composition with or without words; a cinematographic work to which are assimilated works expressed by a process analogous to cinematography; a work of drawing, painting, architecture, sculpture, engraving or lithography; a photographic work to which are assimilated works expressed by a process analogous to photography; a work of applied art; an illustration, map, plan, sketch or three-dimensional work relative to geography, topography, architecture or science; a performance; a broadcast; a phonogram; a compilation of data to the extent it is protected as a copyrightable work; or a work performed by a variety or circus performer to the extent it is not otherwise considered a literary or artistic work.
g. **"You"** means an individual or entity exercising rights under this License who has not previously violated the terms of this License with respect to the Work, or who has received express permission from the Licensor to exercise rights under this License despite a previous violation.
h. **"Publicly Perform"** means to perform public recitations of the Work and to communicate to the public those public recitations, by any means or process, including by wire or wireless means or public digital performances; to make available to the public Works in such a way that members of the public may access these Works from a place and at a place individually chosen by them; to perform the Work to the public by any means or process and the communication to the public of the performances of the Work, including by public digital performance; to broadcast and rebroadcast the Work by any means including signs, sounds or images.
i. **"Reproduce"** means to make copies of the Work by any means including without limitation by sound or visual recordings and the right of fixation and reproducing fixations of the Work, including storage of a protected performance or phonogram in digital form or other electronic medium.

2. Fair Dealing Rights. Nothing in this License is intended to reduce, limit, or restrict any uses free from copyright or rights arising from limitations or exceptions that are provided for in connection with the copyright protection under copyright law or other applicable laws.

3. License Grant. Subject to the terms and conditions of this License, Licensor hereby grants You a worldwide, royalty-free, non-exclusive, perpetual (for the duration of the applicable copyright) license to exercise the rights in the Work as stated below:

a. to Reproduce the Work, to incorporate the Work into one or more Collections, and to Reproduce the Work as incorporated in the Collections;
b. to create and Reproduce Adaptations provided that any such Adaptation, including any translation in any medium, takes reasonable steps to clearly label, demarcate or otherwise identify that changes were made to the original Work. For example, a translation could be marked "The original work was translated from English to Spanish," or a modification could indicate "The original work has been modified.";
c. to Distribute and Publicly Perform the Work including as incorporated in Collections; and,
d. to Distribute and Publicly Perform Adaptations.

e. For the avoidance of doubt:

    i. **Non-waivable Compulsory License Schemes**. In those jurisdictions in which the right to collect royalties through any statutory or compulsory licensing scheme cannot be waived, the Licensor reserves the exclusive right to collect such royalties for any exercise by You of the rights granted under this License;
    ii. **Waivable Compulsory License Schemes**. In those jurisdictions in which the right to collect royalties through any statutory or compulsory licensing scheme can be waived, the Licensor waives the exclusive right to collect such royalties for any exercise by You of the rights granted under this License; and,
    iii. **Voluntary License Schemes**. The Licensor waives the right to collect royalties, whether

individually or, in the event that the Licensor is a member of a collecting society that administers voluntary licensing schemes, via that society, from any exercise by You of the rights granted under this License.

The above rights may be exercised in all media and formats whether now known or hereafter devised. The above rights include the right to make such modifications as are technically necessary to exercise the rights in other media and formats. Subject to Section 8(f), all rights not expressly granted by Licensor are hereby reserved.

4. Restrictions. The license granted in Section 3 above is expressly made subject to and limited by the following restrictions:

a. You may Distribute or Publicly Perform the Work only under the terms of this License. You must include a copy of, or the Uniform Resource Identifier (URI) for, this License with every copy of the Work You Distribute or Publicly Perform. You may not offer or impose any terms on the Work that restrict the terms of this License or the ability of the recipient of the Work to exercise the rights granted to that recipient under the terms of the License. You may not sublicense the Work. You must keep intact all notices that refer to this License and to the disclaimer of warranties with every copy of the Work You Distribute or Publicly Perform. When You Distribute or Publicly Perform the Work, You may not impose any effective technological measures on the Work that restrict the ability of a recipient of the Work from You to exercise the rights granted to that recipient under the terms of the License. This Section 4(a) applies to the Work as incorporated in a Collection, but this does not require the Collection apart from the Work itself to be made subject to the terms of this License. If You create a Collection, upon notice from any Licensor You must, to the extent practicable, remove from the Collection any credit as required by Section 4(b), as requested. If You create an Adaptation, upon notice from any Licensor You must, to the extent practicable, remove from the Adaptation any credit as required by Section 4(b), as requested.
b. If You Distribute, or Publicly Perform the Work or any Adaptations or Collections, You must, unless a request has been made pursuant to Section 4(a), keep intact all copyright notices for the Work and provide, reasonable to the medium or means You are utilizing: (i) the name of the Original Author (or pseudonym, if applicable) if supplied, and/or if the Original Author and/or Licensor designate another party or parties (e.g., a sponsor institute, publishing entity, journal) for attribution ("Attribution Parties") in Licensor's copyright notice, terms of service or by other reasonable means, the name of such party or parties; (ii) the title of the Work if supplied; (iii) to the extent reasonably practicable, the URI, if any, that Licensor specifies to be associated with the Work, unless such URI does not refer to the copyright notice or licensing information for the Work; and (iv) , consistent with Section 3(b), in the case of an Adaptation, a credit identifying the use of the Work in the Adaptation (e.g., "French translation of the Work by Original Author," or "Screenplay based on original Work by Original Author"). The credit required by this Section 4 (b) may be implemented in any reasonable manner; provided, however, that in the case of a Adaptation or Collection, at a minimum such credit will appear, if a credit for all contributing authors of the Adaptation or Collection appears, then as part of these credits and in a manner at least as prominent as the credits for the other contributing authors. For the avoidance of doubt, You may only use the credit required by this Section for the purpose of attribution in the manner set out above and, by exercising Your rights under this License, You may not implicitly or explicitly assert or imply any connection with, sponsorship or endorsement by the Original Author, Licensor and/or Attribution Parties, as appropriate, of You or Your use of the Work, without the separate, express prior written permission of the Original Author, Licensor and/or Attribution Parties.
c. Except as otherwise agreed in writing by the Licensor or as may be otherwise permitted by applicable law, if You Reproduce, Distribute or Publicly Perform the Work either by itself or as part of any Adaptations or Collections, You must not distort, mutilate, modify or take other derogatory action in relation to the Work which would be prejudicial to the Original Author's honor or reputation. Licensor agrees that in those jurisdictions (e.g. Japan), in which any exercise of the right granted in Section 3(b) of this License (the right to make Adaptations) would be deemed to be a distortion, mutilation, modification or other derogatory action prejudicial to the Original Author's honor and reputation, the Licensor will waive or not assert, as appropriate, this Section, to the fullest extent permitted by the applicable national law, to enable You to reasonably exercise Your right under

Section 3(b) of this License (right to make Adaptations) but not otherwise.

5. Representations, Warranties and Disclaimer

UNLESS OTHERWISE MUTUALLY AGREED TO BY THE PARTIES IN WRITING, LICENSOR OFFERS THE WORK AS-IS AND MAKES NO REPRESENTATIONS OR WARRANTIES OF ANY KIND CONCERNING THE WORK, EXPRESS, IMPLIED, STATUTORY OR OTHERWISE, INCLUDING, WITHOUT LIMITATION, WARRANTIES OF TITLE, MERCHANTIBILITY, FITNESS FOR A PARTICULAR PURPOSE, NONINFRINGEMENT, OR THE ABSENCE OF LATENT OR OTHER DEFECTS, ACCURACY, OR THE PRESENCE OF ABSENCE OF ERRORS, WHETHER OR NOT DISCOVERABLE. SOME JURISDICTIONS DO NOT ALLOW THE EXCLUSION OF IMPLIED WARRANTIES, SO SUCH EXCLUSION MAY NOT APPLY TO YOU.

6. Limitation on Liability. EXCEPT TO THE EXTENT REQUIRED BY APPLICABLE LAW, IN NO EVENT WILL LICENSOR BE LIABLE TO YOU ON ANY LEGAL THEORY FOR ANY SPECIAL, INCIDENTAL, CONSEQUENTIAL, PUNITIVE OR EXEMPLARY DAMAGES ARISING OUT OF THIS LICENSE OR THE USE OF THE WORK, EVEN IF LICENSOR HAS BEEN ADVISED OF THE POSSIBILITY OF SUCH DAMAGES.

7. Termination

a. This License and the rights granted hereunder will terminate automatically upon any breach by You of the terms of this License. Individuals or entities who have received Adaptations or Collections from You under this License, however, will not have their licenses terminated provided such individuals or entities remain in full compliance with those licenses. Sections 1, 2, 5, 6, 7, and 8 will survive any termination of this License.
b. Subject to the above terms and conditions, the license granted here is perpetual (for the duration of the applicable copyright in the Work). Notwithstanding the above, Licensor reserves the right to release the Work under different license terms or to stop distributing the Work at any time; provided, however that any such election will not serve to withdraw this License (or any other license that has been, or is required to be, granted under the terms of this License), and this License will continue in full force and effect unless terminated as stated above.

8. Miscellaneous

a. Each time You Distribute or Publicly Perform the Work or a Collection, the Licensor offers to the recipient a license to the Work on the same terms and conditions as the license granted to You under this License.
b. Each time You Distribute or Publicly Perform an Adaptation, Licensor offers to the recipient a license to the original Work on the same terms and conditions as the license granted to You under this License.
c. If any provision of this License is invalid or unenforceable under applicable law, it shall not affect the validity or enforceability of the remainder of the terms of this License, and without further action by the parties to this agreement, such provision shall be reformed to the minimum extent necessary to make such provision valid and enforceable.
d. No term or provision of this License shall be deemed waived and no breach consented to unless such waiver or consent shall be in writing and signed by the party to be charged with such waiver or consent.
e. This License constitutes the entire agreement between the parties with respect to the Work licensed here. There are no understandings, agreements or representations with respect to the Work not specified here. Licensor shall not be bound by any additional provisions that may appear in any communication from You. This License may not be modified without the mutual written agreement of the Licensor and You.
f. The rights granted under, and the subject matter referenced, in this License were drafted utilizing the terminology of the Berne Convention for the Protection of Literary and Artistic Works (as amended on September 28, 1979), the Rome Convention of 1961, the WIPO Copyright Treaty of 1996, the WIPO Performances and Phonograms Treaty of 1996 and the Universal Copyright Convention (as revised on July 24, 1971). These rights and subject matter take effect in the relevant jurisdiction in

which the License terms are sought to be enforced according to the corresponding provisions of the implementation of those treaty provisions in the applicable national law. If the standard suite of rights granted under applicable copyright law includes additional rights not granted under this License, such additional rights are deemed to be included in the License; this License is not intended to restrict the license of any rights under applicable law.

Creative Commons Notice

Creative Commons is not a party to this License, and makes no warranty whatsoever in connection with the Work. Creative Commons will not be liable to You or any party on any legal theory for any damages whatsoever, including without limitation any general, special, incidental or consequential damages arising in connection to this license. Notwithstanding the foregoing two (2) sentences, if Creative Commons has expressly identified itself as the Licensor hereunder, it shall have all rights and obligations of Licensor.

Except for the limited purpose of indicating to the public that the Work is licensed under the CCPL, Creative Commons does not authorize the use by either party of the trademark "Creative Commons" or any related trademark or logo of Creative Commons without the prior written consent of Creative Commons. Any permitted use will be in compliance with Creative Commons' then-current trademark usage guidelines, as may be published on its website or otherwise made available upon request from time to time. For the avoidance of doubt, this trademark restriction does not form part of this License.

Creative Commons may be contacted at https://creativecommons.org/.